SAND2007-2844P

Nanoparticles, Microfluidics and Light: Control over Photochromic Systems

Nelson S. Bell,
Marcin Piech, United Technologies Corp.
Liu Jiang, Tim Long
Dongqing Yang, S. Tom Picraux, U. Arizona
Greg Jamison, SNL
Matt George and Paul Braun, UIUC

Electronic and Nanostructured Materials
Sandia National Laboratories

Albuquerque, New Mexico 87185-0888

Sandia National Laboratories is a multiprogram laboratory operated by Sandia Corporation, a Lockheed Martin Company.
This work was supported by the U.S. DOE under contract DE-AC04-94AL85000.

Sandia National Laboratories

Overview

- Photo-Controlled surfaces
- Directed Particle Interactions using photo-sensitive colloids
- Optical Property Doping of ZnO Semi-conductor nanoparticles
- CINT Microfluidic Discovery Platform™

Motivation

Photochemical control of physical interaction processes on the molecular level

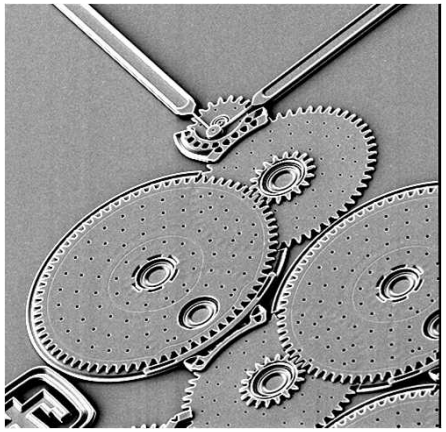

MEMS: ***tribology***

Nano-interaction management

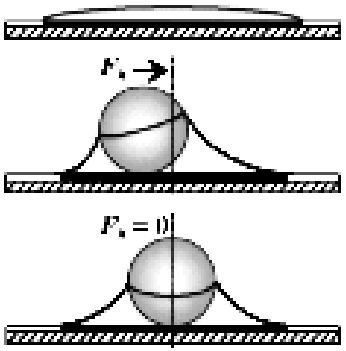

Self-assembled nanostructures:

Microfluidics: ***rheology***

J. Micromech. Microeng.., 13, (2003), p. 261

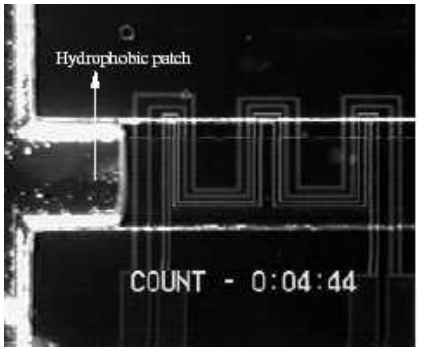

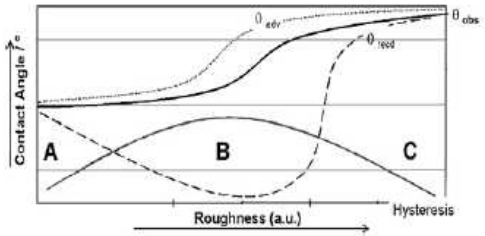

Figure 1. Wettability vs. roughness (schematically). (A) Smooth surface, (B) Wenzel Regime, (C) superhydrophobic surface. θ_{obs}: observable (static) c.a., θ_{adv}: advancing c.a., θ_{recd}: receding c.a.

J. Sol-Gel Sci. Tech., 26, (2003), p.789

- **Fundamental competency for the realization and application of high-surface-area microsystem architectures and the controlled fabrication and utilization of nanostructured materials**

Sandia National Laboratories

Photochromic Molecules

- Azobenzene
- Spiropyran

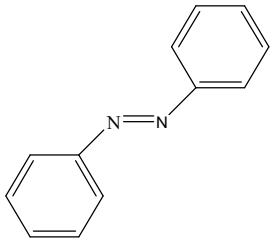

trans

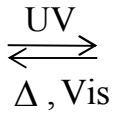

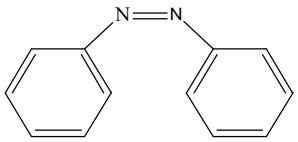

cis

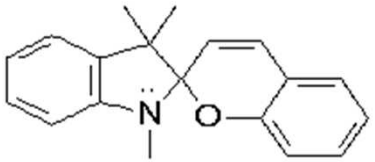

Closed

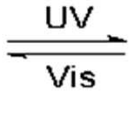

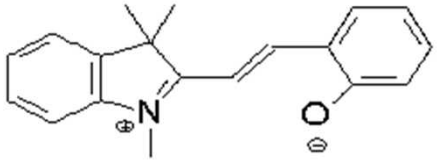

Open

- changes in optical profile (UV/Vis spectrum)
- alteration of surface energy (contact angle measurements)

Surface Design with Azobenzene

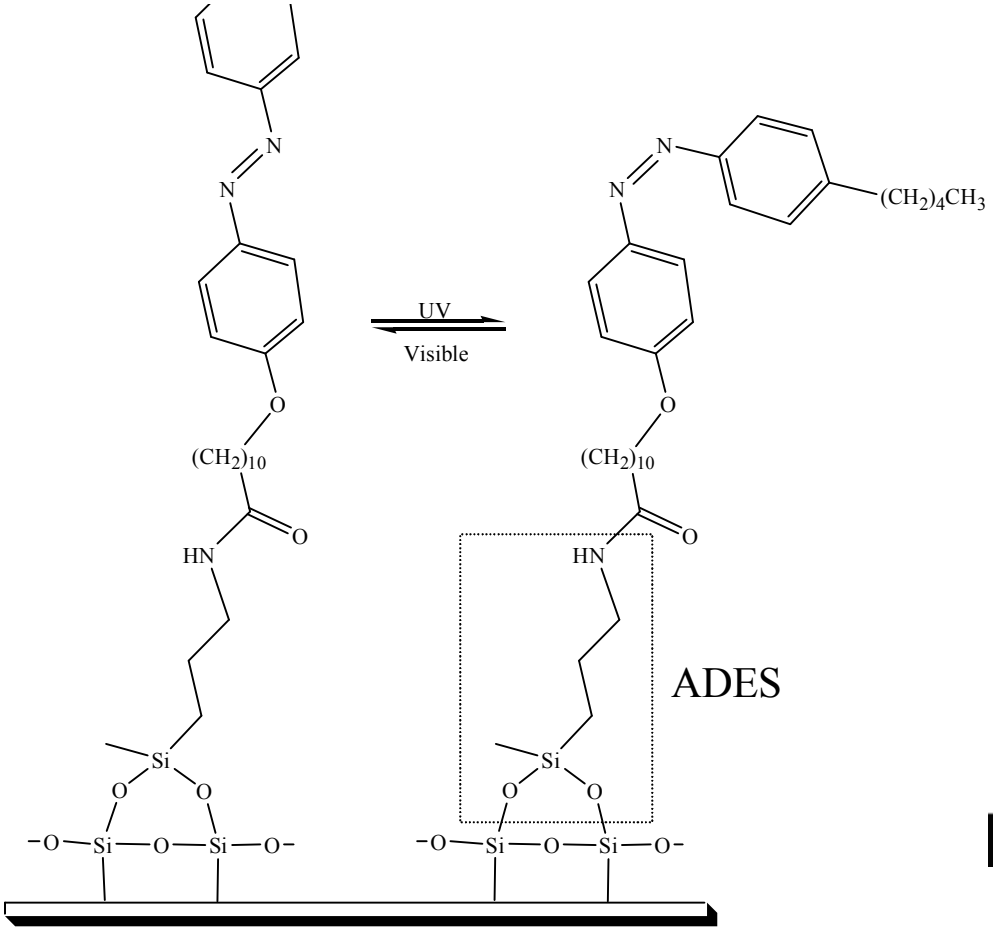

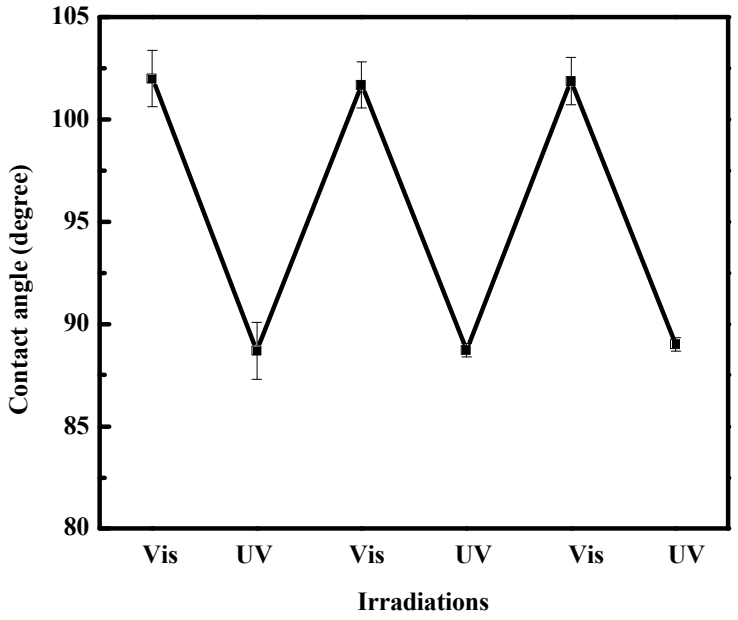

Wetting angle

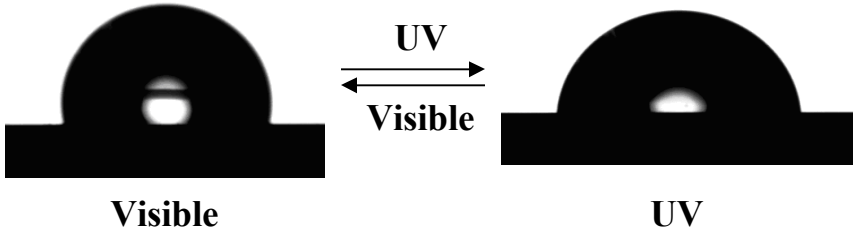

Azobenzene molecules attach to the surface through aminopropylmethyldiethoxysilane(ADES)

Visible	UV
100° -102°	88° -90°

Modeling of Surface Energy from Contact Angle Measurements

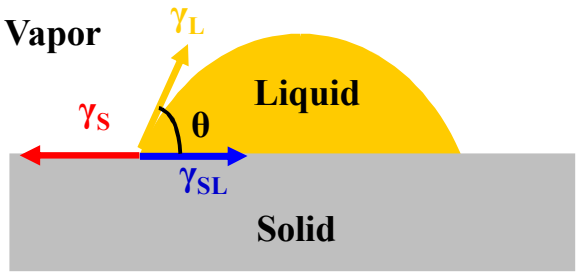

Young's equation

$$\gamma_S = \gamma_{SL} + \gamma_L \cos\theta$$

Van Oss theory

$$\gamma_S = \gamma_S^{LW} + \gamma_S^{AB} \qquad \gamma_S^{AB} = 2\sqrt{\gamma_S^- \gamma_S^+}$$

$$\gamma_L(1+\cos\theta) = 2\left(\sqrt{\gamma_S^{LW}\gamma_L^{LW}} + \sqrt{\gamma_S^-\gamma_L^+} + \sqrt{\gamma_S^+\gamma_L^-}\right)$$

Surface energy separated into dispersive (LW), electron donating (-) and electron accepting (+) components

Van Oss Modeling of Azobenzene Surfaces

Azobenzene modified surface energy (mJ/m^2) was calculated by using three fluids of known dispersive, acid and base components.

$$\gamma_L(1+\cos\theta) = 2\left(\sqrt{\gamma_S^{LW}\gamma_L^{LW}} + \sqrt{\gamma_S^{-}\gamma_L^{+}} + \sqrt{\gamma_S^{+}\gamma_L^{-}}\right)$$

Table: Surface tensions and components of probe liquids (mJ/m^2) suggested by Van Oss

Liquid	γ_L	γ_L^{LW}	γ_L^{-}	γ_L^{+}	γ_L^{AB}
Polar					
DI water	72.8	21.8	25.5	25.5	51.0
ethylene glycol	48.0	29.0	47.0	1.92	19.0
formamide	58.0	39.0	39.6	2.28	19.0
Nonpolar					
diiodomethane	50.8	50.8	--	0	0
1-bromonaphthalene	44.4	44.4	0	0	0

Van Oss Modeling of Azobenzene

Contact Angle Measurements using three fluids of known dispersive, acid and base character.

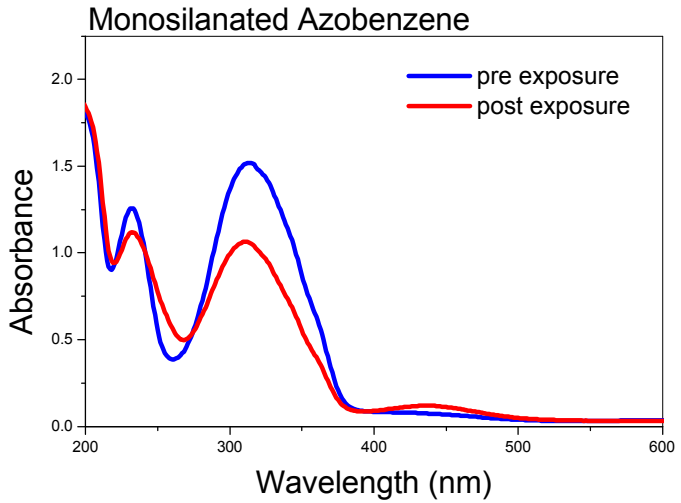

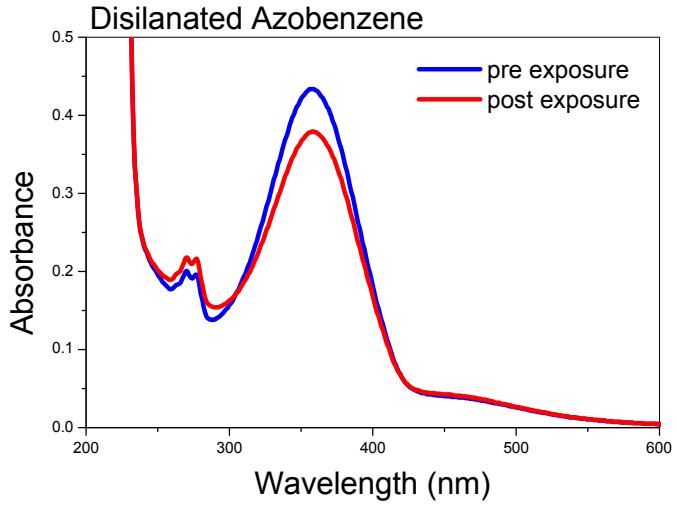

Solvent Parameters	σL	σD	σ-	σ+
Water	72.8	21.8	25.5	25.5
Diiodomethane	50.8	50.8	0	0
Formamide	58.2	39	39.6	2.28

$$\sqrt{\left(\sigma_l^D\right)\left(\sigma_s^D\right)}+\sqrt{\left(\sigma_l^-\right)\left(\sigma_s^+\right)}+\sqrt{\left(\sigma_l^+\right)\left(\sigma_s^-\right)}=\frac{\sigma_l\left(Cos\Theta+1\right)}{2}$$

Azobenzene (Monosilanated)	σ^D	σ^+	σ^-
Unexposed	40.08	0.10	1.23
Exposed	40.44	0.07	7.89
Azobenzene (Disilanated)			
Unexposed	29.10	0.02	7.24
Exposed	29.44	0.95	7.15

Sandia National Laboratories

Van Oss Modeling of Azobenzene Surfaces

Azobenzene modified surface energy (mJ/m^2) was calculated by using three fluids of known dispersive, acid and base components.

$$\gamma_L(1+\cos\theta) = 2\left(\sqrt{\gamma_S^{LW}\gamma_L^{LW}} + \sqrt{\gamma_S^{-}\gamma_L^{+}} + \sqrt{\gamma_S^{+}\gamma_L^{-}}\right)$$

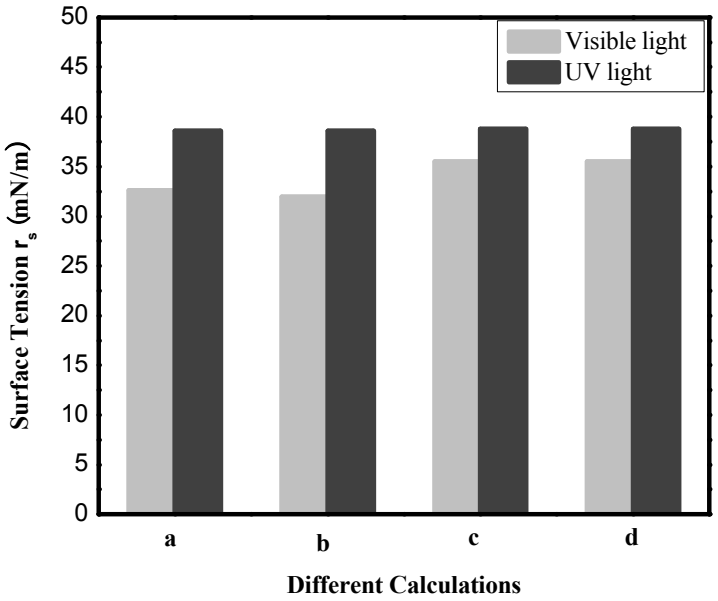

Calculations	Illumination	γ_S^{LW}	$(\gamma_S^{+})^2$	γ_S^{-}	γ_S
a)	Visible	32.59	-0.09	0.42	32.59
	UV	38.59	-0.21	3.23	38.59
b)	Visible light	32.02	-0.69	1.99	32.02
	UV	38.59	-0.55	4.57	38.59
c)	Visible	35.49	-0.28	0.36	35.49
	UV	38.83	-0.22	3.22	38.83
d)	Visible	35.49	-1.00	2.07	35.49
	UV	38.83	-0.57	4.58	38.83

a) Using DI water, Ethylene glycol, diiodomethane to calculate; b) Using DI water, Formamide, diiodomethane to calculate; c) Using DI water, Ethylene glycol, 1-Bromonaphtalene to calculate; d) Using DI water, Formamide, 1-Bromonaphtalene to calculate

Contact Angle Measurement with Liquids

Table: Contact angle on azobenzene modified surface with various solvents (degree).

Solvents	trans	cis	Surface Tension (mN/m)	Switching Angle ($\theta^{trans}_{adv} - \theta^{cis}_{adv}$)
	θ_{adv}	θ_{adv}		
acetonitrile	27.0±0.55	11.5±0.87	27	15.5
benzonitrile	32.0±2.0	17.0±0.76	38.65	15
DI water	101.3±0.98	88.9±0.86	72.8	12.4
diiodomethane	54.1±0.49	42.1±1.08	50.8	12
dimethylformamide	37.5±1.74	26.8±0.53	36.8	10.7
formamide	82.2±1.36	71.5±0.66	58.2	10.7
1-methylnaphthalene	33.3±1.09	23.3±0.34	40.5	10
ethylene Glycol	73.2±0.73	63.9±0.71	48	9.3
1-bromonaphthalene	38.0±0.67	29.7±0.40	44.4	8.3

Linear relationship between surface tension of solvents and its contact angle on azobenzene surface

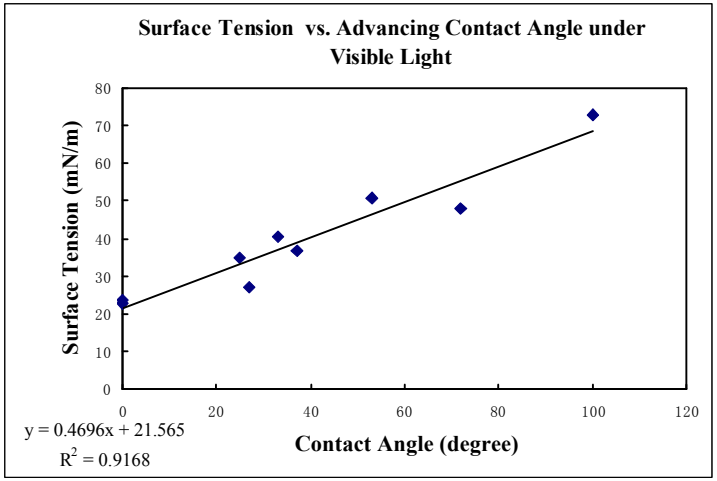

Droplet Mobility Requirements

Requirement: The receding contact angle (trans-isomer) under visible light must be larger than advancing contact angle (cis-isomer)

Table: Contact angle measurements (degree) on azobenzene modified surface with various solvents.

Liquid	trans		cis	
	θ_{adv}	θ_{rec}	θ_{adv}	θ_{rec}
Fulfill motion requirement				
benzonitrile	32.0±2.0	26.2± 1.25	17.0± 0.76	--
diiodomethane	54.1± 0.49	43.7± 0.58	42.1± 1.08	33.1± 1.28
dimethylformamide	37.5± 1.74	29.6± 1.47	26.8± 0.53	19.0± 1.34
1-bromonaphthalene	38.0± 0.67	33.5± 0.5	29.7± 0.40	24.6± 0.51
acetonitrile	27.0± 0.55	19.4± 1.41	11.5± 0.87	--
1-methylnaphthalene	33.3± 1.09	23.5± 0.77	23.3± 0.34	13.5± 0.56
Not fulfill motion requirement				
DI water	101.3± 0.98	76.0± 2.0	88.9± 0.86	69.8± 1.4
formamide	82.2± 1.36	62.8± 1.18	71.5± 0.66	58.2± 1.01
ethylene glycol	73.2± 0.73	49.0± 1.15	63.9± 0.71	41.5± 0.49

Motion of 1-Bromonaphthalene by UV Light

We demonstrate the idea of using light to move liquids on a photoresponsive surface.

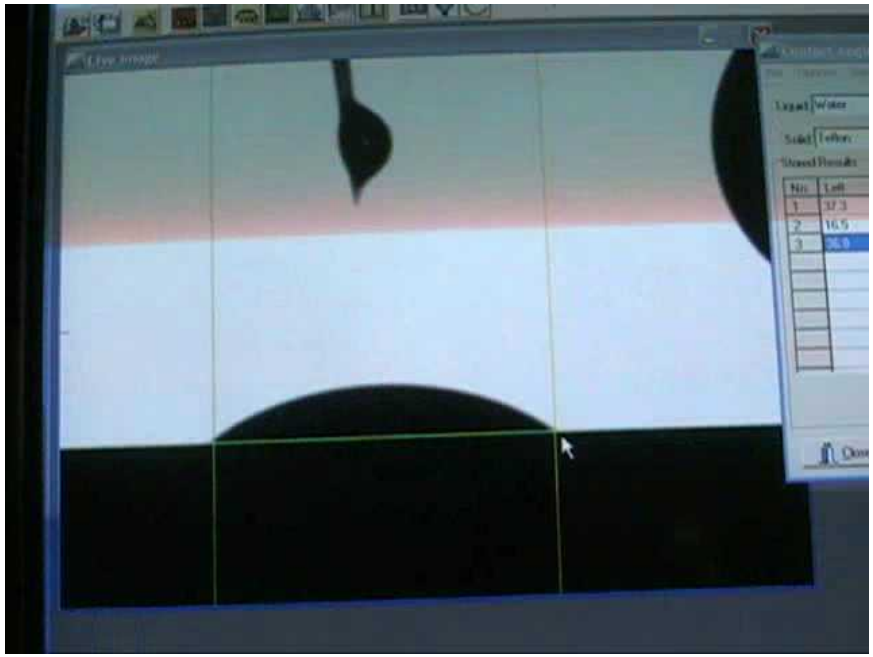

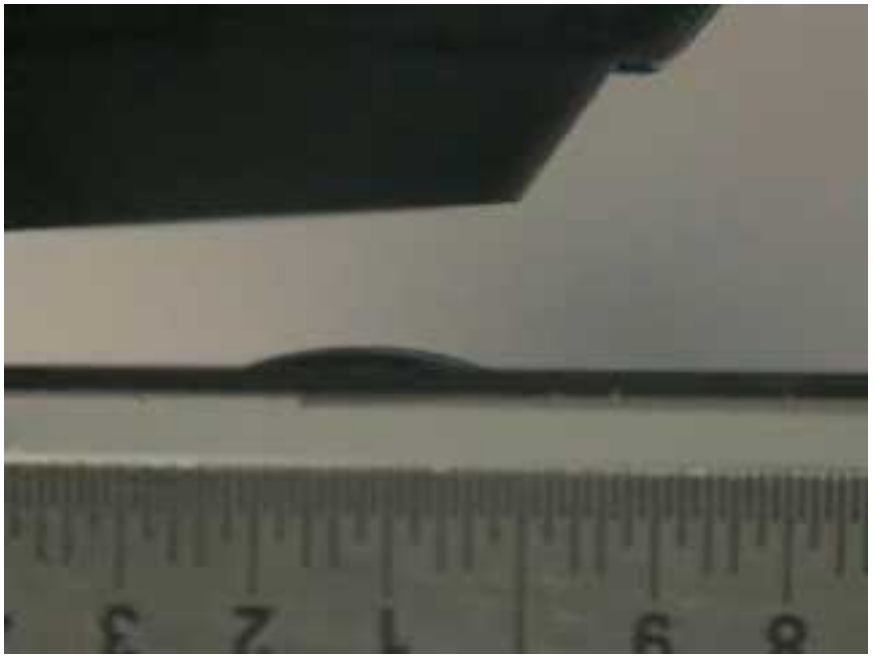

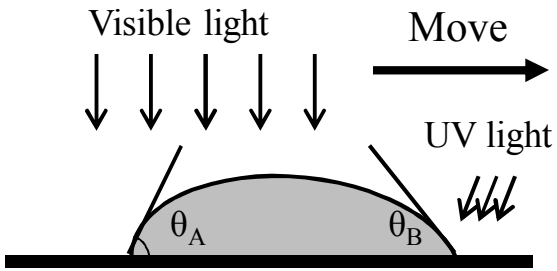

Surface Templating of Particle Assembly

Cationic/anionic functionalization of particles and substrates enables
-single particle spectroscopy
-definition of ABAB composite architectures for energy transfer

Particle templating via microcontact printing (mCP) of heterogeneous monolayers:

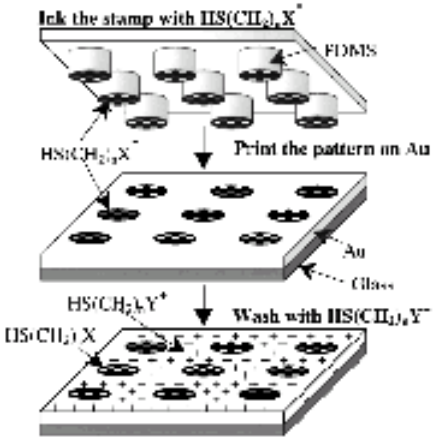

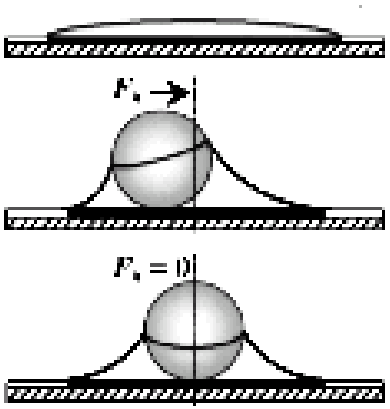

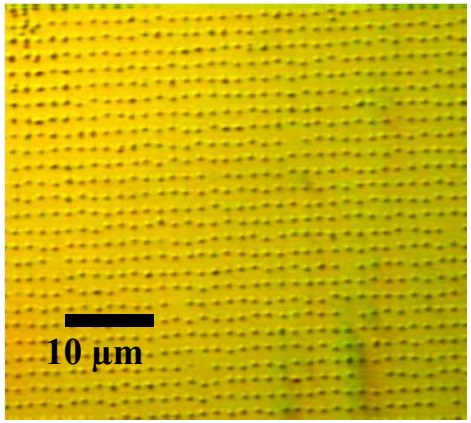

Particle templating allows:

- more complicated structures: FCC, BCC, diamond cubic
- introduction of defects (superlattices)
- stamping of waveguides

Clem and Payne, "Monolayer-mediated patterning of electroceramics," J. Electroceram, 3(2), 163 (1999).
Aizenberg, Braun, and Wiltzius, "Patterned colloidal deposition by electrostatic and capillary forces, Phys. Rev. Lett. **84**(13), 29973000 (2000).

Sandia National Laboratories

Heterogeneous Particle Assembly

Are there analogs to directed assembly at the colloidal scale?

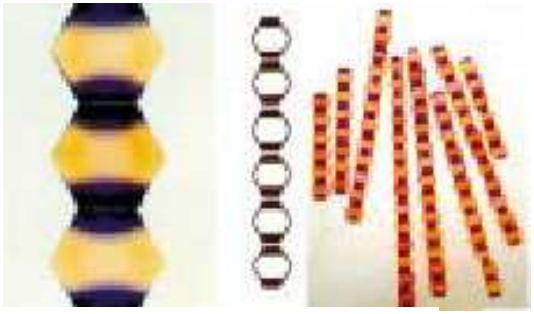

Ned Bowden, et al. *J. Am. Chem. Soc.* **121** (1999) 5373-5391

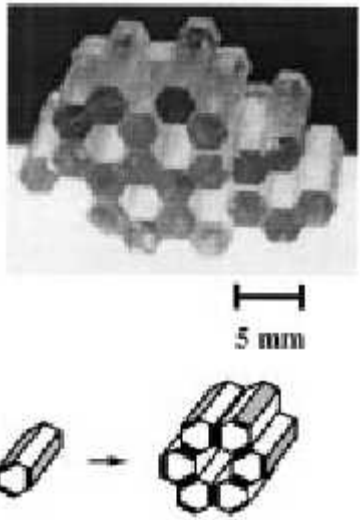

S.R.J. Oliver at al. *J. Colloid Interface Sci.*, **224** (2000) 425-428.

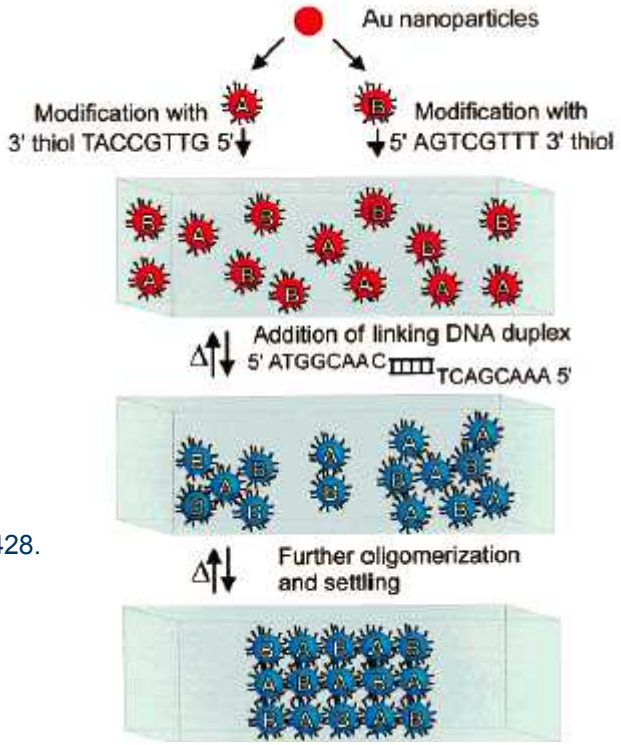

* Chad Mirkin, *Inorg. Chem.* 39 (2000)
Hiddessen et al. *Langmuir*, 16 (2000)

There are <u>novel</u> systems to study with these methods…

- Electrostatic Assembly (i.e. Ionomeric Gel).
- Photosensitive stabilization mechanisms or bonding.
  (Zaitsev SY, et al. Supramolecular Science, **4** (1997) 519-524.)
- Biological Surface Recognition*
  DNA, nucleotides, peptides, lipids …
  Observed structures include colloidal micelles, clusters, rings, and chains.
- Structured layer deposition using non-spherical particles
  (Choi et al. Langmuir (2000) **16**, 2997-2999.)

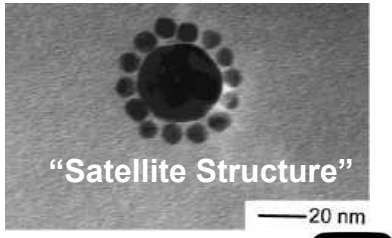

Sandia National Laboratories

Photochemical Control of Surface Interactions

Photochemical alteration of an organic moiety resulting in a change in steric, electrostatic parameters

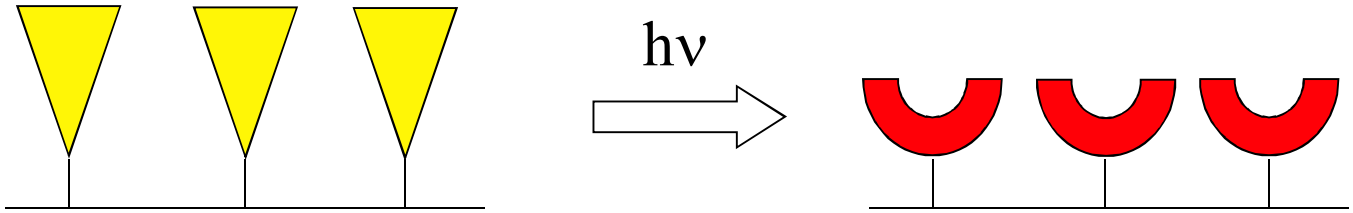

- Real-time manipulation of surface properties
- Switchable/reversible (new operational modes)
- High photoefficiency ~ low power LED's
- Non-invasive/remote

Manifested in:

- changes in optical profile (UV/Vis spectrum)
- alteration of surface energy
- photocontrolled colloidal stability

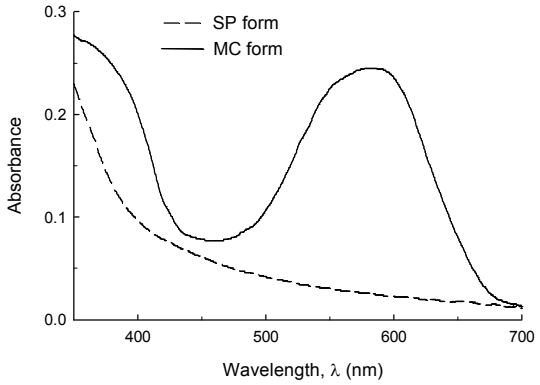

Sandia National Laboratories

Reversible Light-regulated Colloidal Interactions?

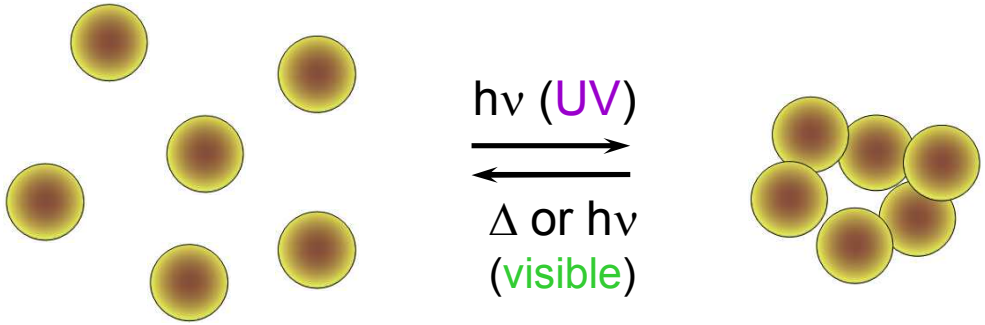

Approach: Utilize reversible photochemical reaction

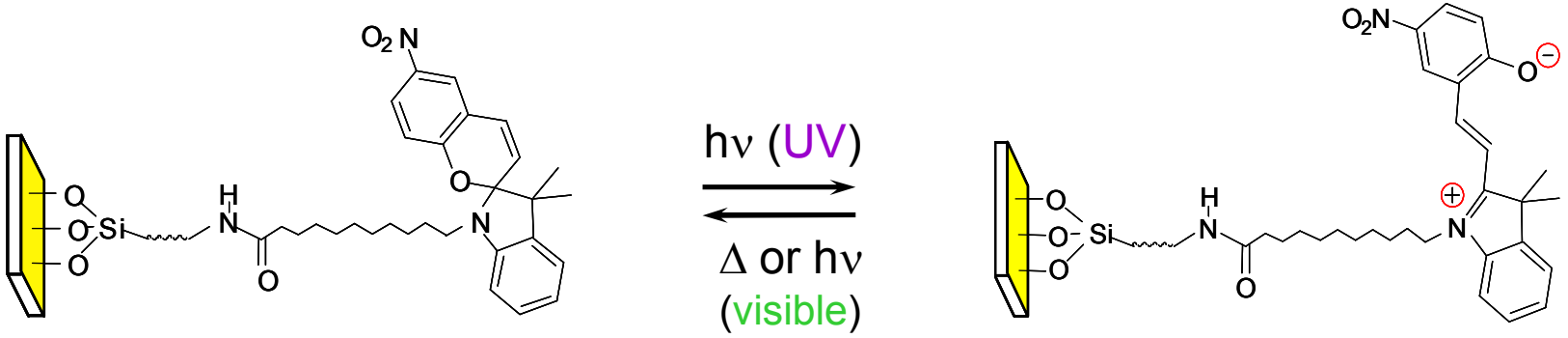

closed form

Spirobenzopyran (SP)

zwitterionic form

Merocyanine (ME)

- Reversible aggregation of SP-coated colloidal particles in non-polar solvents
  K. Ichimura, et al. *J. Mat. Chem.* **4**, 883 (1994)

Azobenzene Derivatized Surface and Colloid Aggregation Response

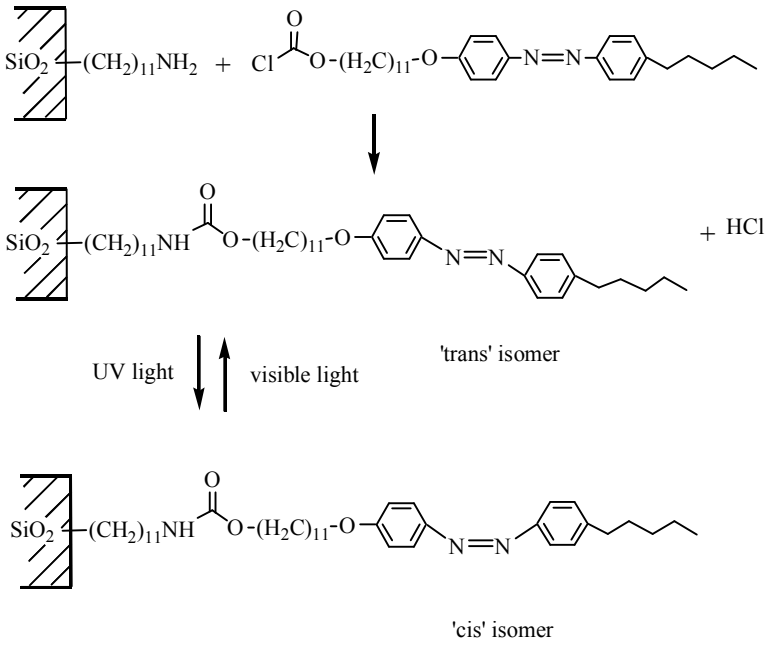

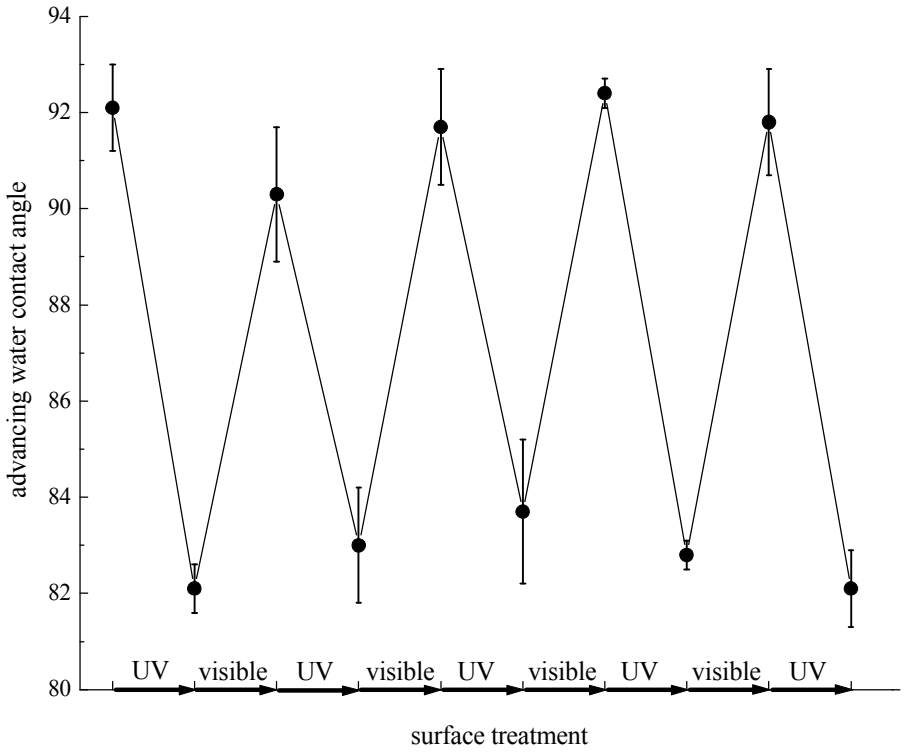

Left sample is visible exposed
Right sample is UV exposed

Sedimentation Rate Difference

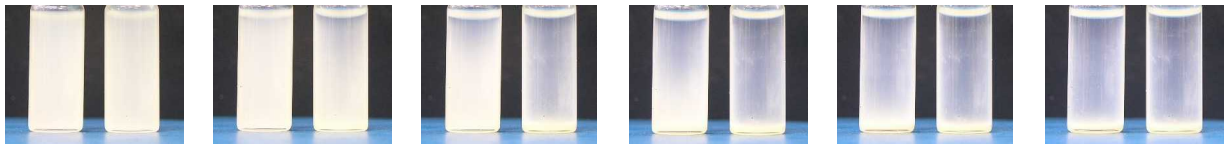

12 sec 60 sec 120 sec 180 sec 240 sec 300 sec

Sandia National Laboratories

Interfacial Energy Calculation

A transition from negative to positive interfacial energy is desired for photo control of wetting characteristics.

$$\Delta G_{131} = -2\left(\sqrt{\gamma_1^D} - \sqrt{\gamma_3^D}\right)^2 - 4\left(\sqrt{\gamma_1^+\gamma_1^-} + \sqrt{\gamma_3^+\gamma_3^-} - \sqrt{\gamma_1^+\gamma_3^-} - \sqrt{\gamma_3^+\gamma_1^-}\right)$$

	Pre exposure	Post Exposure	Change in Surface Energy
Cyclohexane	-4.69	-7.03	-2.34
Chloroform	2.72	13.51	10.78
Tetrahydrofuran	-12.29	-16.31	-4.02
Diiodomethane	-2.67	-3.83	-1.16
Water	-80.14	-49.41	30.73
Formamide	-24.77	-17.46	7.31
Glycerol	-43.54	-33.54	10.00
Ethylene Glycol	-26.37	-20.52	5.85

Strategic Approach to forming a Photosensitive Colloidal System

Demonstrate Reversible aggregation and dispersion of colloidal particles by light based methods.

Particle system: Silica

- monodisperse,
- spherical
- common model system
- surface chemistry can be modified using silanes

Organic component: spiropyran

- large dipole moment change
- forms a zwitterionic state
- literature states solubility changes of SPMMA polymers in nonaqueous solvents

Approach: derivatize particles with layers of photo-switchable polymer.

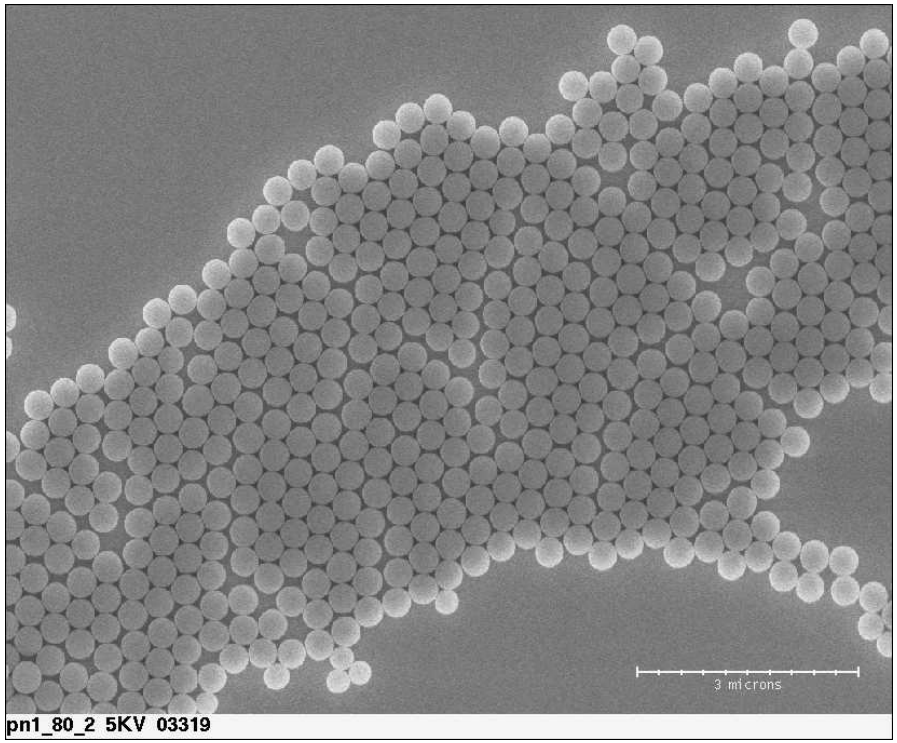

Sandia National Laboratories

Atom Transfer Radical Polymerization Reaction Mechanism

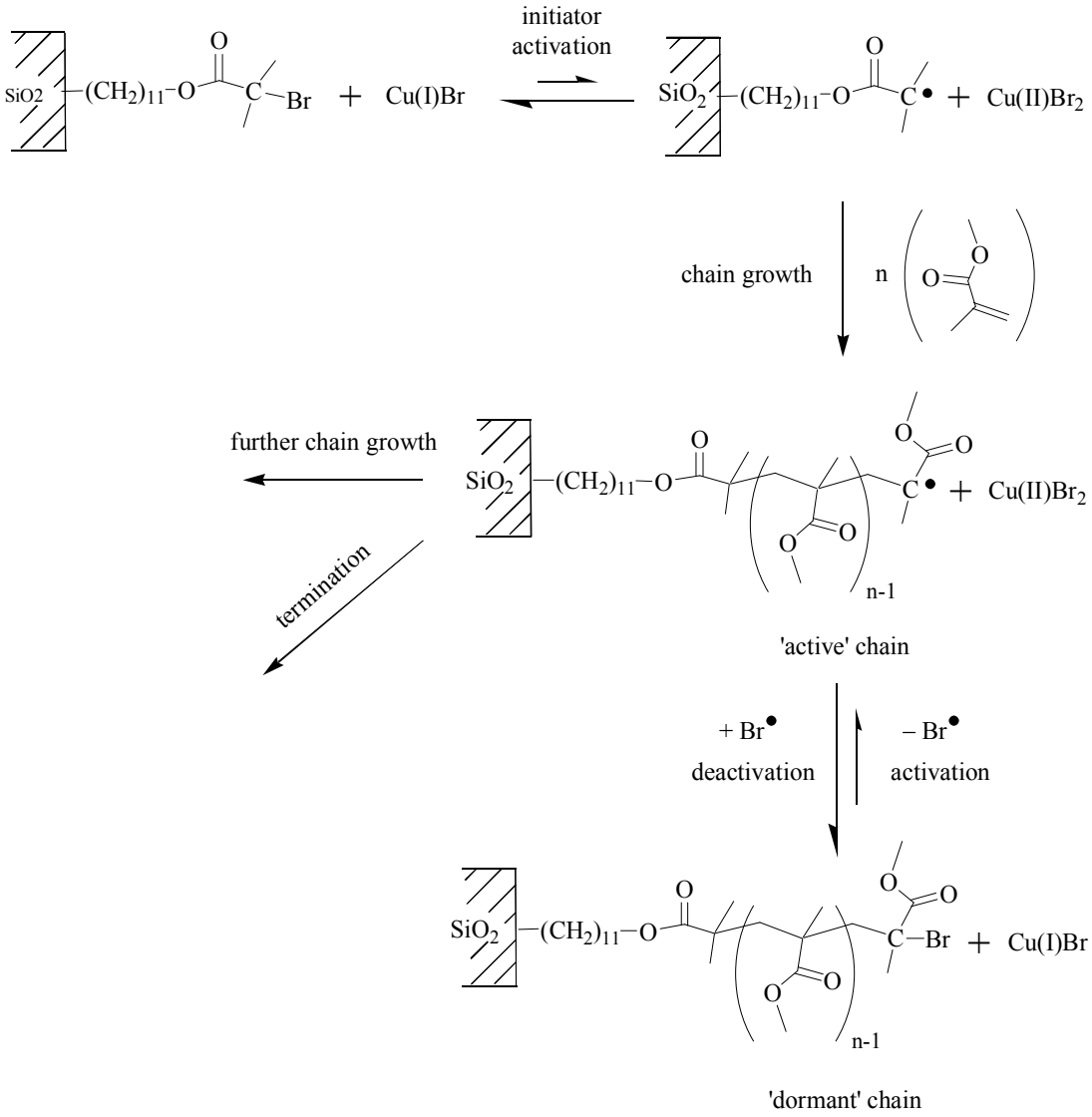

Properties:

- Controlled growth of uniform layers
- Reaction kinetics allow for thickness control
- Requires oxygen free environment or techniques
- Large number of catalyst systems to test

Sandia National Laboratories

ATRP Reaction Kinetics for SP/MMA Colloids

Model

$$\frac{d[A]}{dt} = -k_1[A]^2$$

$$\frac{dh}{dt} = k_2[A]$$

$$h = (k_2/k_1)\ln(1 + k_1[A]_0 t)$$

- Fit to the model of Kim *et al.*† indicates the presence of termination reactions

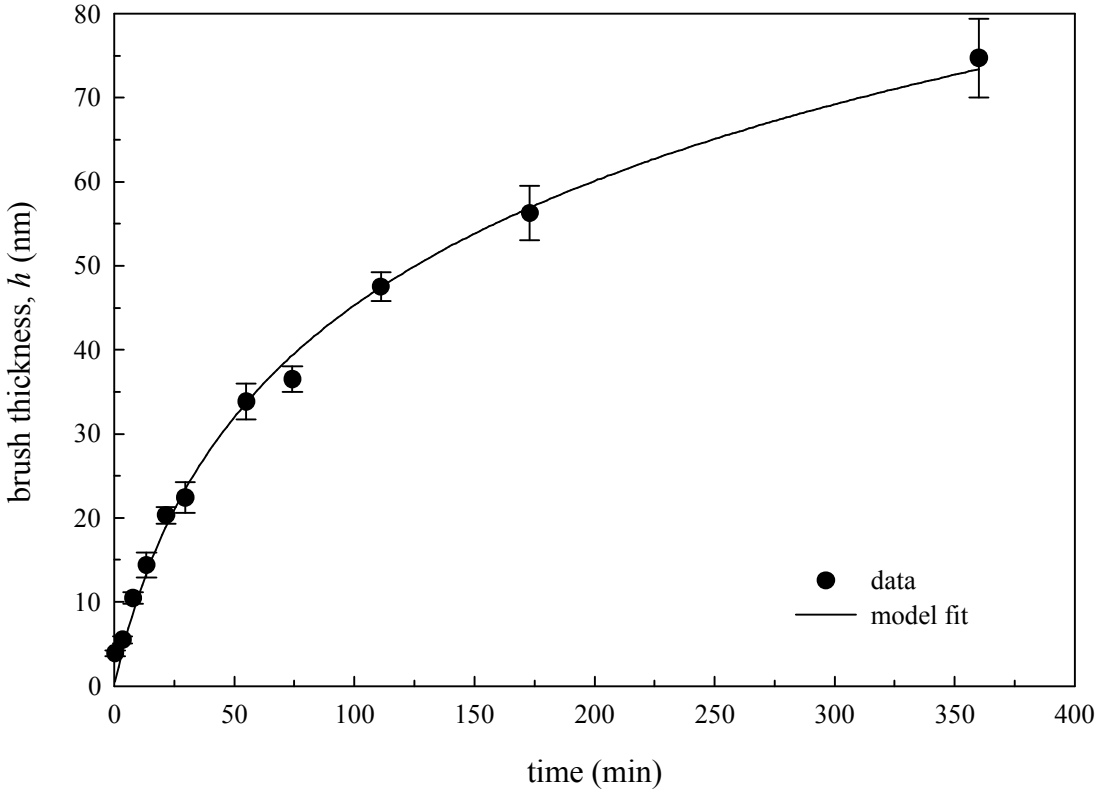

† J. –B. Kim, W. Huang, M. L. Bruening, G. L. Baker, "Synthesis of Triblock Copolymer Brushes by Surface-Initiated Atom Transfer Radical Polymerization," *Macromolecules* **35** (2002) 5410-5416.

Sandia National Laboratories

Photo-induced switching

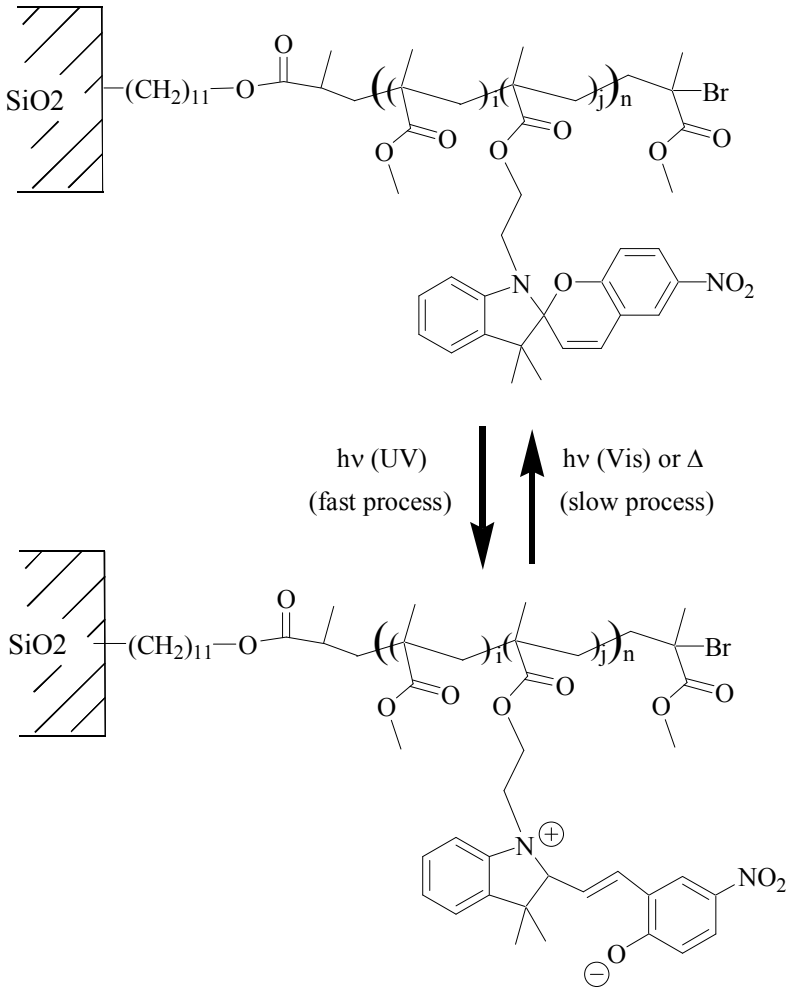

- In non-polar solvents spyrobenzopyran (SP) molecule exists in closed form
- UV excitation causes ring-opening photoisomerization
- After UV treatment molecule exists in zwitterionic merocyanine (ME) form
- Corresponding polarity change alters polymer conformation and polymer-solvent interactions
- Process is reversible (albeit slower) upon exposure to visible light or heat

Sandia National Laboratories

Behavior of core-shell silica/polymer particles in toluene

(data shown for 284 nm silica core and 20 nm SP/MMA polymer shell containing 20 mol % of SP molecules)

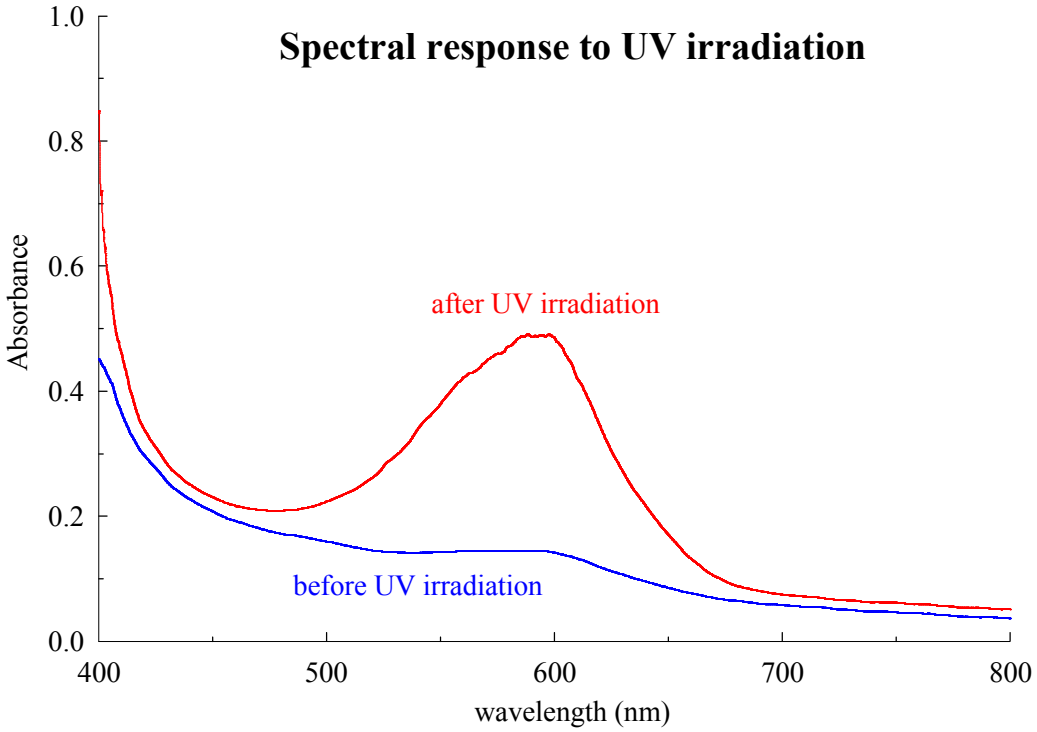

Photo-induced aggregation

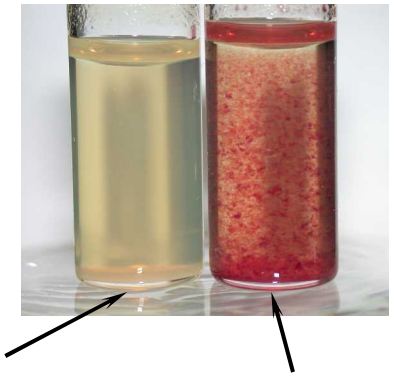

before UV
particles well dispersed with SP molecules in closed, non-polar form

after UV
particles aggregate and sediment with SP molecules in more polar, open form

– aggregation induced in < 1min by λ=366 nm light from a hand-held lamp

– particles easily re-disperse upon shaking after visible light irradiation (λ>420 nm) or heating

Sandia National Laboratories

Wetting of SPMMA monolayers versus SPMMA-*co*-MMA (20% SP) polymers

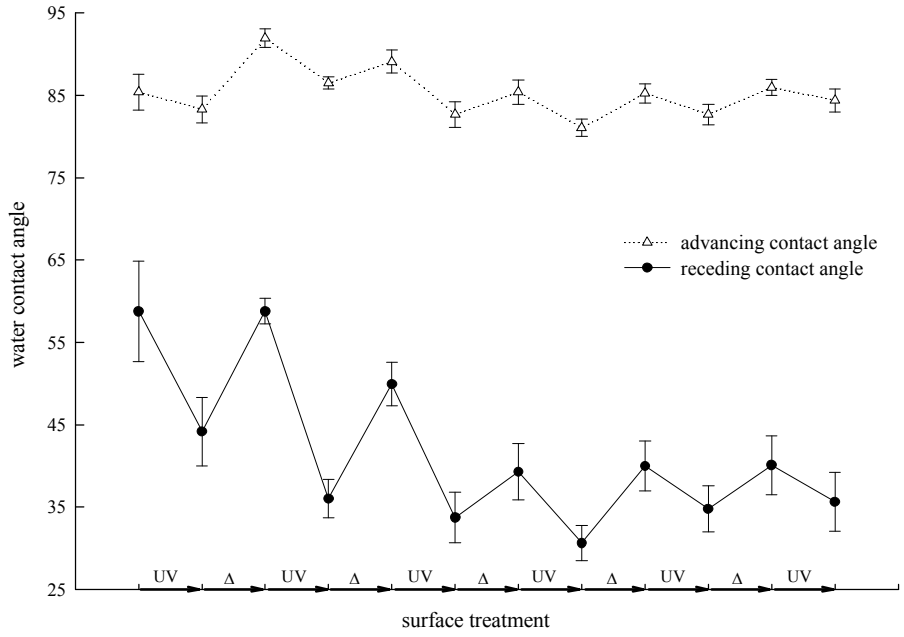

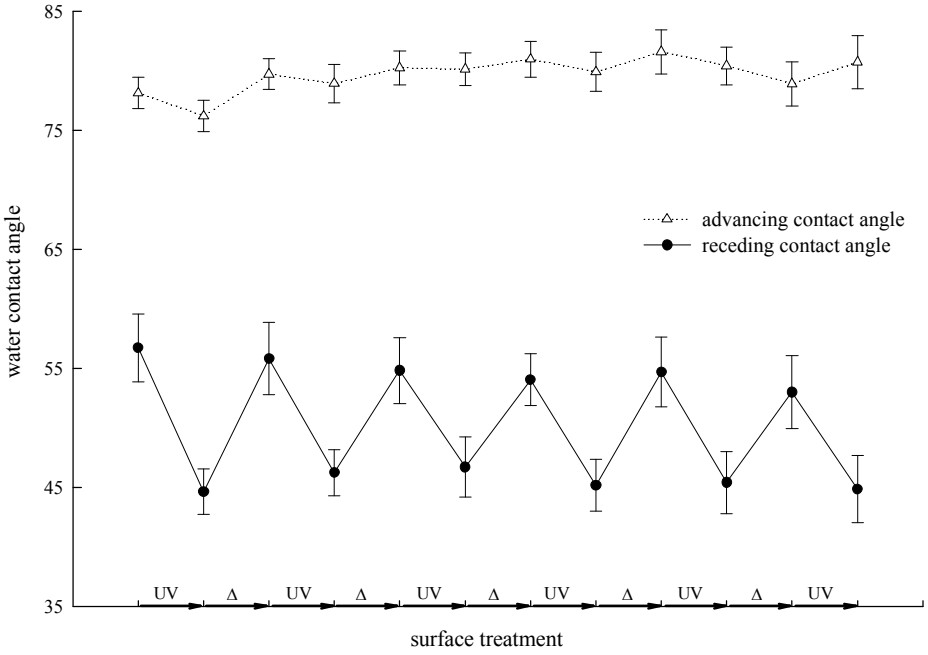

✓ Loss of switching ability is prevented by using polymeric layers instead of organic monolayers.

Sandia National Laboratories

Photo-control of viscosity in colloidal systems

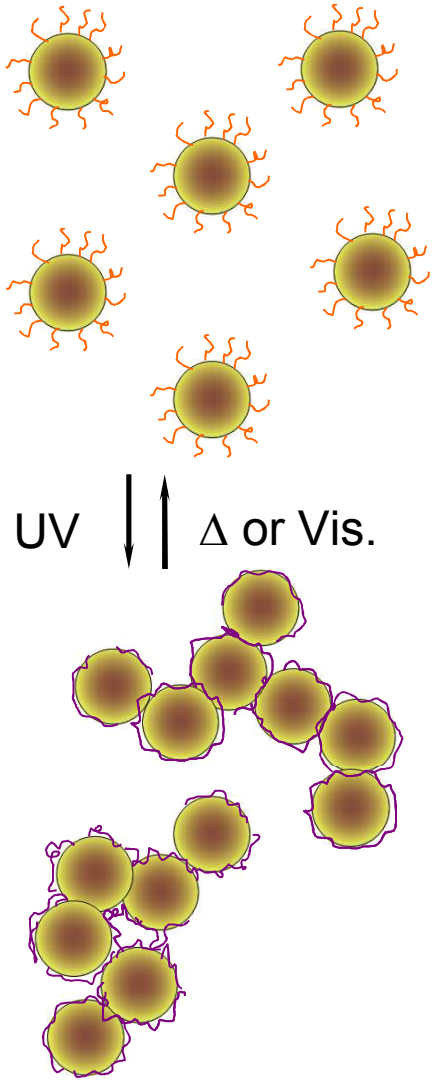

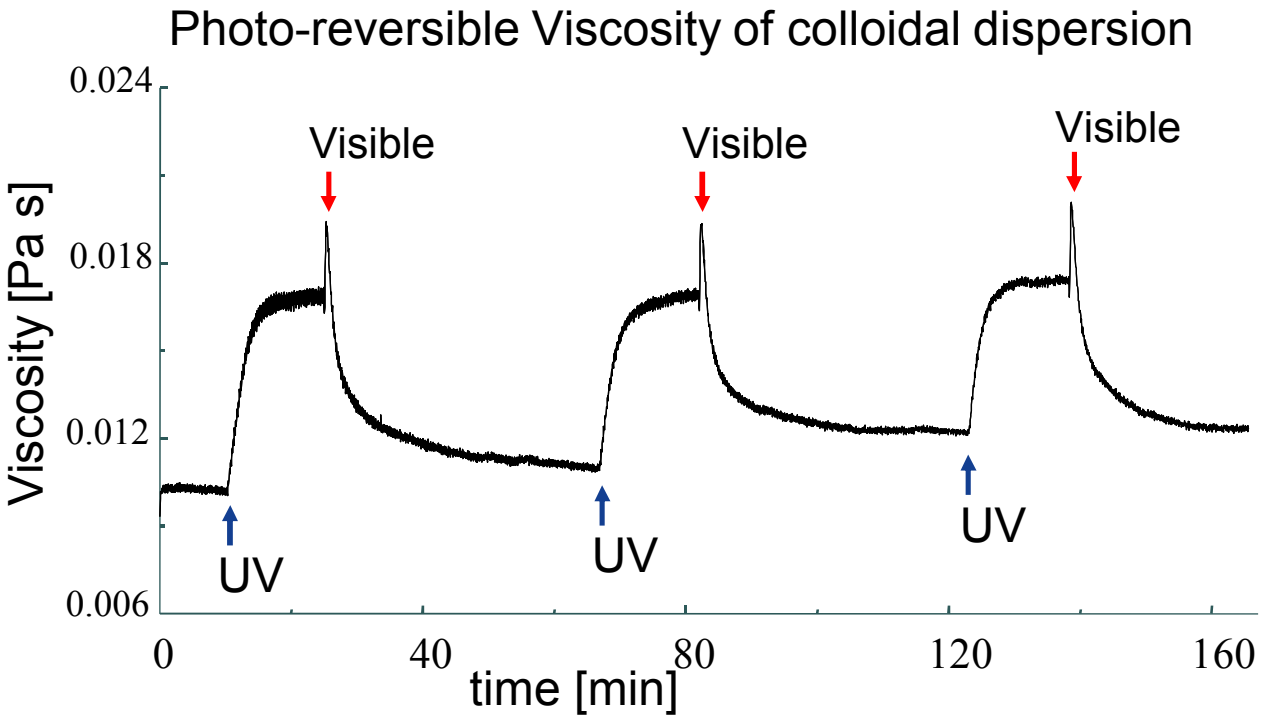

1 μm SP/MMA modified colloids (20% SP) in toluene at ~30 vol.%

Photo-control of colloidal interactions, CINT Workshop Poster, Martin Piech and Nelson S. Bell (Sandia National Laboratories, NM), Paul Braun and Matthew George (University of Illinois at Urbana-Champaign)

Effects of photo-isomerization on SP/MMA polymers

- Free SP/MMA polymers reduce solution viscosity upon UV irradiation due to polymer chain shrinkage (Irie *et al.*, Golburt *et al.*)
- Chain shrinkage is most pronounced in non-polar solvents (*e.g.*, toluene) and disappears in polar media (*e.g.*, dichloroethane)
- Process caused by specific intramolecular solvation of polar merocyanine form by MMA ester side groups in competition with solvation by solvent
- Polymer shrinkage also demonstrated on flat surfaces by as much as 30 nm for 45 nm thick films in non-polar solvents (Ito, *et al.*)

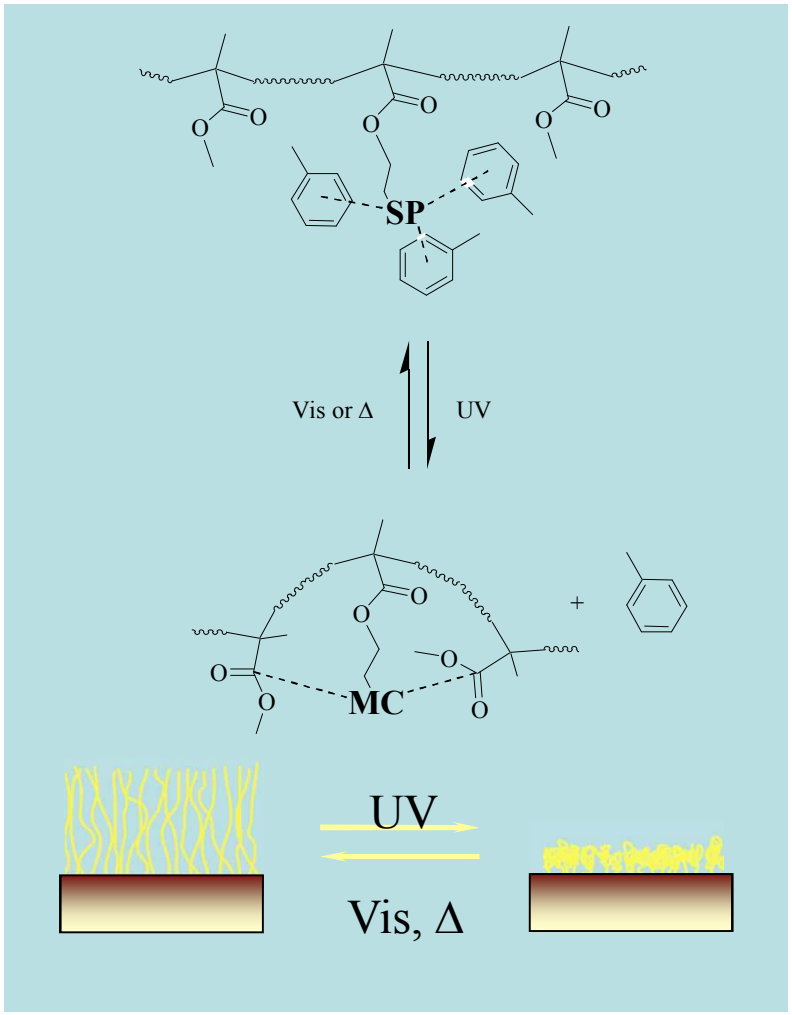

Effects of Photo-Isomerization on Spiropyran Monolayers

- Spyrobenzopyran monolayers on flat surfaces demonstrate reversible wettability change
- Contact angle altered by as much as 13° (Garcia, *et al.*)
- Colloidal particles covered with SP monolayers and dispersed in non-polar solvents undergo reversible aggregation (Ichimura, *et al.*)
- Change brought about by marked polarity difference between closed SP and open ME forms

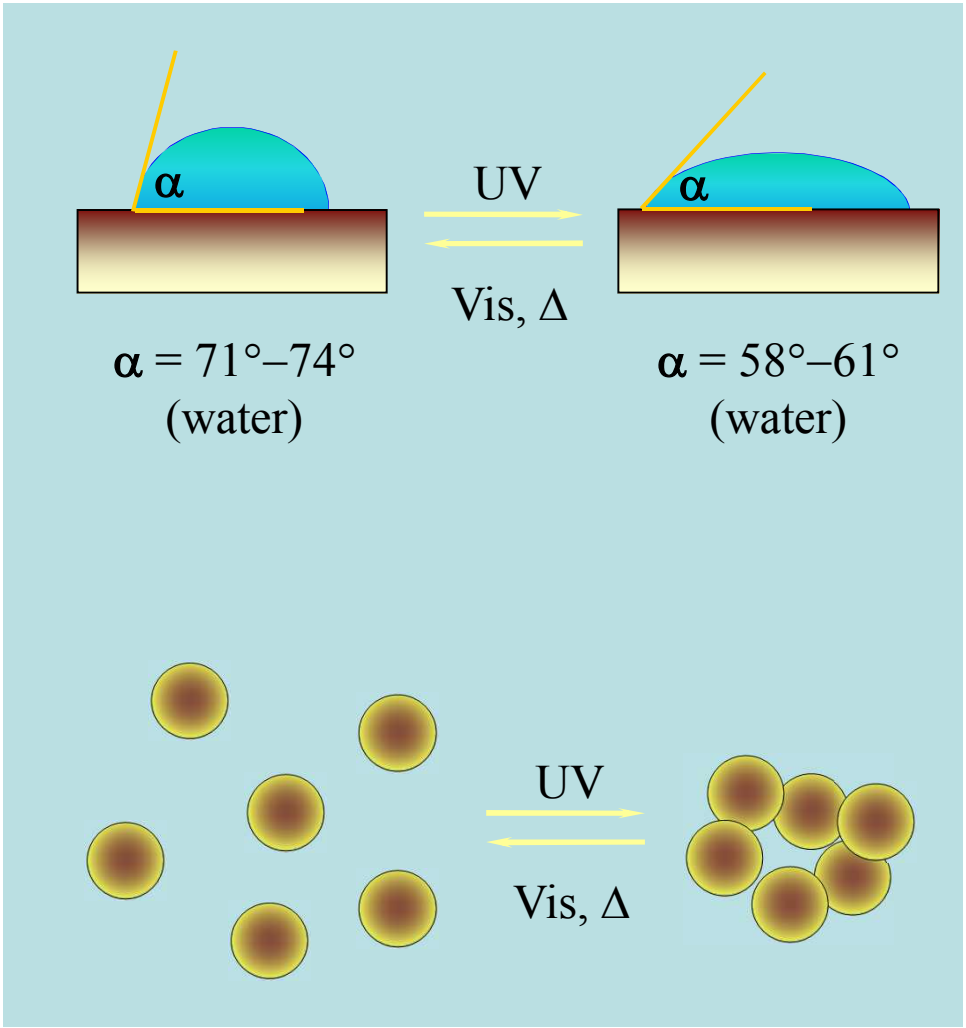

Sandia National Laboratories

UV-Vis Characterization

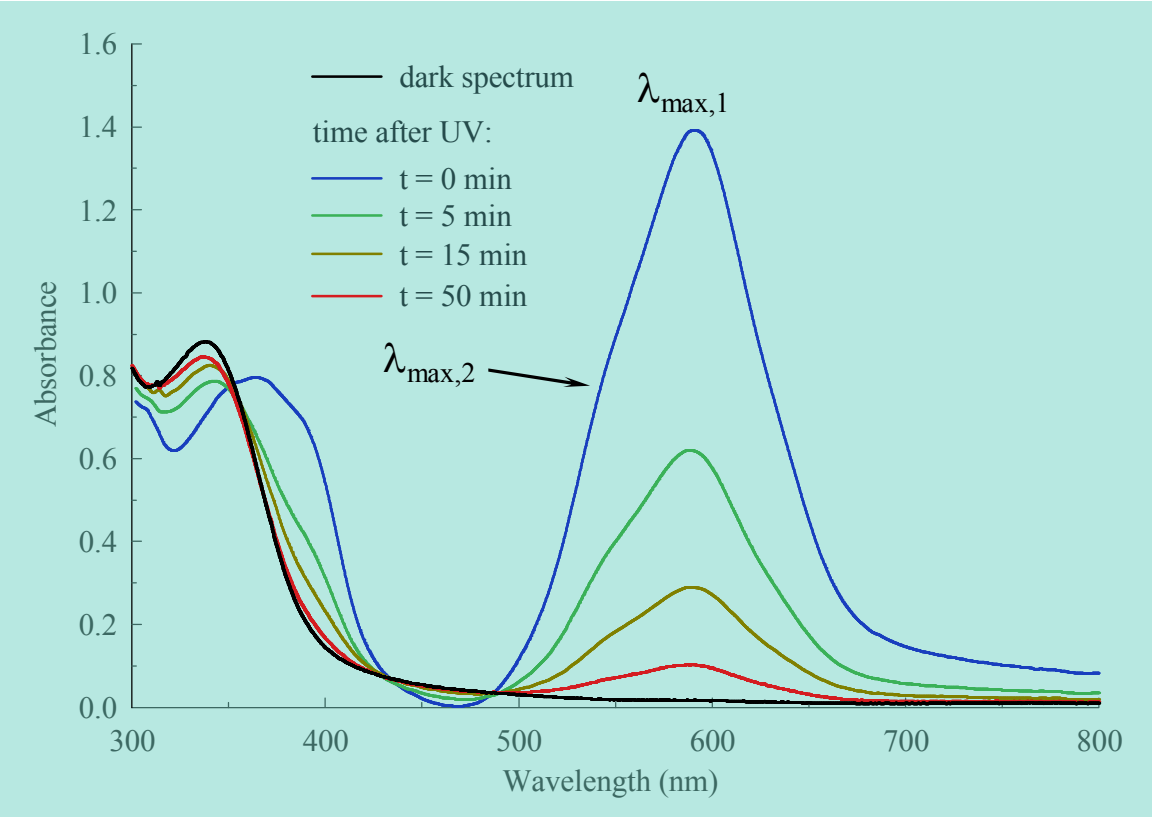

Spectrum of 20% SP / 80% MMA polymer attached to 1 μm SiO_2 colloids at concentration of 0.079% wt/wt in THF

- $\lambda_{max,1}$ = 589 nm due to ME
- $\lambda_{max,2} \approx$ 550 nm due to ME-SP aggregates
- identical spectra obtained for attached and free polymers
- SP monomer shows only $\lambda_{max,1}$ = 587 nm due ME
- SP micro-environment within SP/MMA polymers favors ME-SP aggregation

Sandia National Laboratories

UV-Vis Characterization

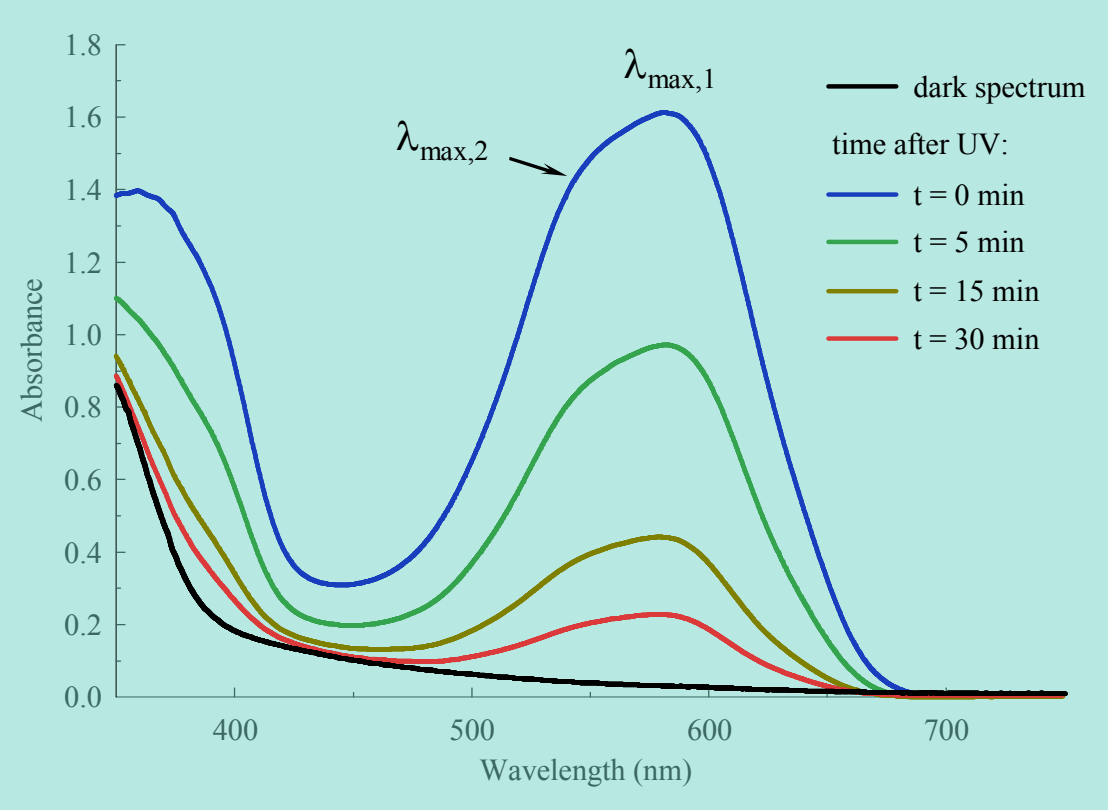

Spectrum of 20% SP / 80% MMA polymer attached to 1 μm SiO_2 colloids at concentration of 0.20% wt/wt in toluene

- $\lambda_{max,1}$ = 581 nm due to ME
- $\lambda_{max,2}$ ≈ 545 nm due to ME-SP aggregates
- $\lambda_{max,1}$ diminished relative to $\lambda_{max,2}$ in toluene compared to THF
- This points to better ME solvation by THF vs. toluene
- $\lambda_{max,1}$ and $\lambda_{max,2}$ blue shifted in toluene compared to THF
- This points to more polar ME micro-environment in toluene vs. THF

Sandia National Laboratories

Sedimentation in different solvents

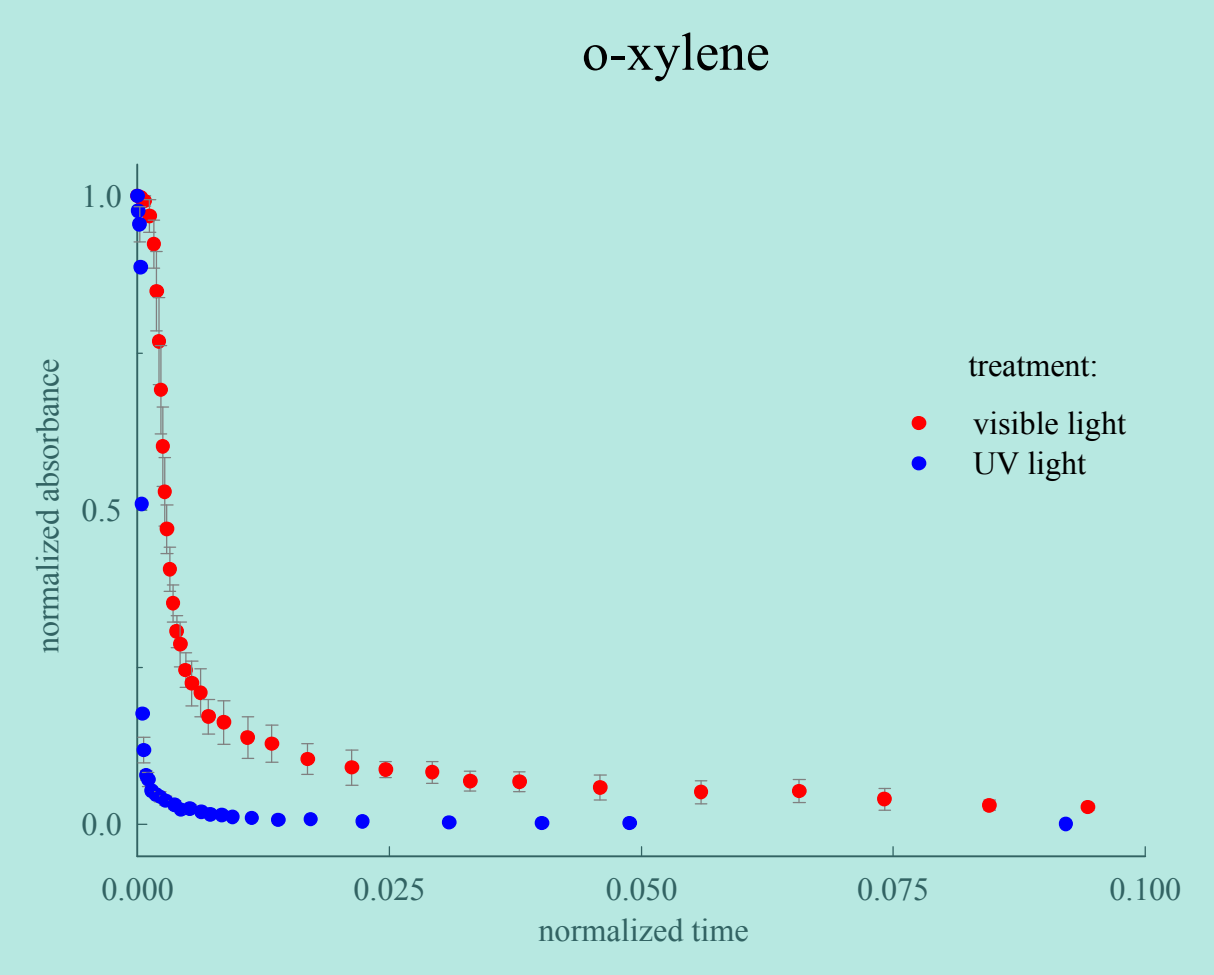

- Surface Layers contain 20 mol% spirobenzopyran molecules in PMMA shell.
- Time axis normalized by theoretical sedimentation time
- Decrease in solvent polarity causes stronger aggregation
- UV irradiation precipitates stronger aggregation in in border-line solvents

Sandia National Laboratories

Sedimentation with different spiropyran content particles

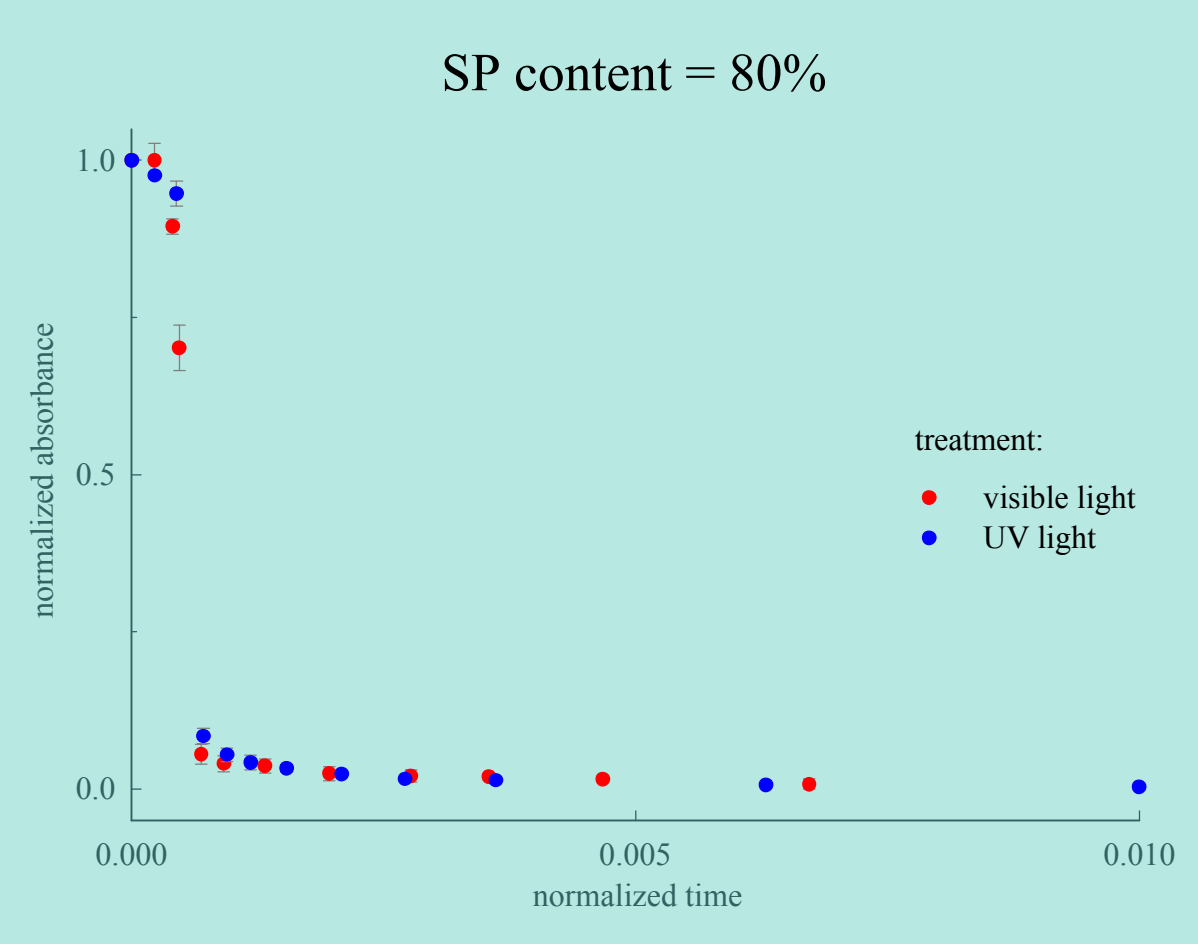

- Sedimentation studied in toluene solvent for each SP concentration
- Increase in SP content causes stronger aggregation
- UV irradiation precipitates stronger aggregation in in border-line solvents

Sandia National Laboratories

Sediment Comparison via SEM

No UV exposure

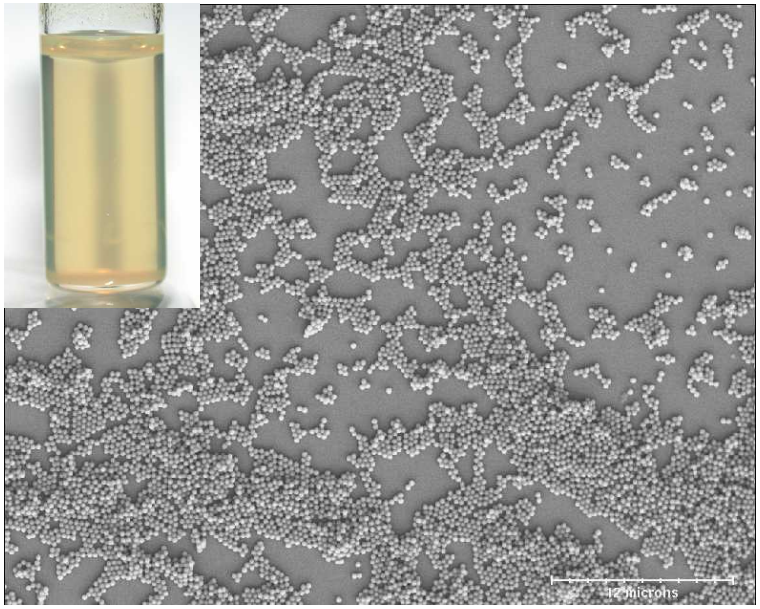

After 1 min UV irradiation (λ=366 nm)

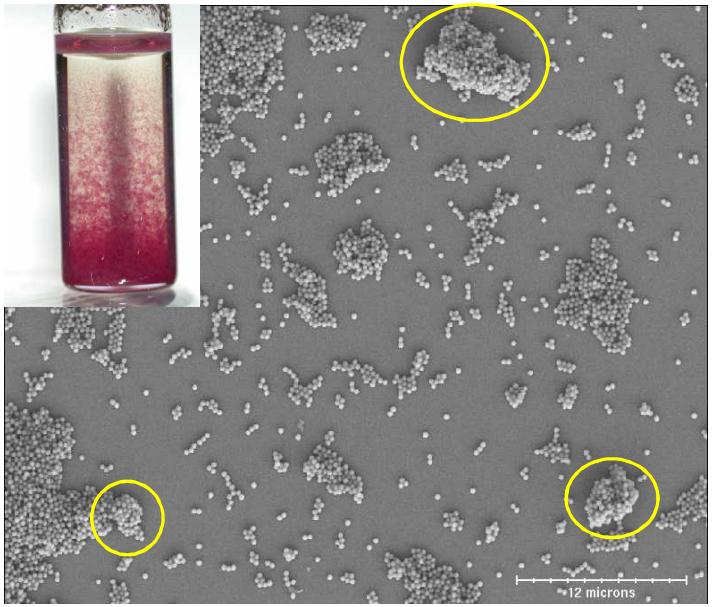

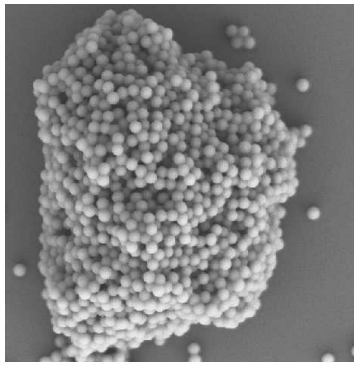

- particles form well spread mono- and multi-layers
- predominant hexagonally packed domains

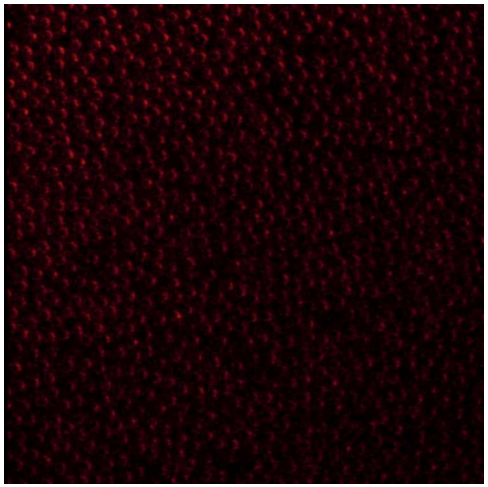

- larger aggregates present in addition to mono- and multi-layers
- aggregates characterized by random particle packing

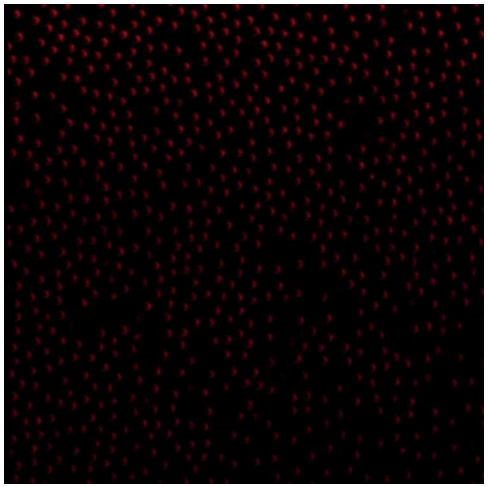

2D Photo-defined Colloidal Adsorption

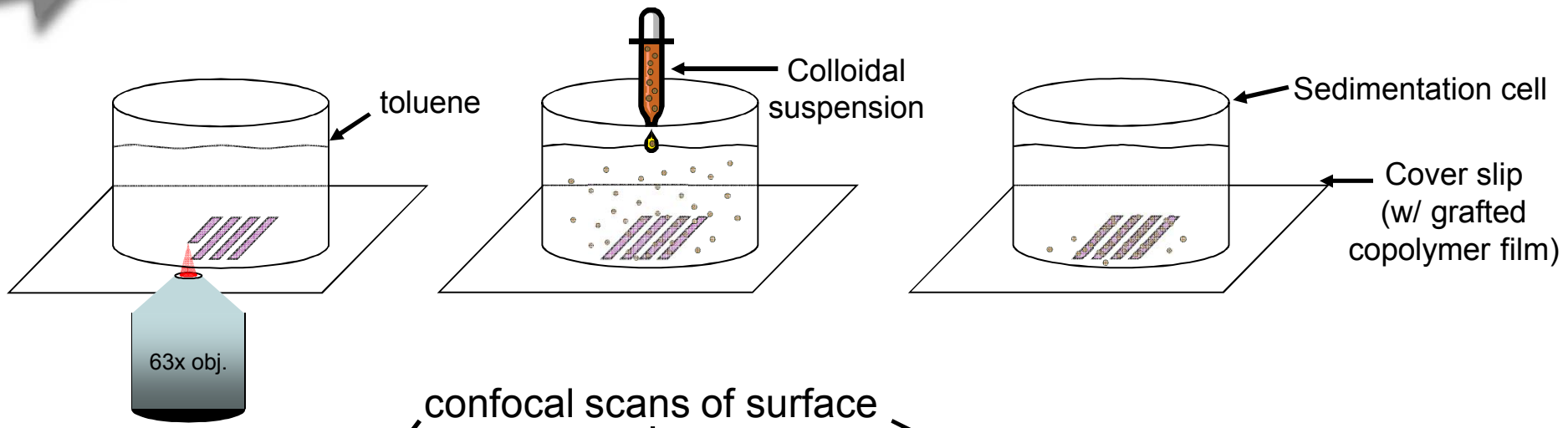

confocal scans of surface

2D patterning example

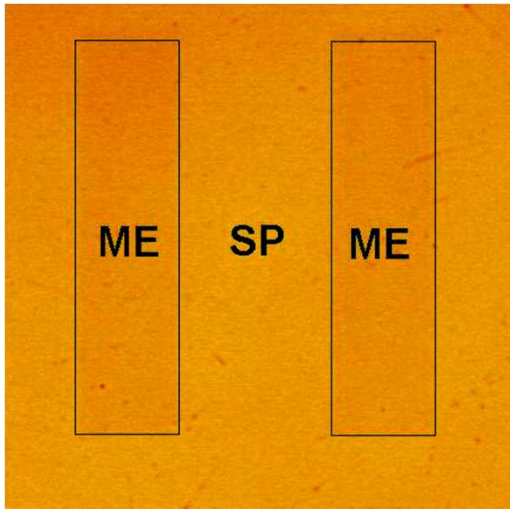

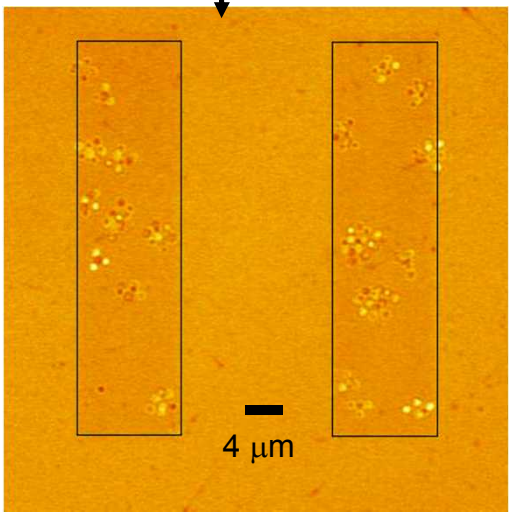

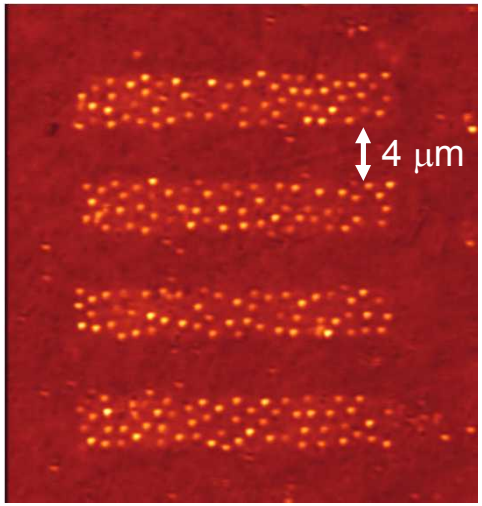

exp. start, t = 0

clusters, t = 660 s

M. Piech, M. C. George, N. S. Bell and P. V. Braun:, *Langmuir*, **22**, 1379-1382 (2006)

Photo-Actuated Deposition in Toluene

SPMMA-*co*-MMA coated glass slide in toluene

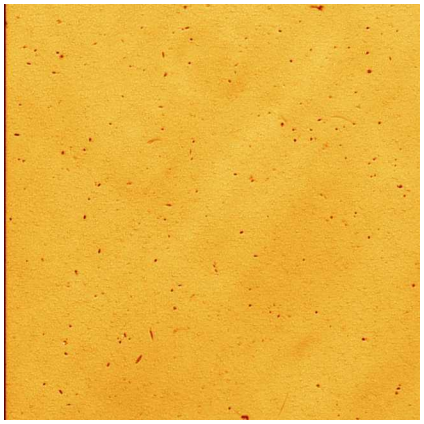

Photo-isomerizing SP in dark regions

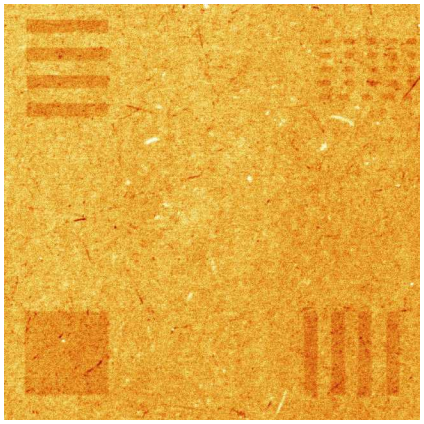

After settling dilute colloidal suspension

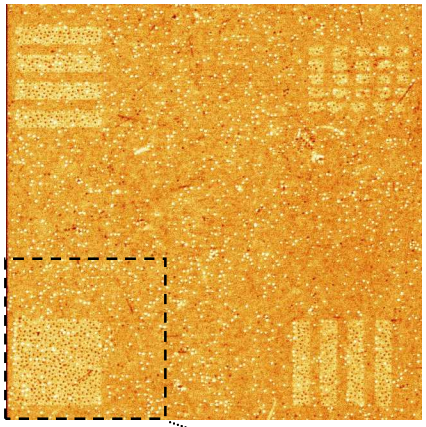

After drying

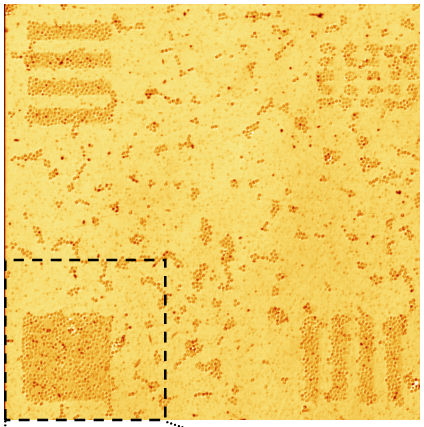

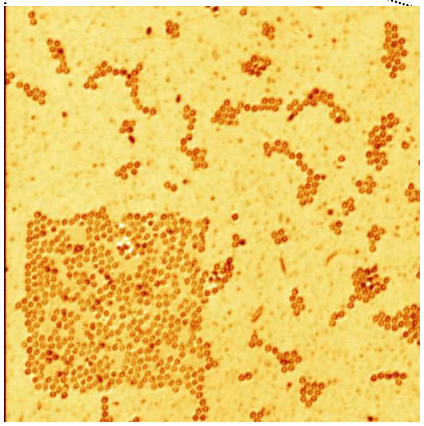

particle adsorption kinetics

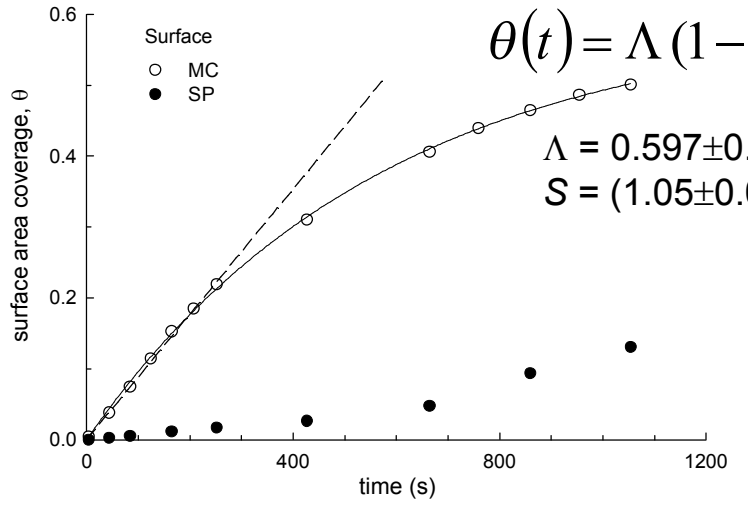

$$\theta(t) = \Lambda\left(1 - e^{-S\,t/\Lambda}\right)$$

Λ = 0.597±0.007,
S = (1.05±0.02)×10^{-3} s^{-1}

The deposition behavior falls between random sequential adsorption and ballistic deposition models, with a time constant near the sedimentation rate.

Sandia National Laboratories

Kinetics of photo-actuated deposition

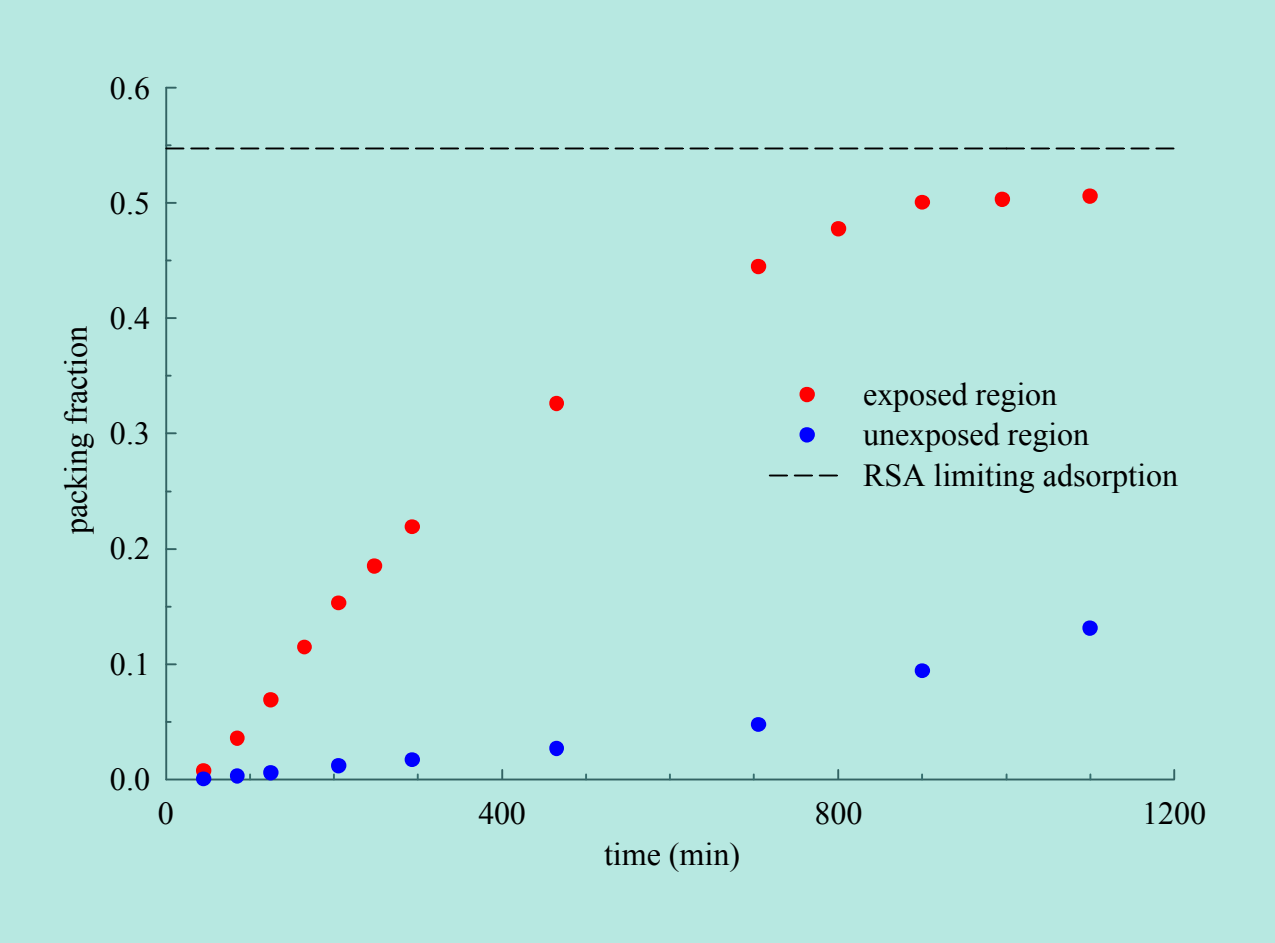

- Initially particles adsorb 14× more selectively to the exposed regions containing ME

- Following rinsing and drying particle density is 10× higher in exposed regions

Sandia National Laboratories

3D laser gel-writing in colloidal sediments

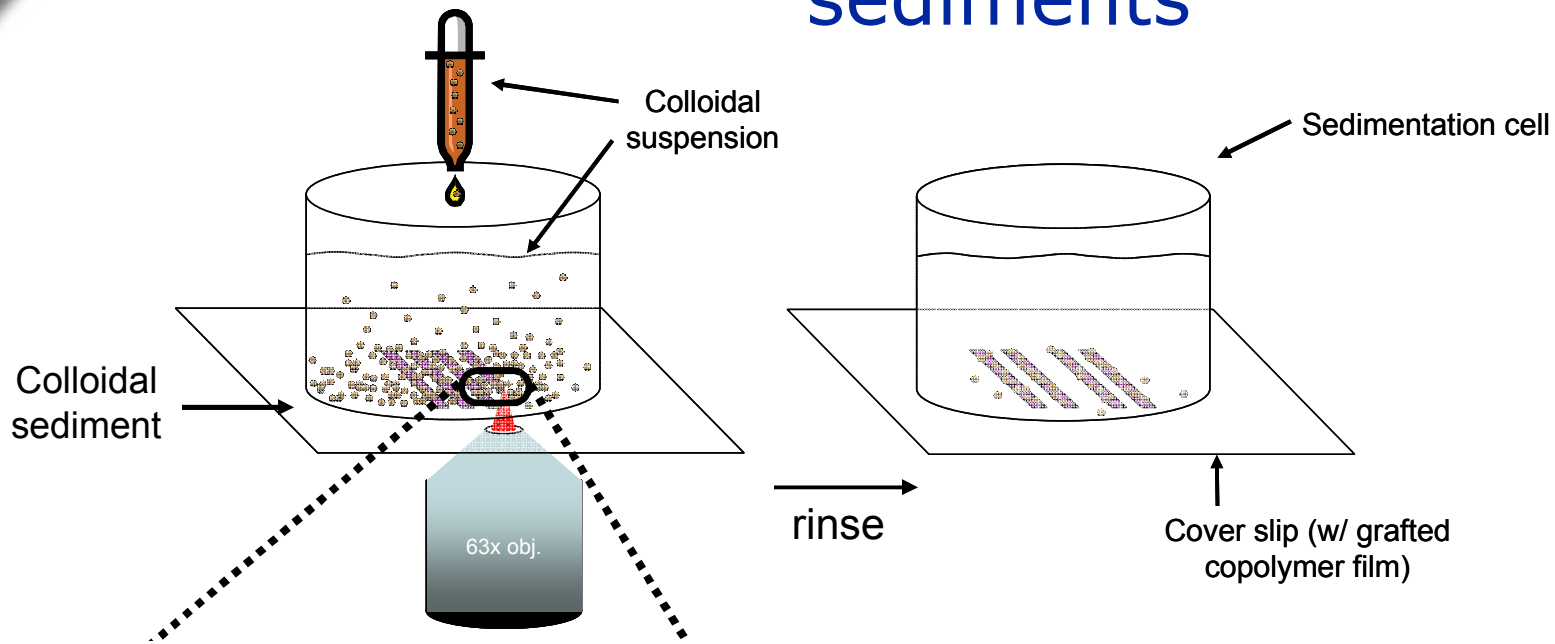

Photo-Patterned Colloidal Gel Micro-channels

Processing Steps

- Introduce colloids, form sediment
- Write walls (via 2PA)
- Write channel top
- Rinse out un-gelled colloids

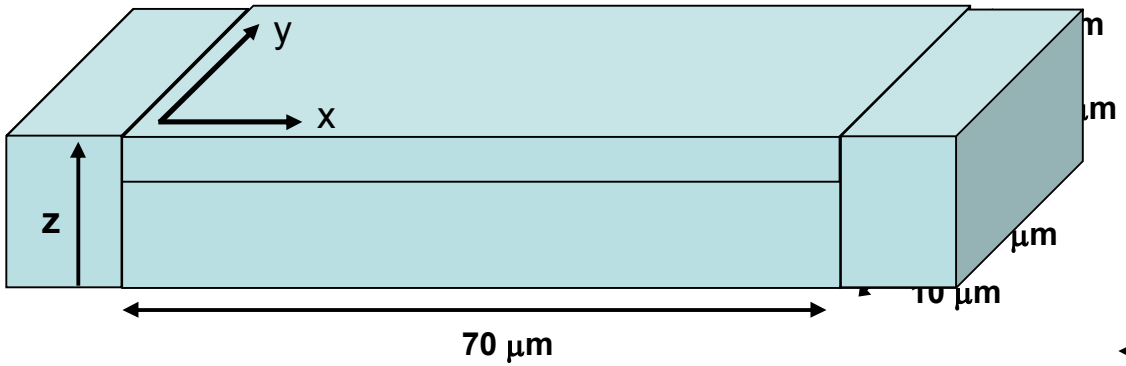

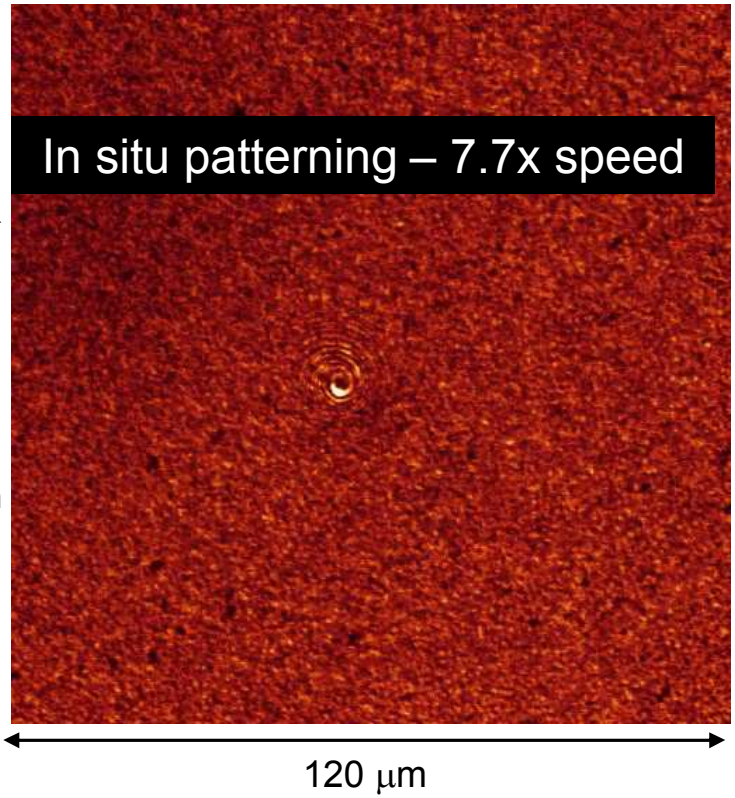

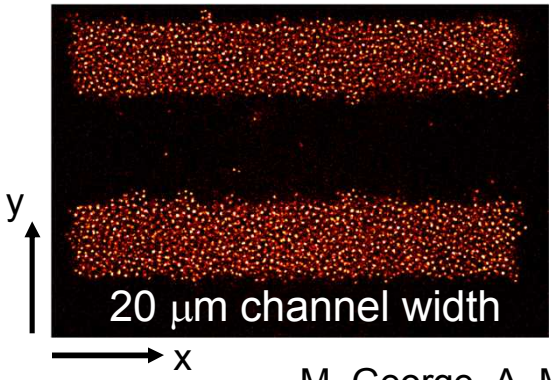

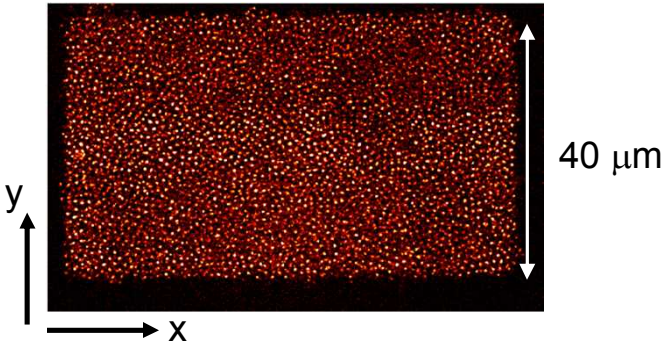

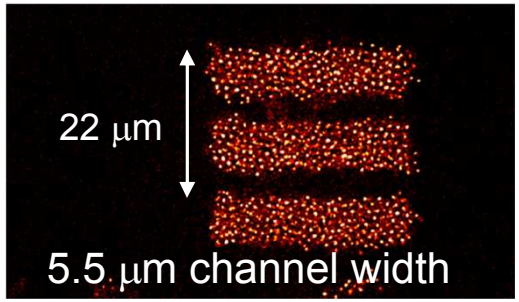

M. George, A. Mohraz, M. Piech, N. Bell, J. Lewis, and P. Braun (unpublished work)

Photo-Patterned Colloidal Gel Micro-cavity

confocal xy reflectance sections

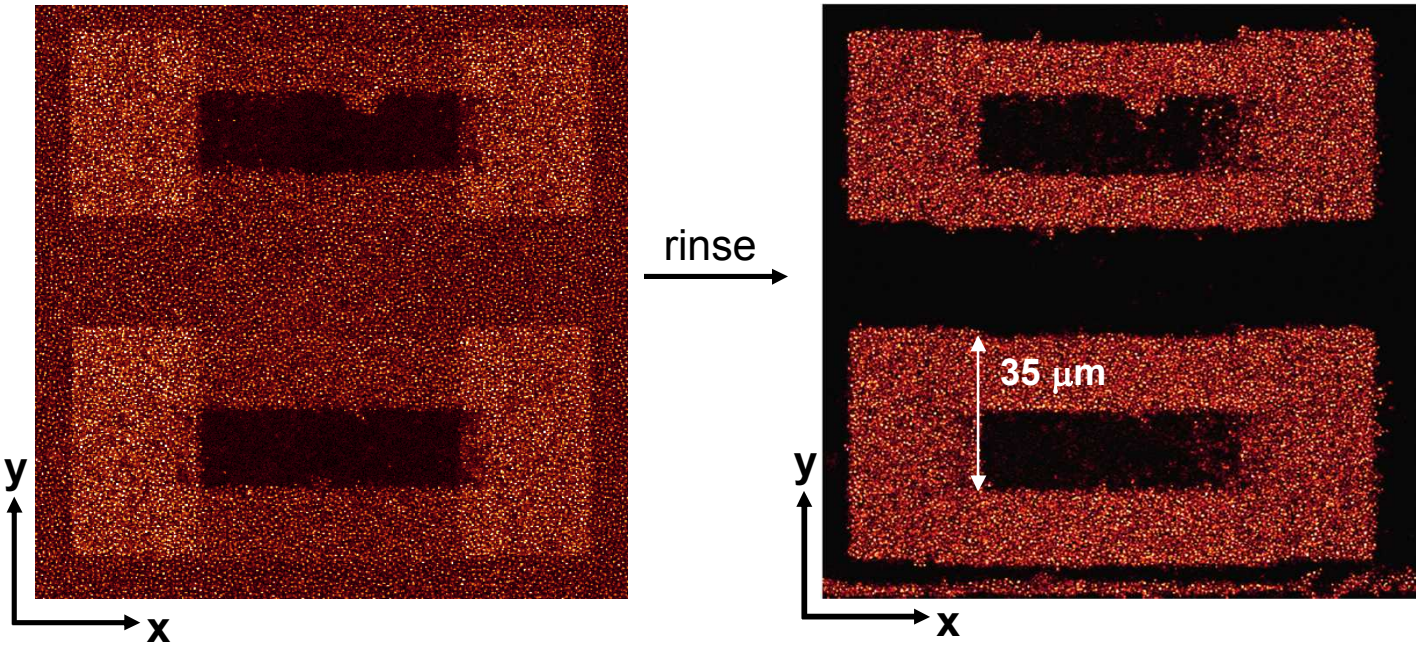

confocal reflectance cross-sections (xz)

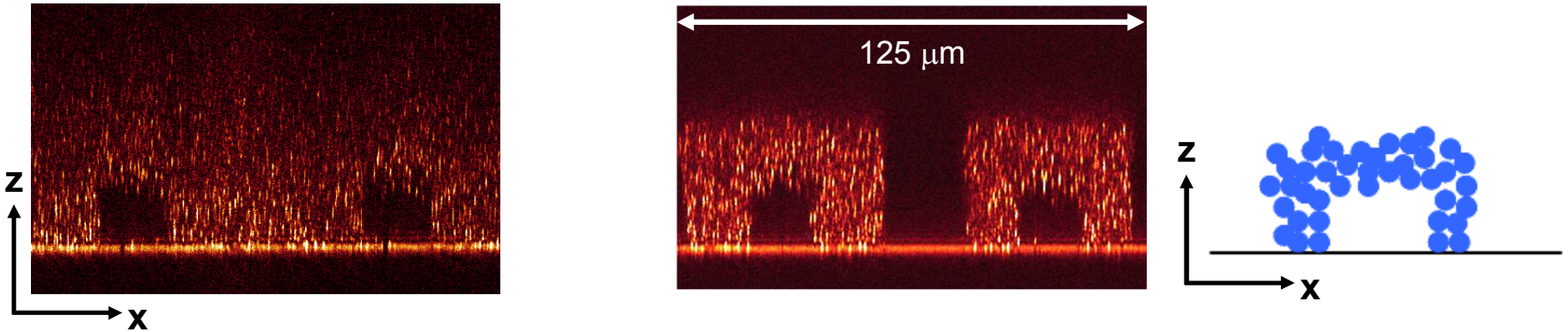

Trapped Colloidal Particles

<u>Processing Steps</u>

- form a colloidal sediment
- Write walls (via 2PA)
- Write channel top
- Rinse out un-gelled colloids
- Observe Brownian motion of contained colloids

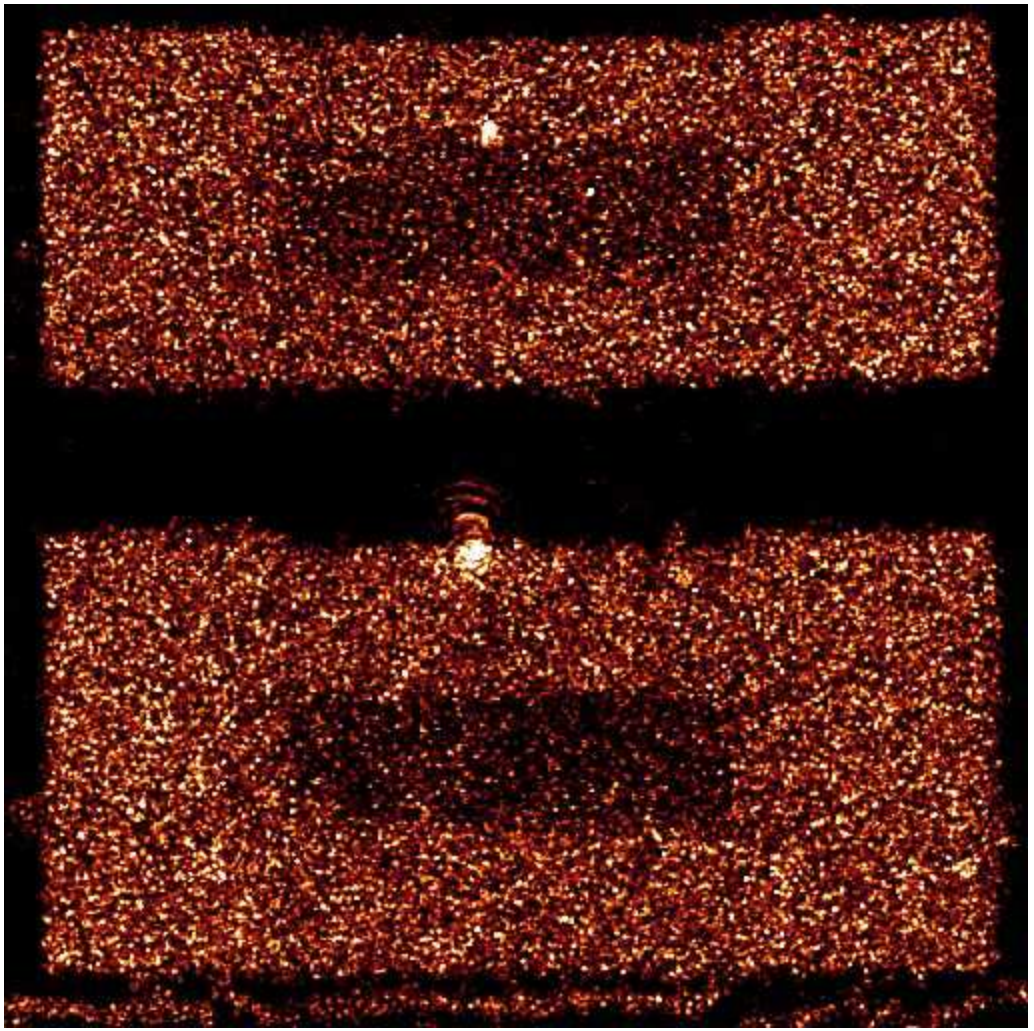

Conclusions

1. Photochromic molecules show the capability to influence macroscopic phenomena
2. Changes in optical and surface energy of modified surfaces have been detected by UV/VIS and contact angle measurements, respectively.
3. Modeling of Surface Energy Parameters gives greater insight into the mechanisms of surface energy control and allows screening of systems to generate desired photowetting effects.
4. A colloidal system has demonstrated reversible aggregation and dispersion phenomena.
5. Polymer layers show greater cycle lifetime than monolayers.
6. Chromophoric molecules act as dopants in modifying polymer behavior and show promise for more application.

Fundamental Study of Crystallization and Morphology

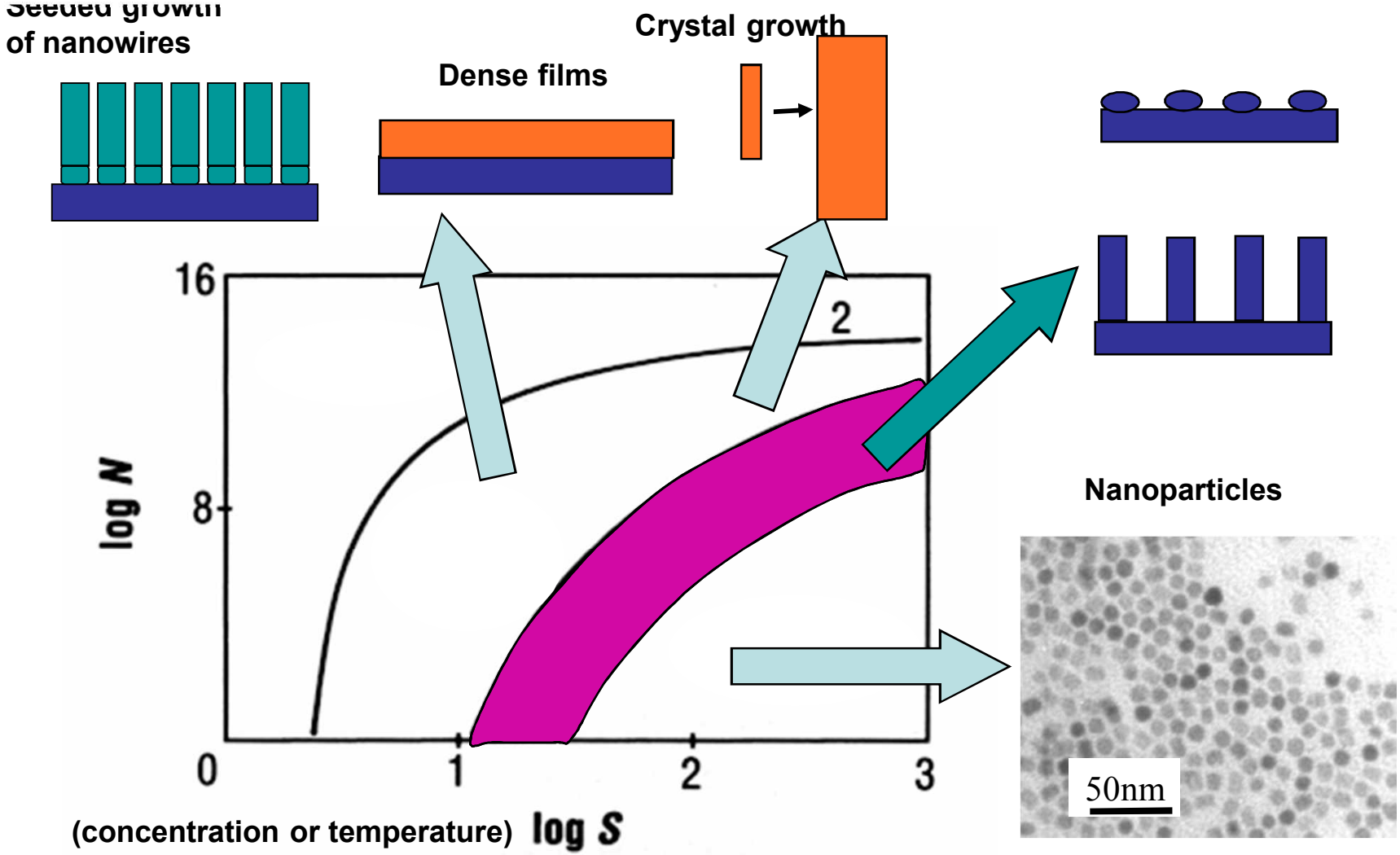

(Bunker et al. Science, 264, 48, 1993)

Stepwise Growth of Complex Nanostructures

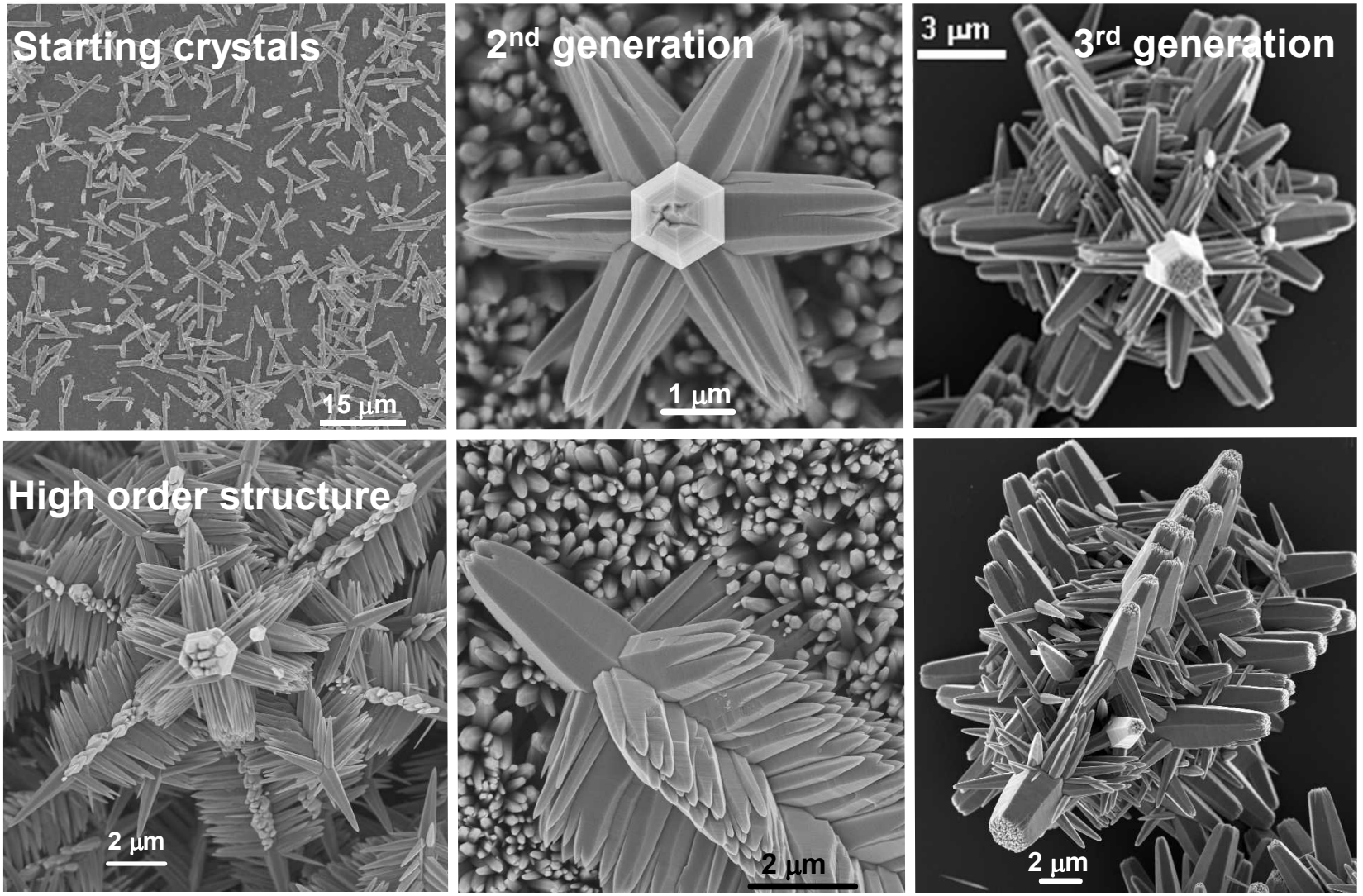

Synthesis of ZnO Nanoparticles and Morphological Control

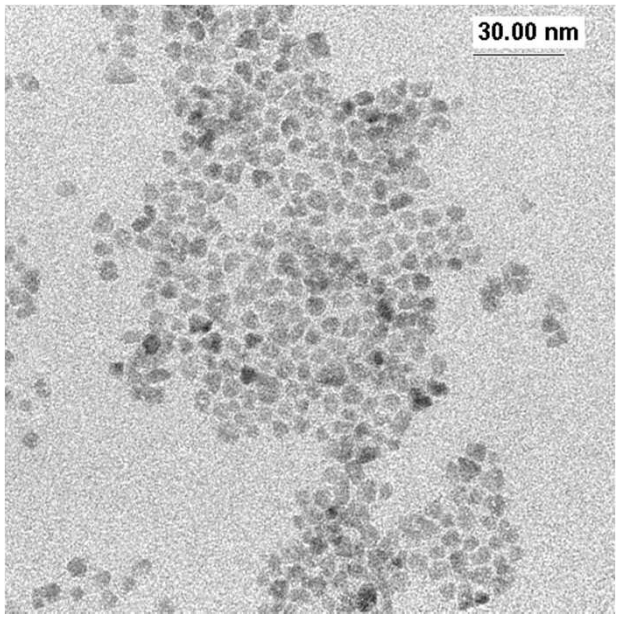

Solvothermal annealing at 90 or 120 ºC promotes the development of nanorods via Ostwald ripening.

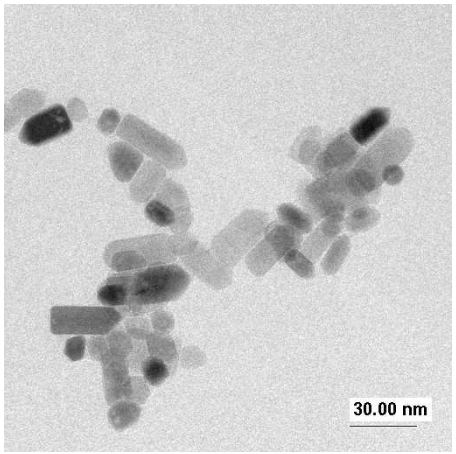

12 hours

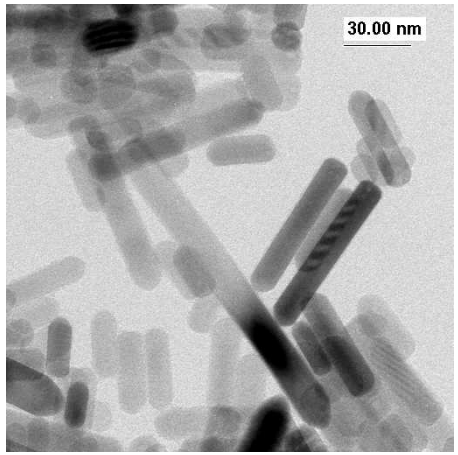

112 hours

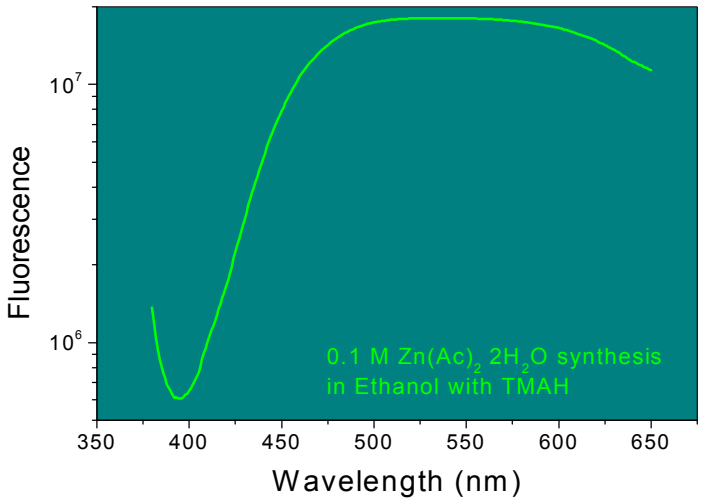

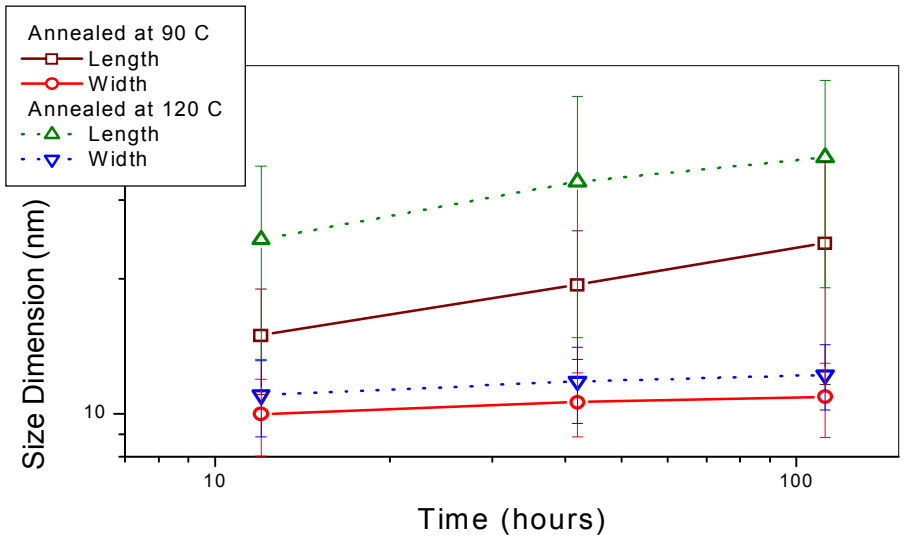

Doping ZnO for Varying Optical Properties
Aqueous Solution Chemistry

Zinc speciation (aqueous)

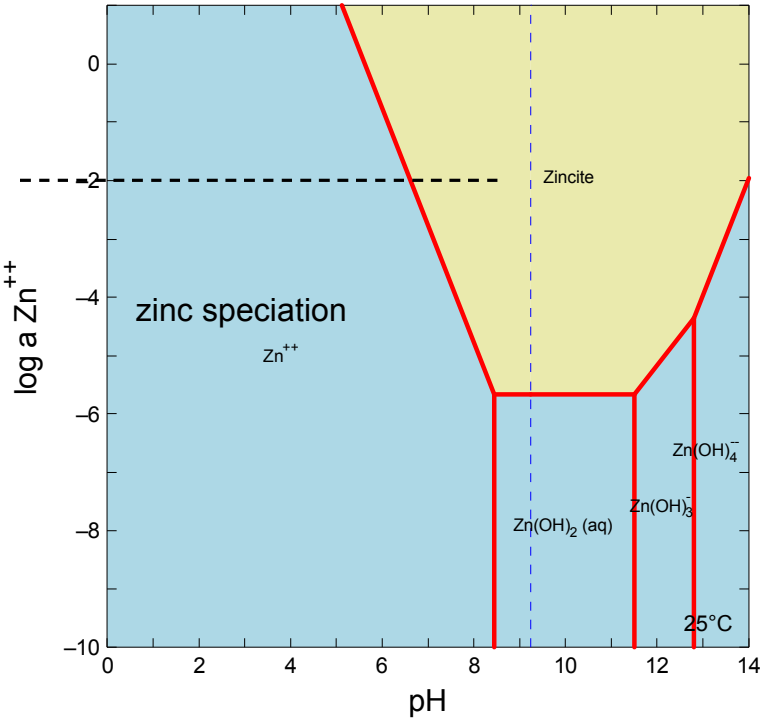

Magnesium speciation (aqueous)

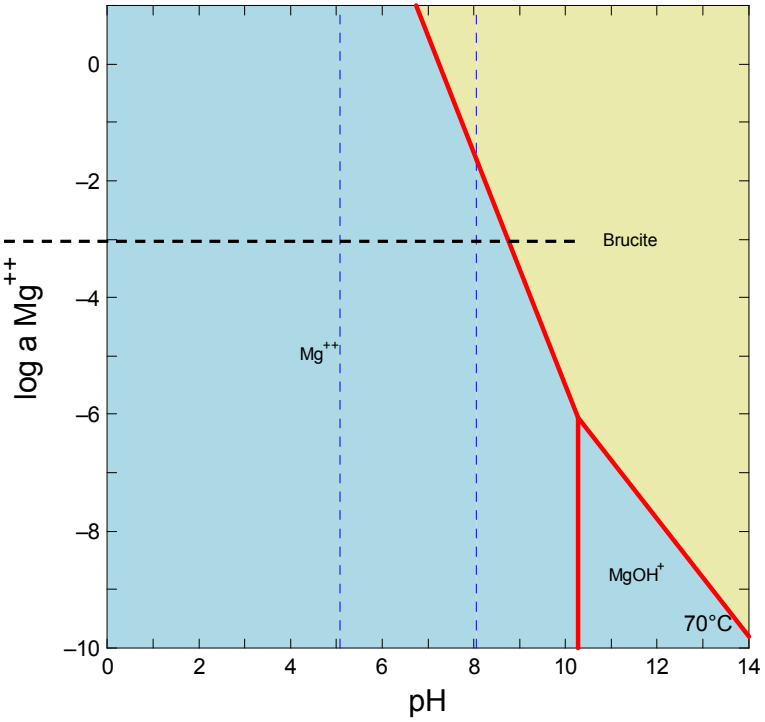

XRD Characterization of ZnO With 20 mol% Mg Doping

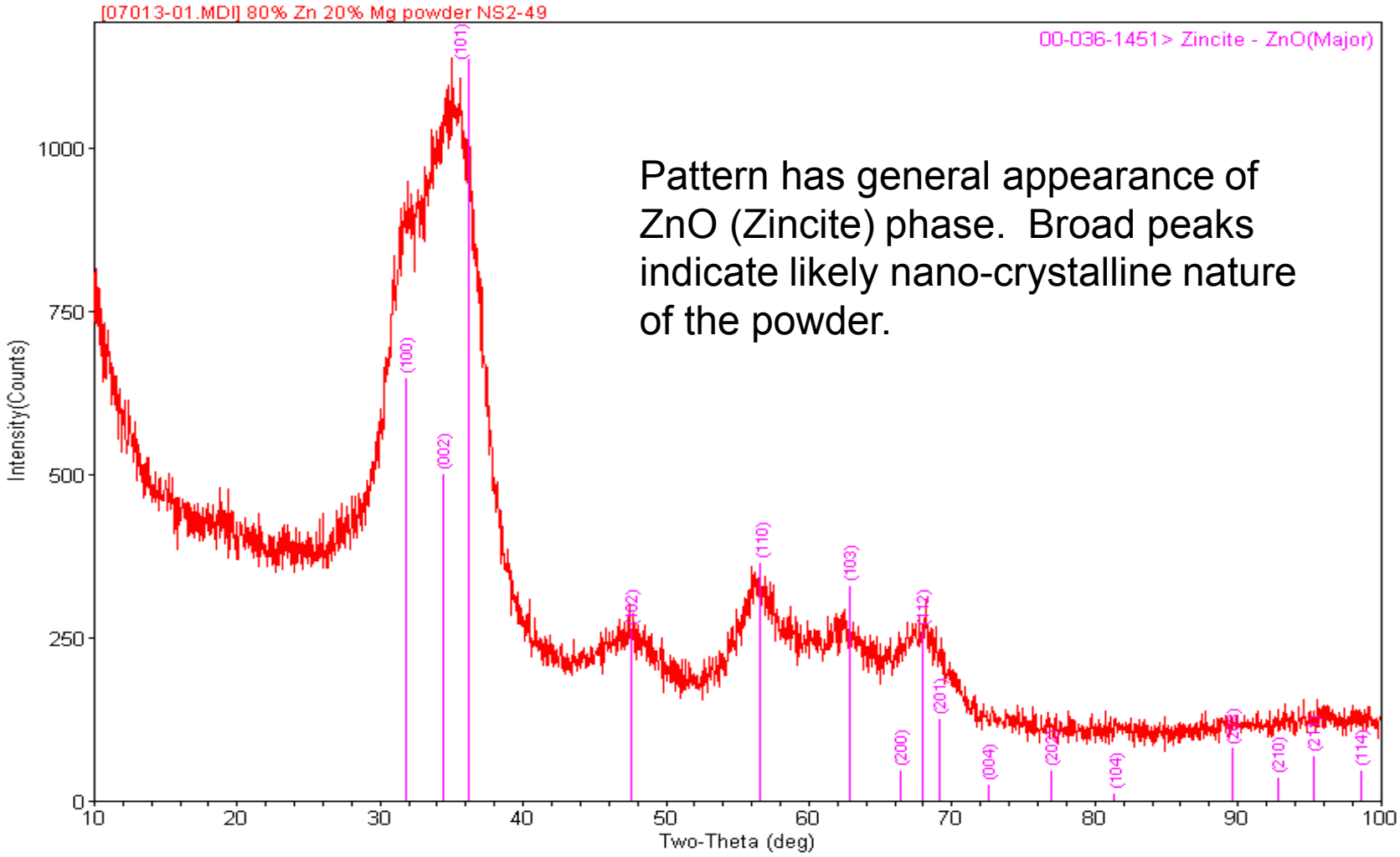

Pattern has general appearance of ZnO (Zincite) phase. Broad peaks indicate likely nano-crystalline nature of the powder.

TEM Characterization of Crystal Size
10 Mol% Mg doping of ZnO

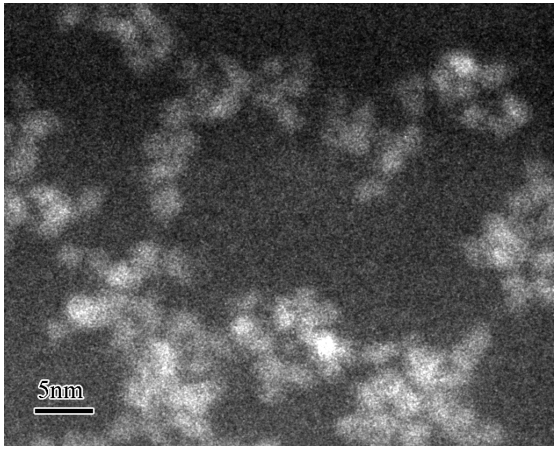

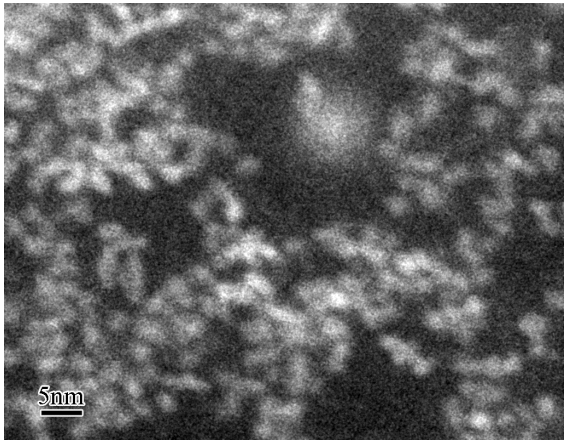

Z-contrast annular dark field (ADF) images showing 4-5nm ZnO particles.

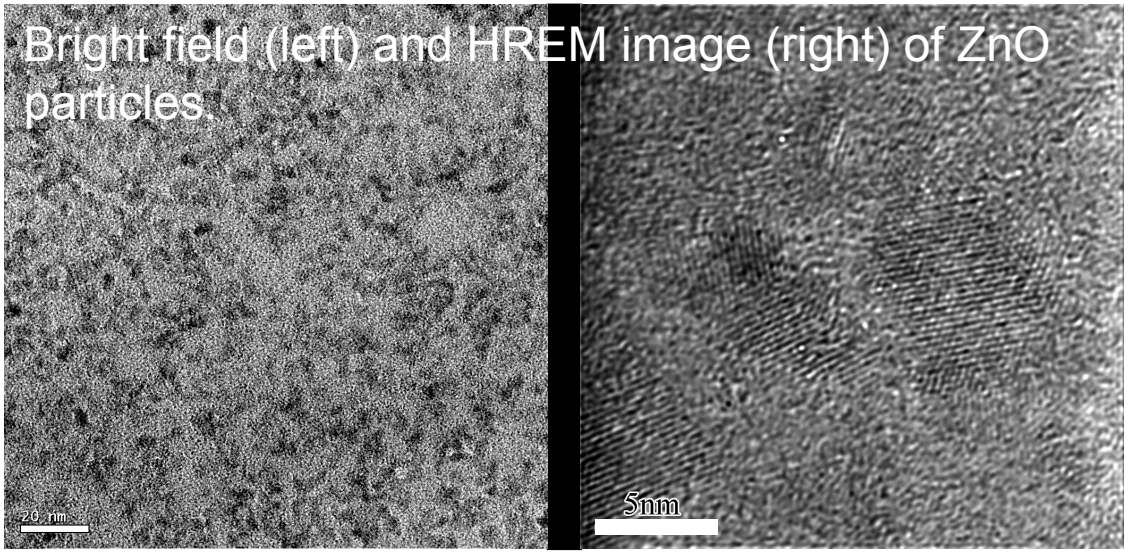

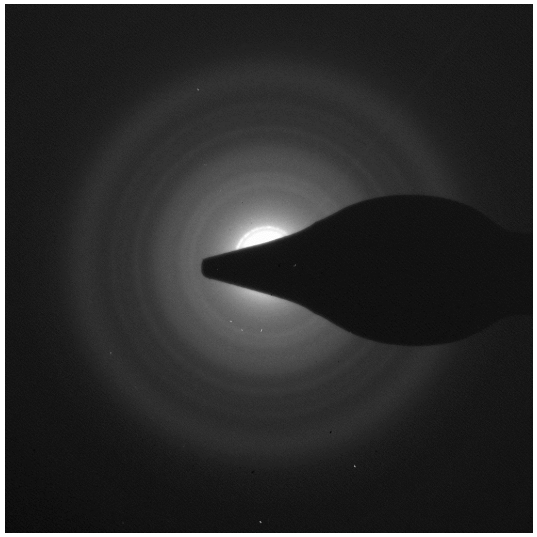

Selected Area Diffraction Pattern from ZnO particles.

Absorption Edge shifting by Mg Doping in ZnO Nanoparticles

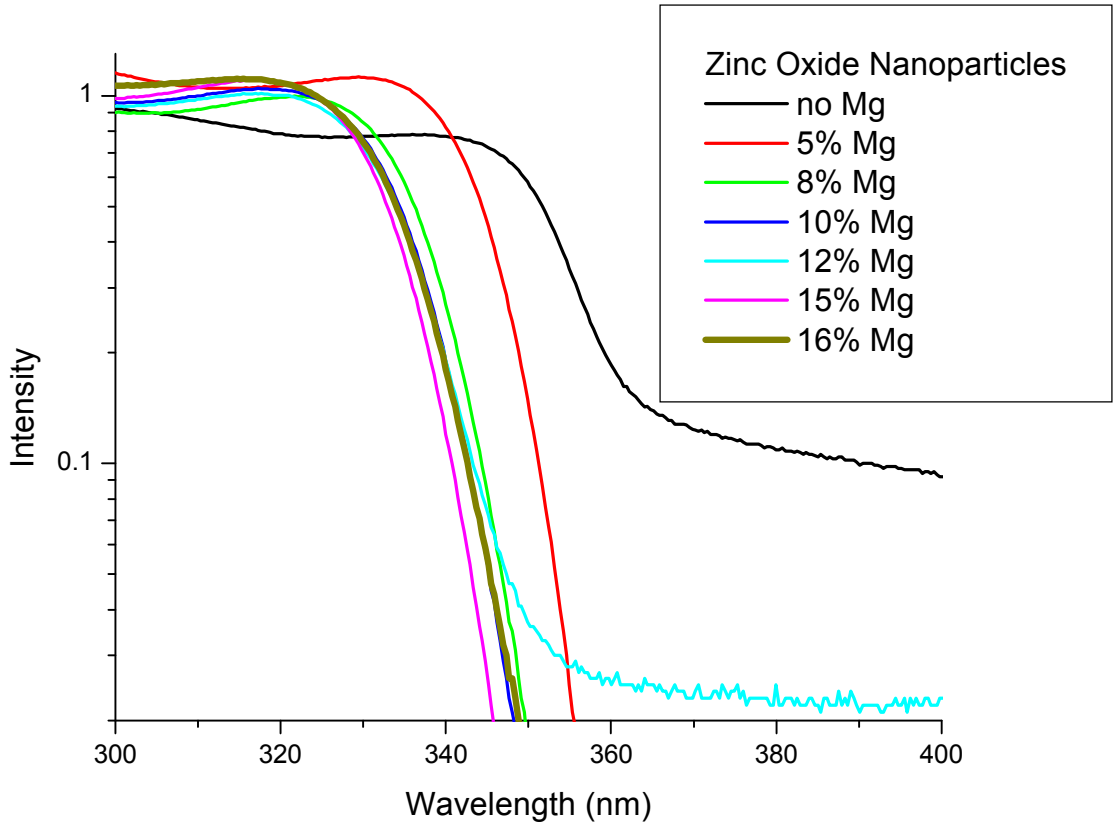

The maximum doping level appears to be 15 mol% at room temperature.

Mg Doping of Zinc Oxide

- Mg acetate does dope ZnO in the sol-gel synthesis technique
- Kinetics are affected leading to quantum confinement
- doping and Q-confinement effects shift the adsorption edge in a non-linear fashion.
- Maximum dopant for colloidal stability is 15 mol%.

Microfluidic Synthesis Motivation

Phase stability and morphology of nanoparticles is thermally and compositionally controlled

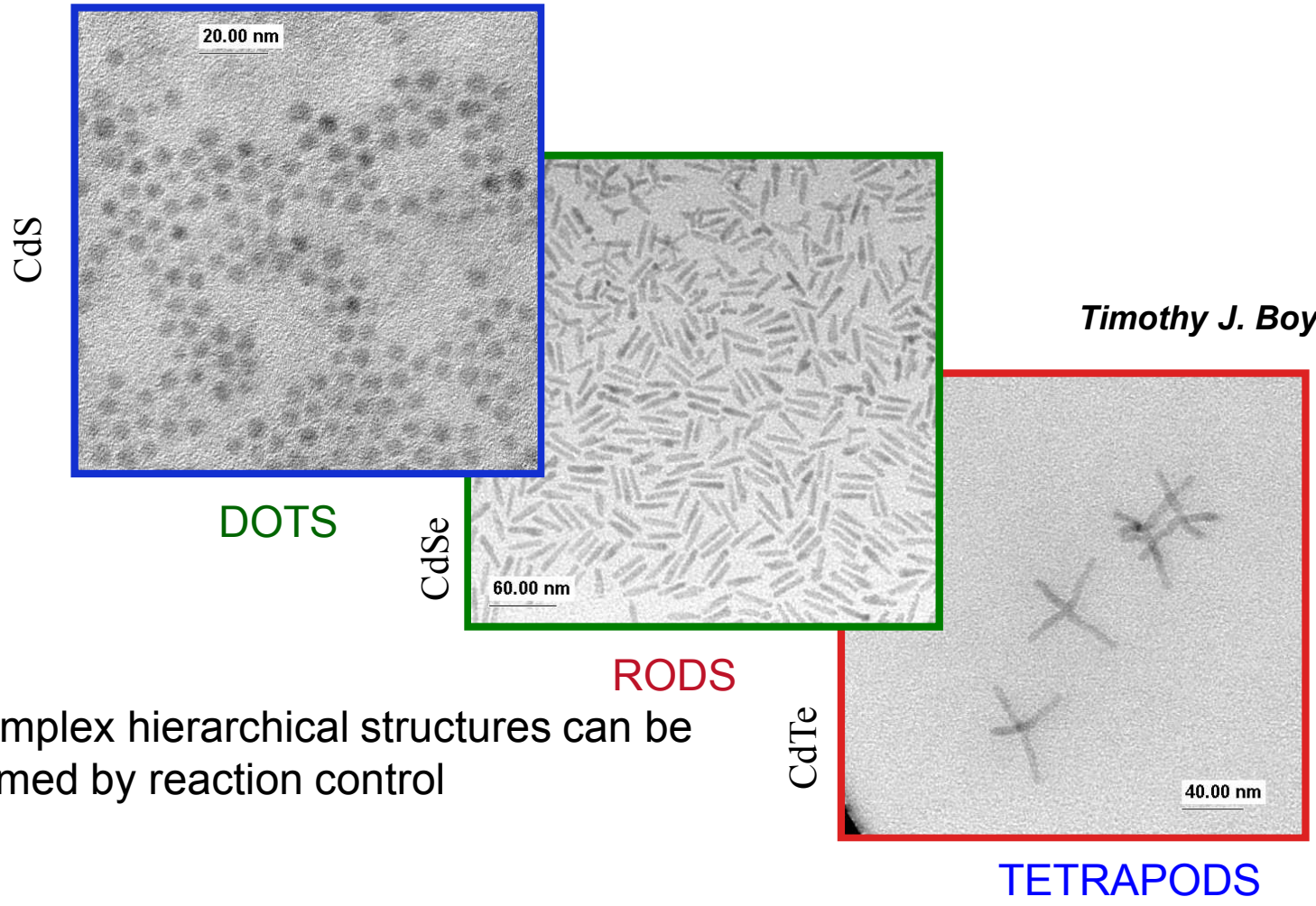

Timothy J. Boyle, Sandia

Complex hierarchical structures can be formed by reaction control

Microfluidic Synthesis Discovery Platform™:

Understanding the Kinetics of Nanomaterial Synthesis

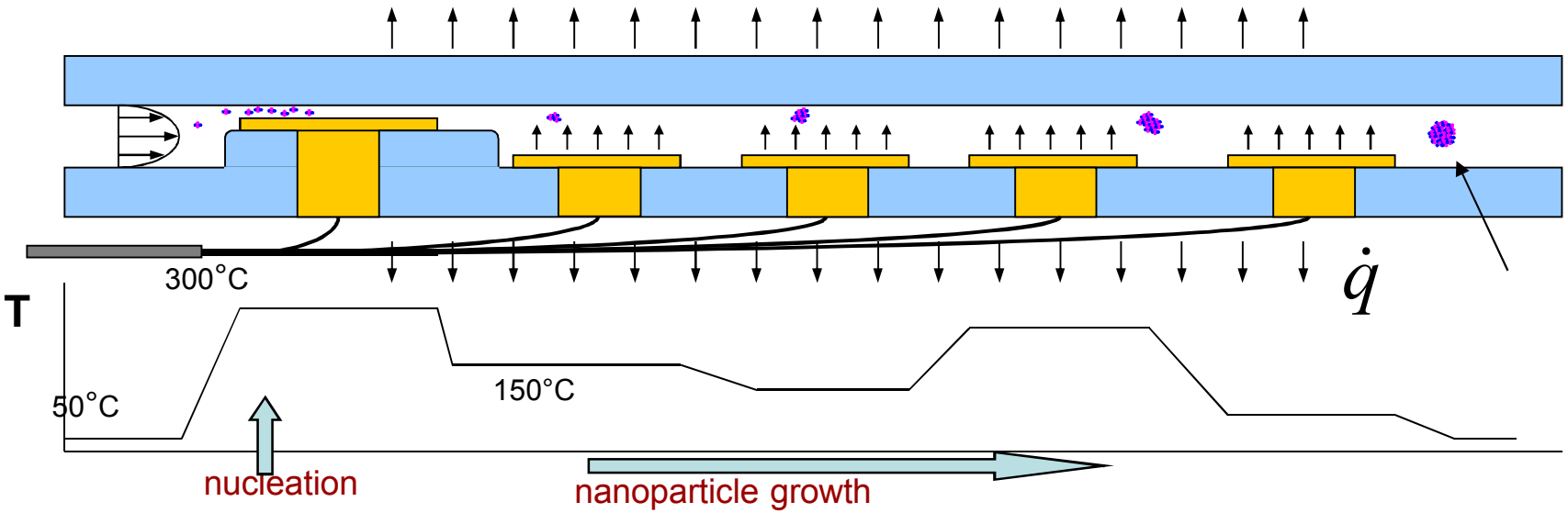

Development of a basic understanding is needed for future "continuous flow" reactors.
Control of thermal profile allows fundamental studies of synthesis reactions.

- What are the values of the thermodynamic parameters that control nanoparticle synthesis? (enthalpy, entropy, surface energy)
- What is the mechanism of nanoparticle nucleation and growth? (i.e. diffusion, surface reaction, self-assembly)
- What is the mechanism of the formation of shell layers around a core nanoparticle?
- How does the surfactant composition relate to the quantum confinement properties of nanoparticles?

- Microfluidic chip will be integrated within a carrier platform
- A SWIFT-light process will be used to develop the heater and sensor elements.
- Users include synthetic chemists, quantum dot material synthesis.

Chip Design

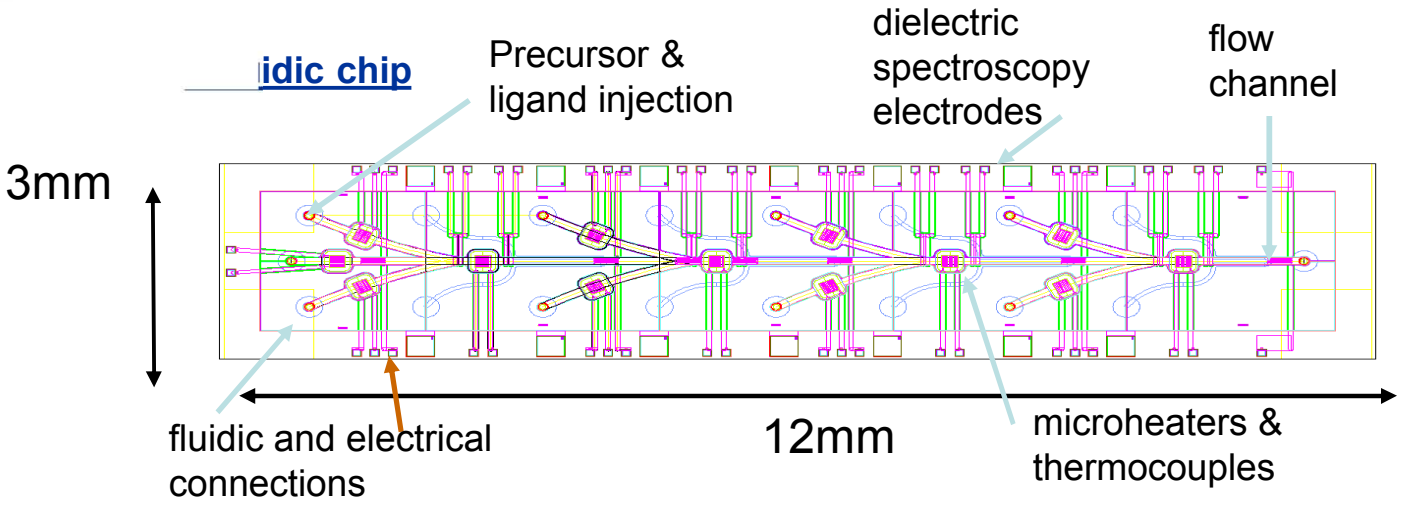
idic chip
Precursor &
ligand injection
dielectric
spectroscopy
electrodes
flow
channel
3mm
fluidic and electrical
connections
12mm
microheaters &
thermocouples

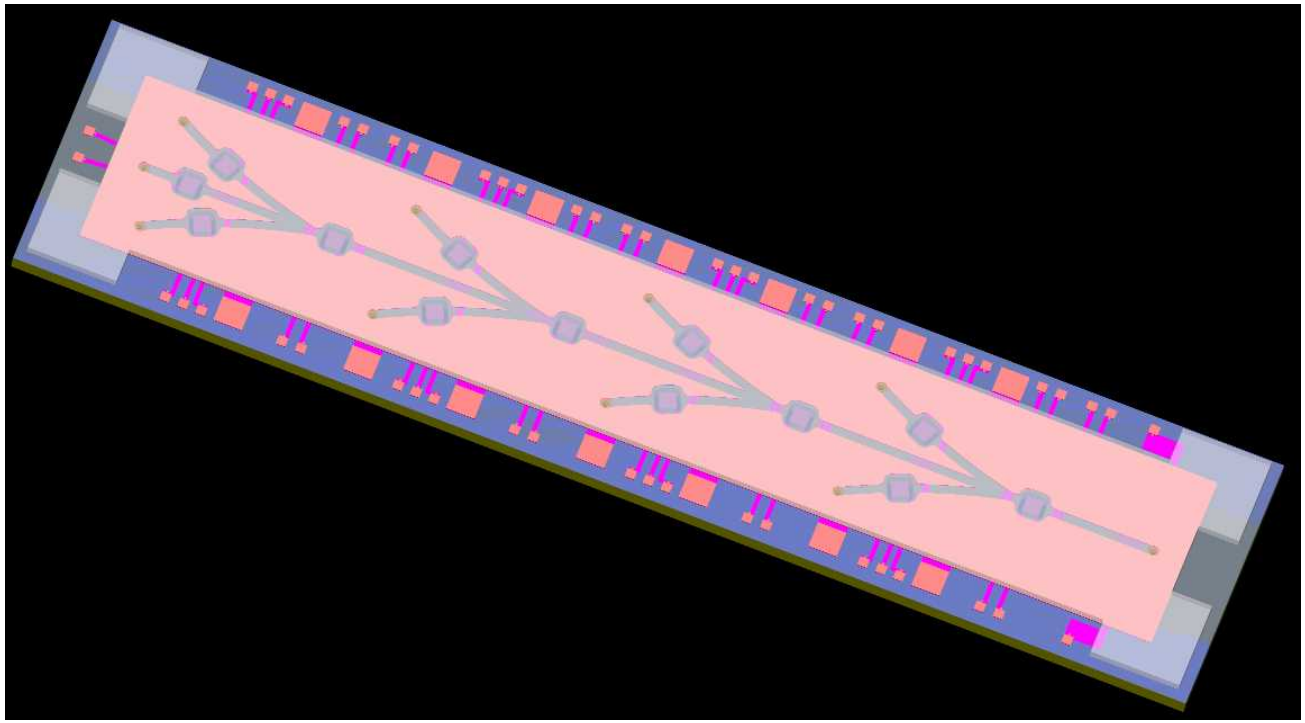

Entry Stage Details

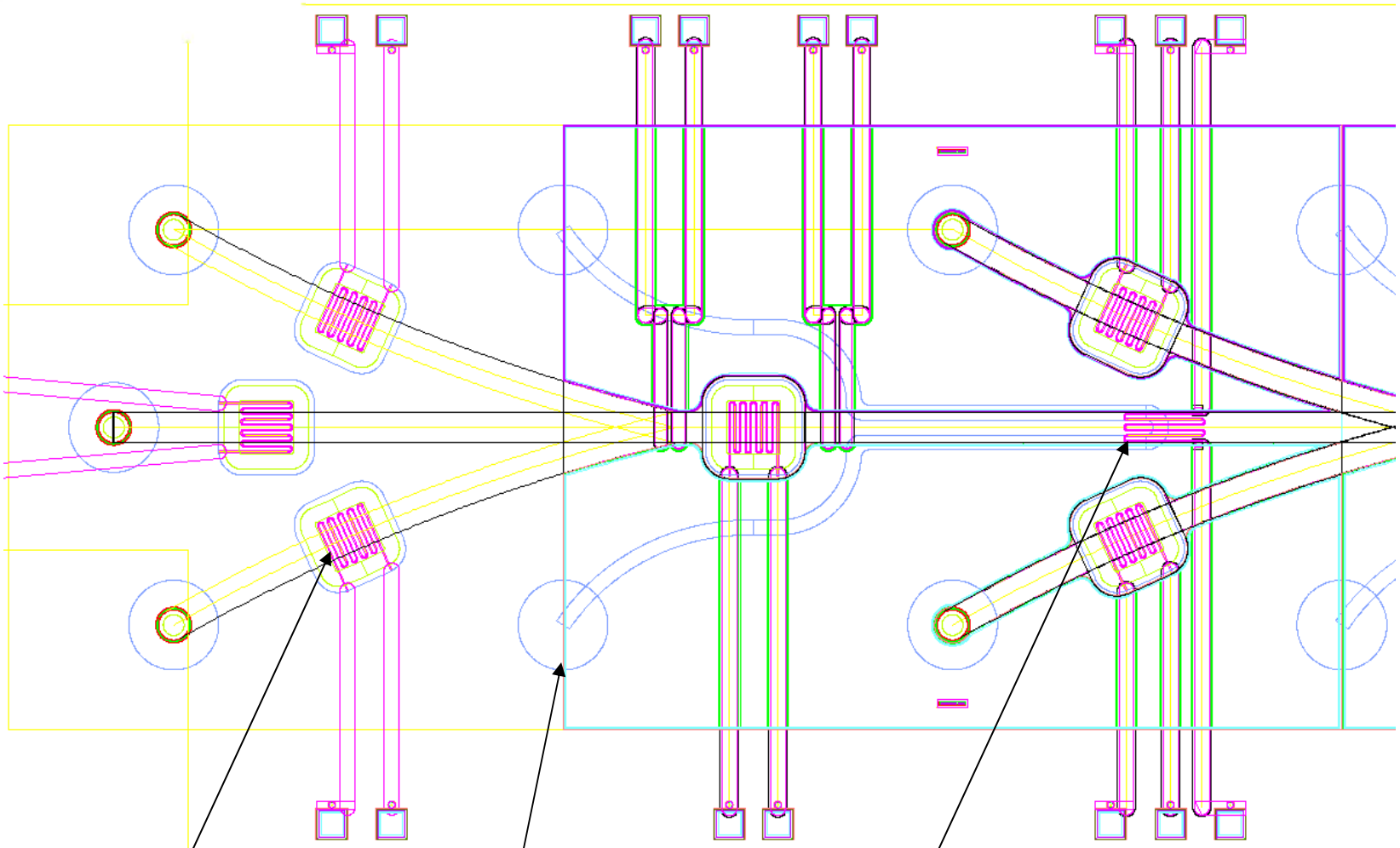

isolated resistors for high temp.

channels for temp. control in silicon bulk

non-isolated resistors for temp. measurement/control

Fluidic and Electrical Connections Through the Platform Manifold

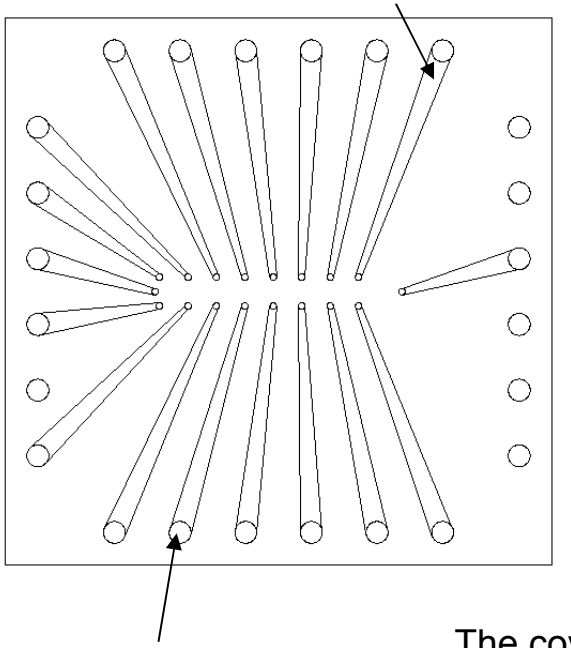

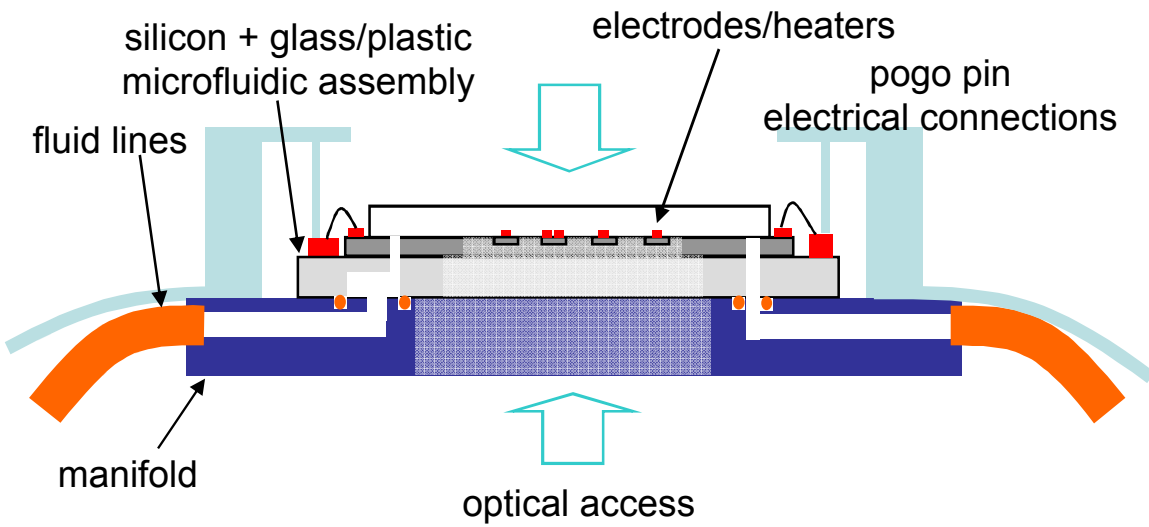

The cover and fan out glass must be anodically bonded to the Microfluidic Synthesis DP.

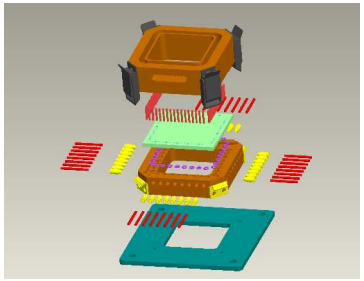

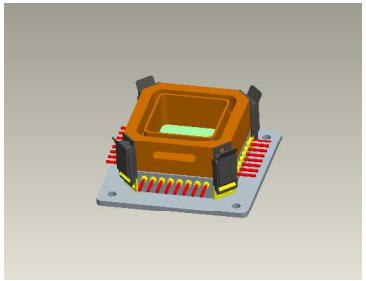

Integration package

- 64 pogo-pin connections utilizing one common interface connector
- 32 fluidic connections
- 1.5 inch square top/bottom access

- O-ring seals to 500 psi
- Dowel pin alignment
- 4-place draw-latch compression

- Circuit board connections soldered directly to pogo-pins
- MDM connector for reliable
- assembly and disassembly

Manifold and Manufactured Platform

The microfluidic Discovery Platform™ has completed the fabrication and anodic bonding phases. Further testing is focused on capability validation.

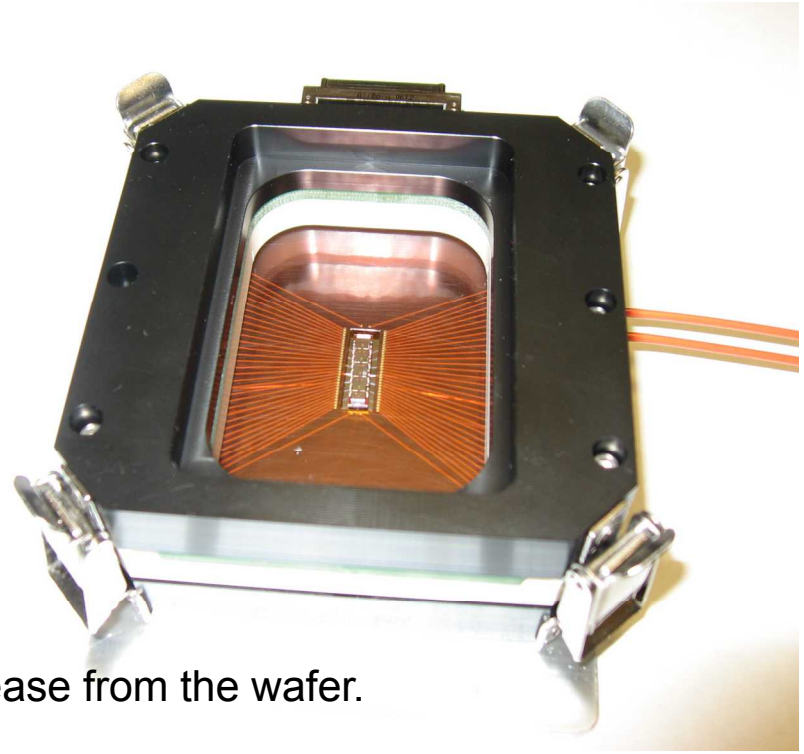

Microfluidic Network before dicing and release from the wafer.

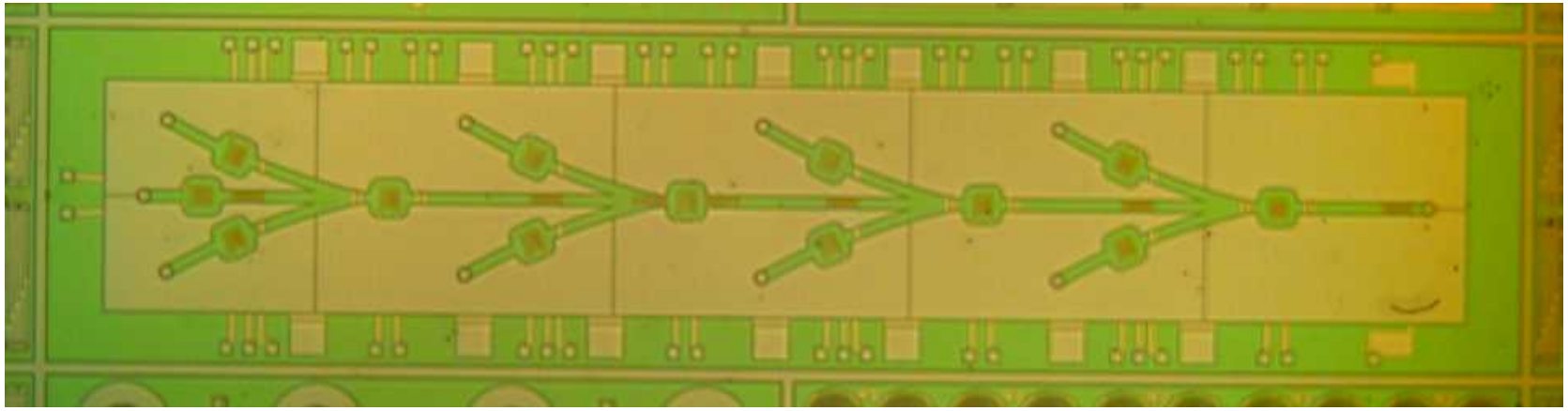

Future Research Focus

Nelson S. Bell

Research Directions

1. characterization of colloidal properties of nanoparticle suspensions
2. control of self-assembly processes in colloidal systems

Microfluidic Discovery Platform

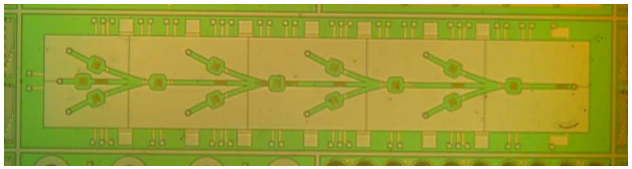

The Microfluidic DP will allow for study of the nucleation and growth of nanoparticle materials, and functionalization of the surface with surfactants for evaluation of interactions between particles and surfaces.

Parameters Affecting the Colloidal Stability of Nanoparticles

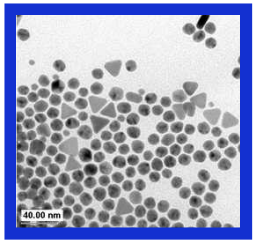

The influence of surfactants and growth conditions on nanoparticle morphology (seen in the gold nanoparticles above, *T. Boyle*) directly affect nanoparticle production and colloidal stability, as well as the ability of these materials to be integrated into functional devices. I will investigate the interaction of dispersants during formation of particles from solutions and how surfactants can be used to form nanostructures from nanoparticle components.

Directed Colloidal Assembly of Colloidal Materials for Novel Properties

Zinc Oxide nanorods give anisotropic optical properties, and can be piezoelectrically actuated. *Electrophoretic fields* are being investigated for the aligned assembly of ZnO Nanocomposites with R. Vaia, AFRL

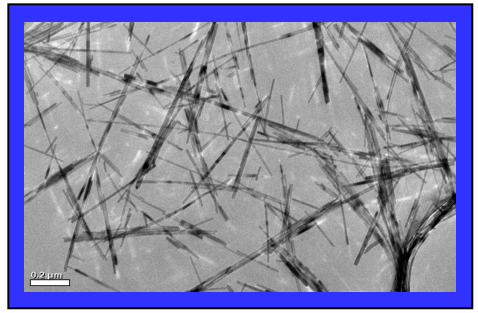

Optically directed assembly results from photo-controlled wetting of surface polymers on colloidal particles. Novel porous structures can be fabricated, and potentially lead to ordered dielectric networks with optically active functionality, done with CINT User P. Braun, UIUC.

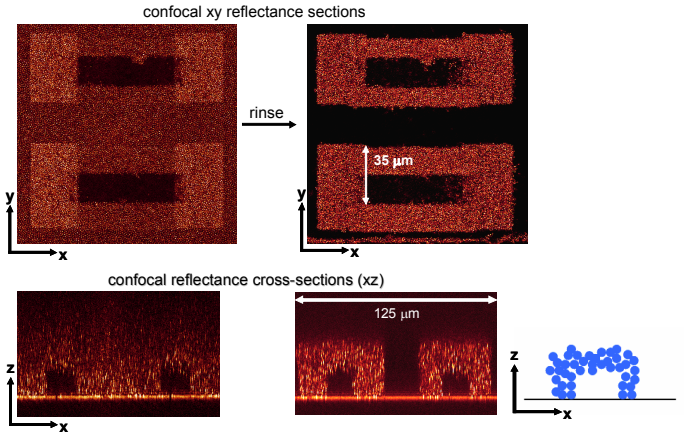

Adsorption kinetics

RSA of Disks $\Rightarrow$ Jamming coverage
0.547 +/- 0.0002

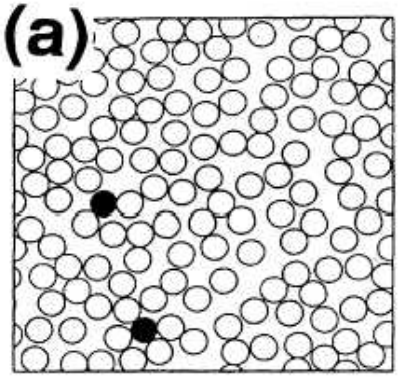

Evans, J.W. *Rev. Mod. Phys.*, **65**, No. 4, (1993)

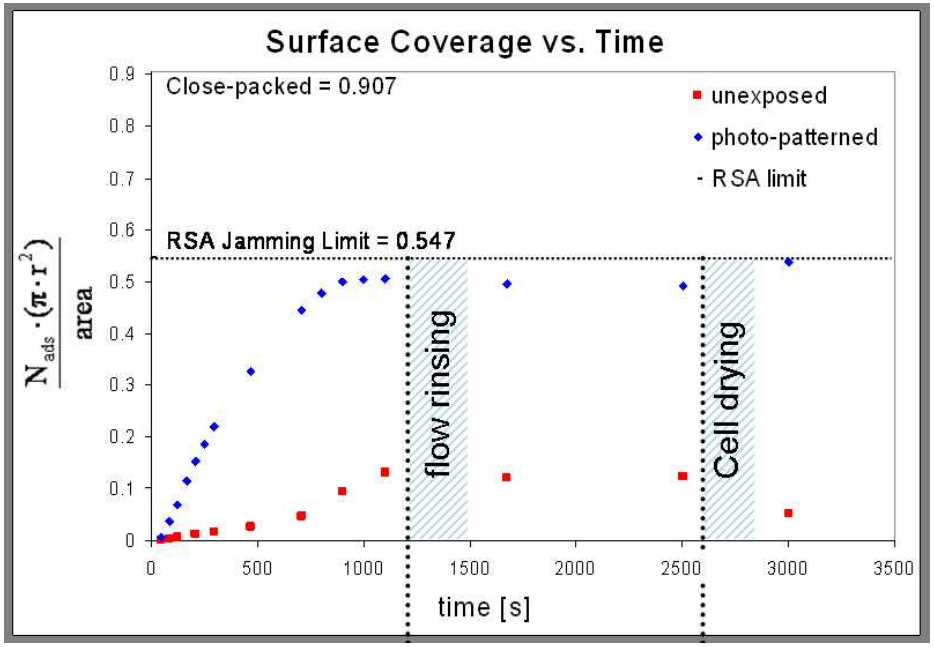

same

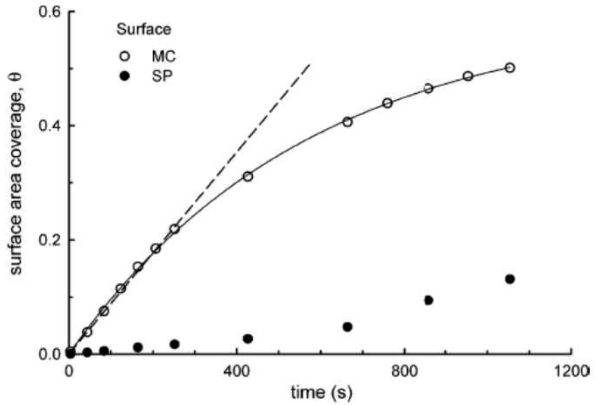

Figure 3. Plot of fractional surface coverage as a function of time for colloids depositing onto the photoswitched (MC) and unexposed (SP) regions of the substrate modified with an SP-*co*-MMA

M. Piech, M. C. George, N. S. Bell and P. V. Braun:, *Langmuir*, **22**, 1379-1382 (2006).

Absorbance spectrum of a complex fluid, containing SP/MMA copolymer

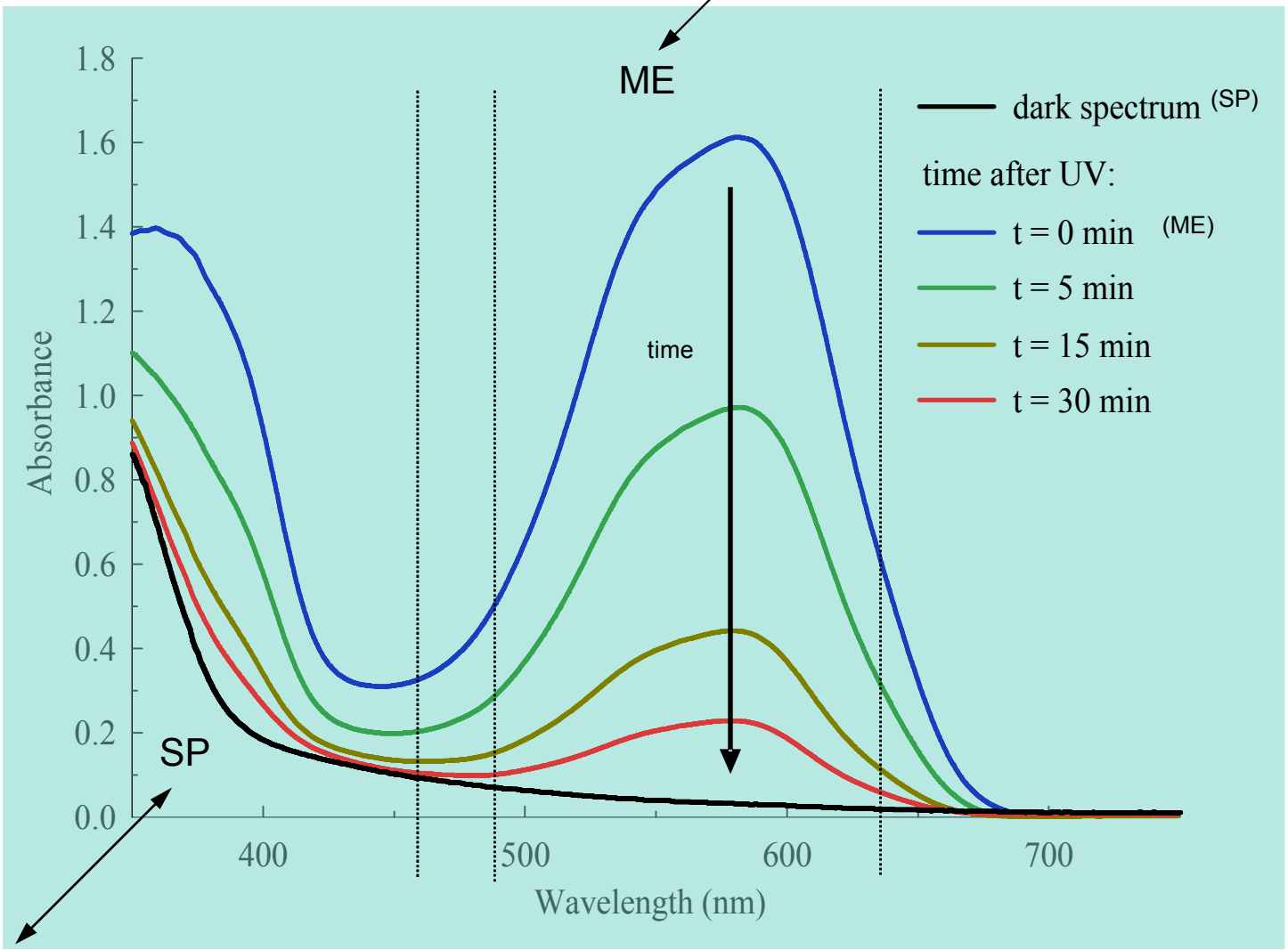

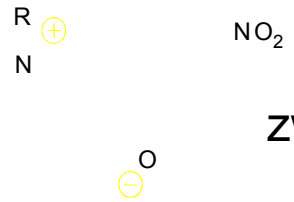

zwitterionic form

closed form

Confocal Reflectance Images (458nm)

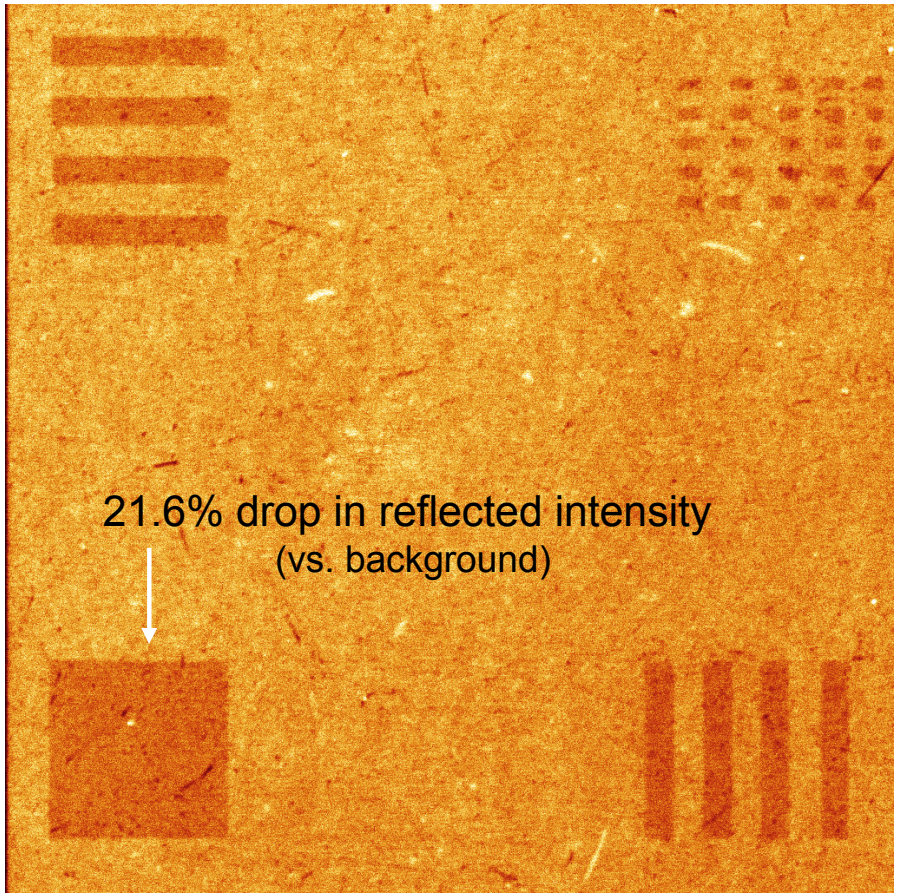

Initial image taken after 2-photon exposure

time

After several minutes (& additional exposure)

- Initial drop in reflected intensity… followed by brightening with time !?!?!

Phase diagram for colloids with hard core repulsive and short range attractive square well potentials

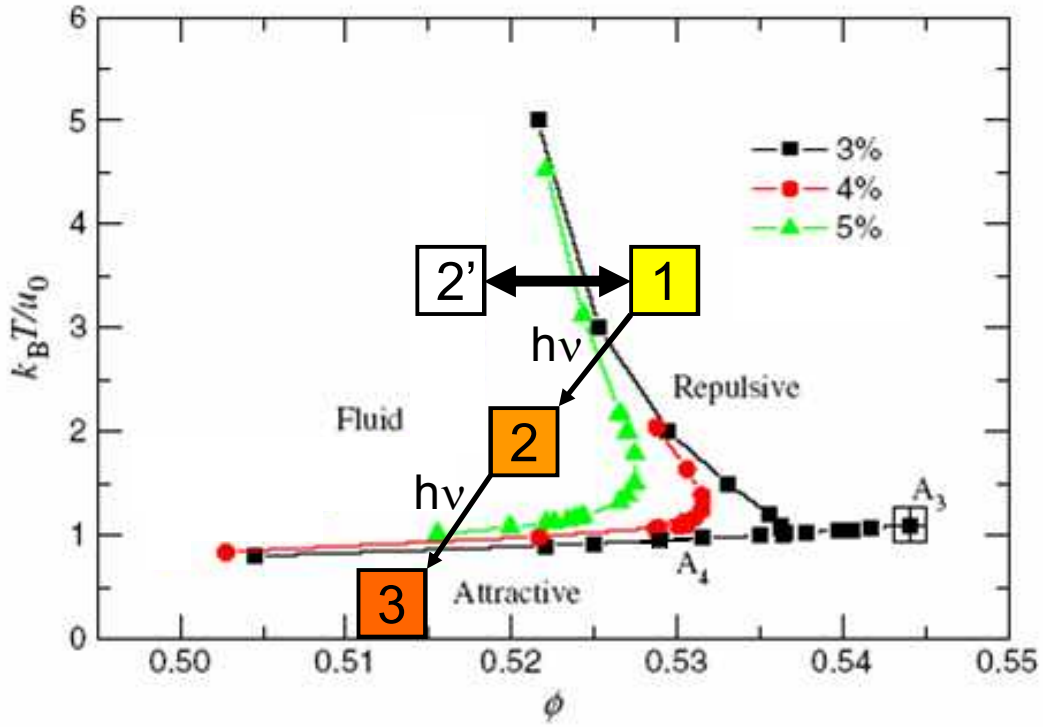

Solution: SP-co-MMA-block-PS (colloids do not aggregate upon UV irradiation)

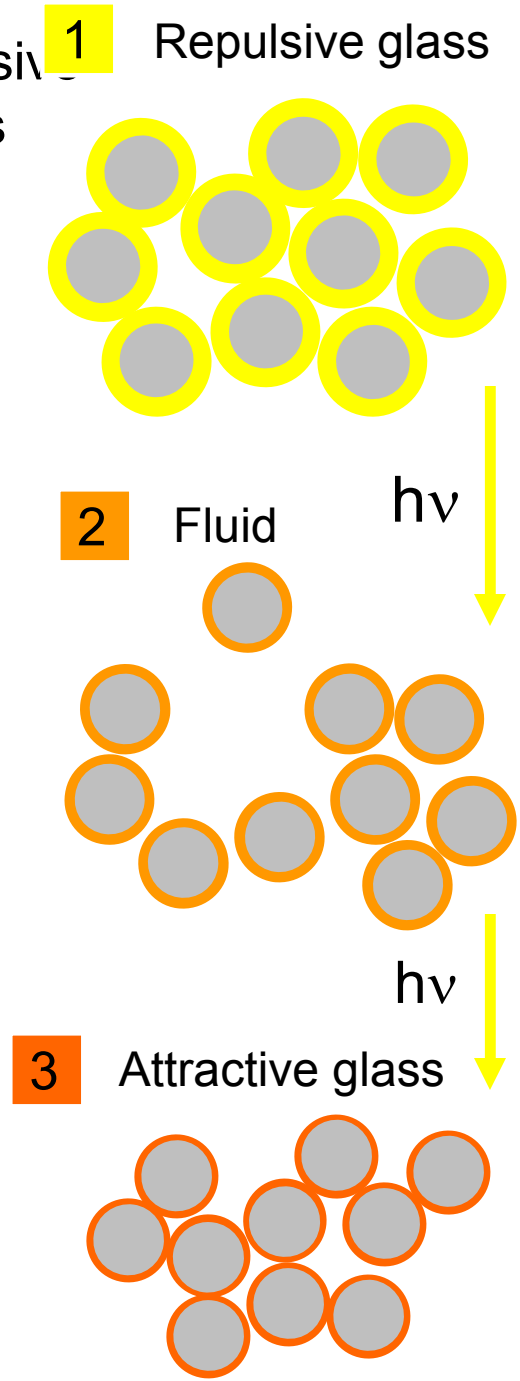

Luca Cipelletti and Laurence Ramos, "Slow dynamics in glassy soft matter", *J. Phys.: Condens. Matter* **17** (2005) R253-R285

Synthesis and Light-induced Assembly of Photo-responsive Colloids

Matthew George[1], Ali Mohraz[1], Kyle Plunkett[2], Martin Piech[3], Nelson Bell[3], Jeffrey Moore[2], Jennifer Lewis[1], and Paul Braun[1]

1. Frederick Seitz Materials Research Laboratory, University of Illinois, Urbana, Illinois
2. Chemistry, University of Illinois, Urbana, Illinois
3. Electronic and Nanostructured Materials, Sandia National Laboratories, Albuquerque, New Mexico.

Acknowledgments

Additional contributors:

- Marcin Piech, United Technologies Corporation
- Dongqing Yang and Tom Picraux, University of Arizona, CINT
- Matt George and Paul Braun, UIUC
- Jacinta Conrad
- Stephanie Pruzinsky

Facilities:

- Sandia National Laboratory; Albuquerque, NM
- Beckman Institute Microscopy Suite; Urbana, IL
- Frederick Seitz Materials Research Laboratory; Urbana, IL

Funding:

- CINT – Sandia National Laboratory
- Army Research Office – MURI Grant
- Department of Energy

Microfluidic Platform – Bosch etched features (back of Si chip)

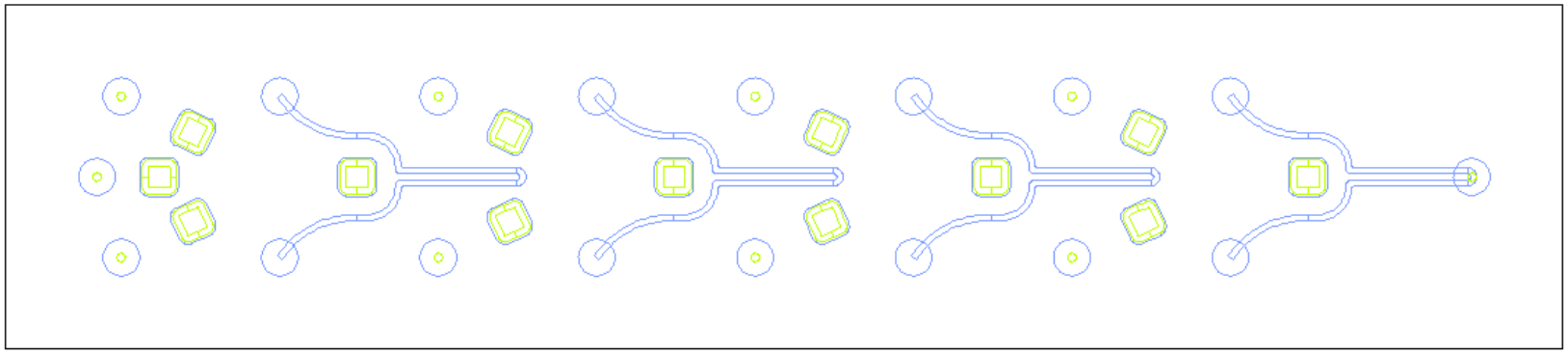

Summary

• Photoswitch wetting/dewetting surfaces were achieved by functionalized azobenzene surface, the dynamic advancing contact angle is 101.3 ° under visible light and 88.9 ° under UV light;

• The dynamic contact angle of various solvents were measured on azobenzene modified surface; we found solvents that can be moved by UV light on this surface;

• Demonstrate the use of light to move liquids on azobenzene modified surface by 1-bromonaphalene;

• The surface energy of azobenzene modified surface which calculated by Van Oss theory, is 38.7mJ/m^2 under UV light, is 33.9mJ/m^2 under Visible light ;

Photo-reversible copolymer brush layer

Silica core, SP-co-MMA shell

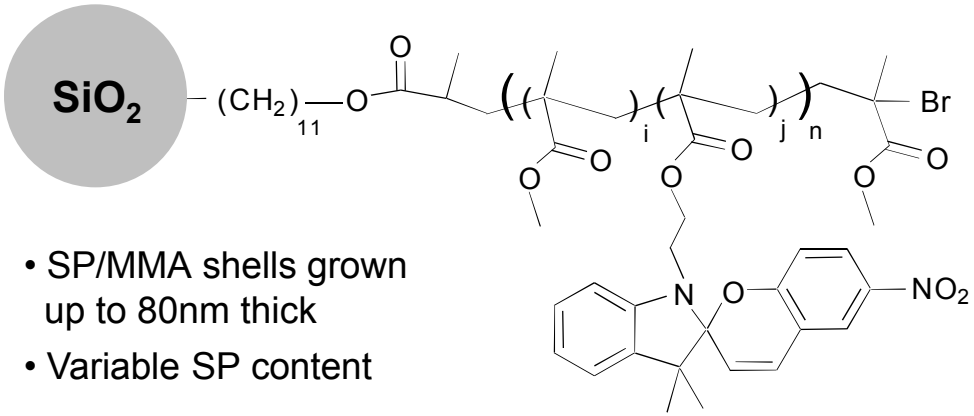

=

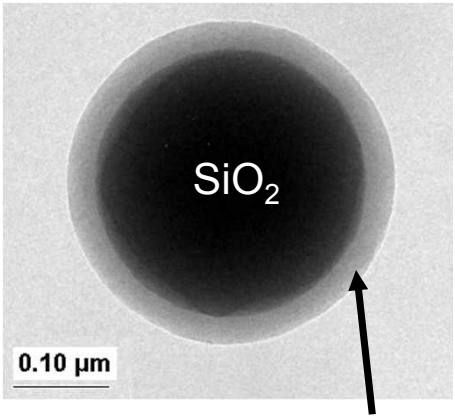

polymer brush layer

- SP/MMA shells grown up to 80nm thick
- Variable SP content

M. Piech, N.S. Bell, *Macromolecules* **39**, 915 (2006)

sterically stabilized, **SP** form

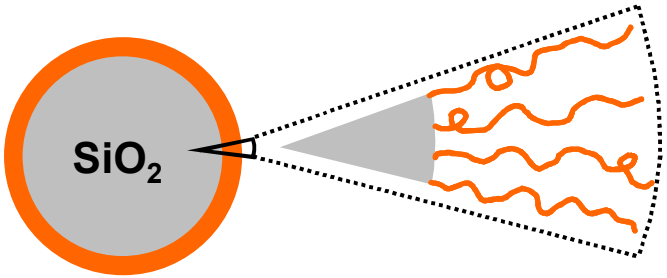

hν (UV)

Δ or hν (visible)

aggregating, **ME** form

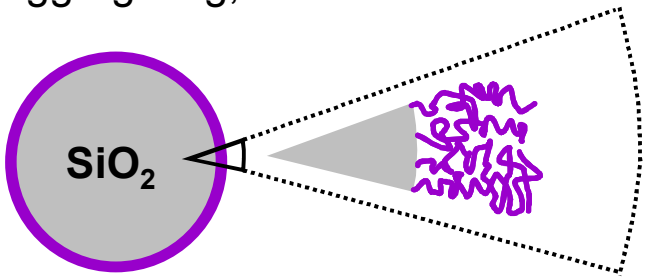

SP = closed form

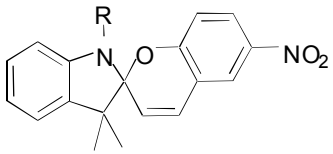

ME = zwitterionic form

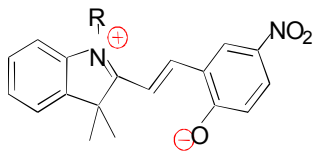

N. S. Bell, M. Piech, *Langmuir*, ***22*** *(2006)* 1420-1427

Sediment Comparison via Confocal Microscopy

No UV exposure

After 1 min UV irradiation (λ=366 nm)

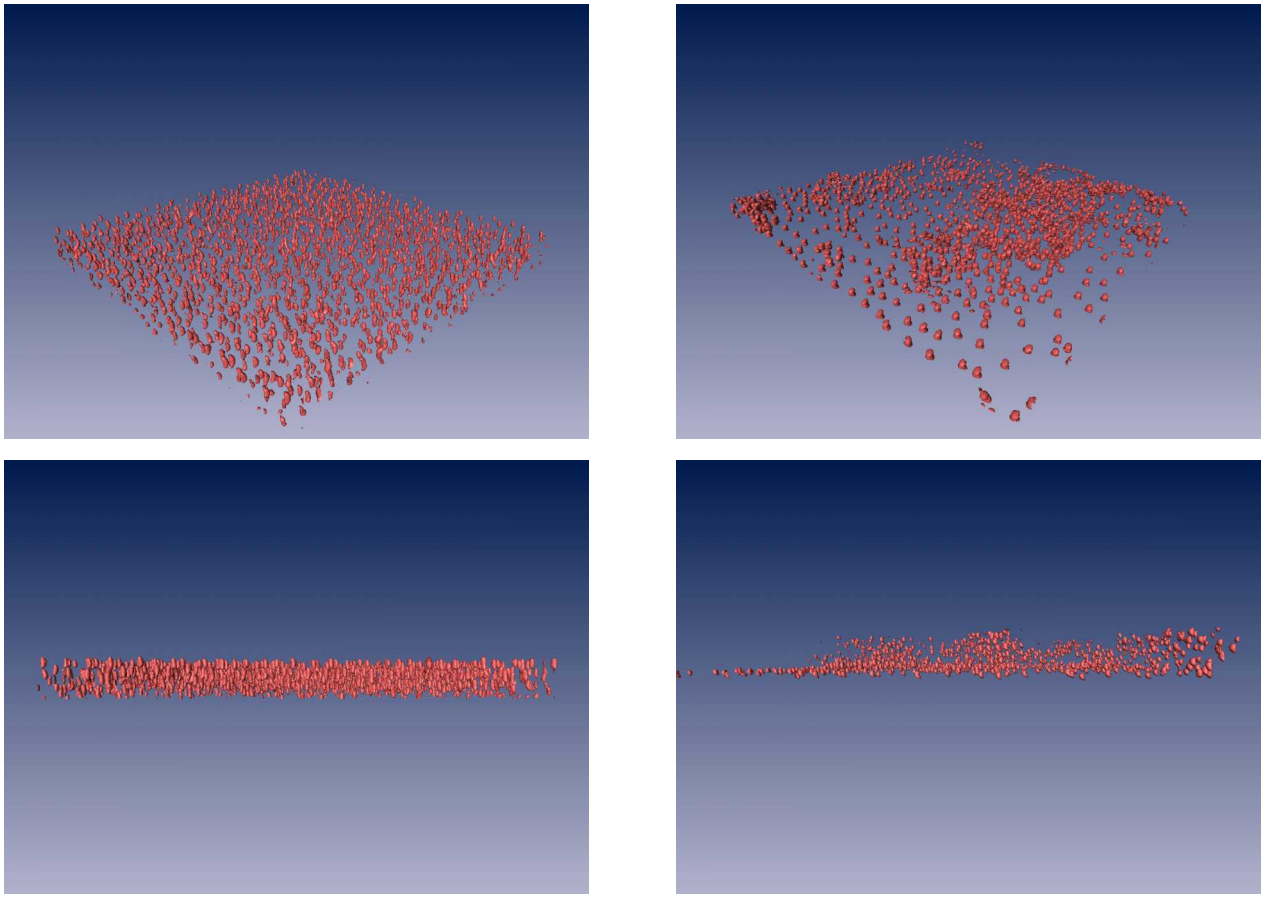

Sandia National Laboratories

Photo-Actuated Deposition (video)

Sedimentation with substrate patterning

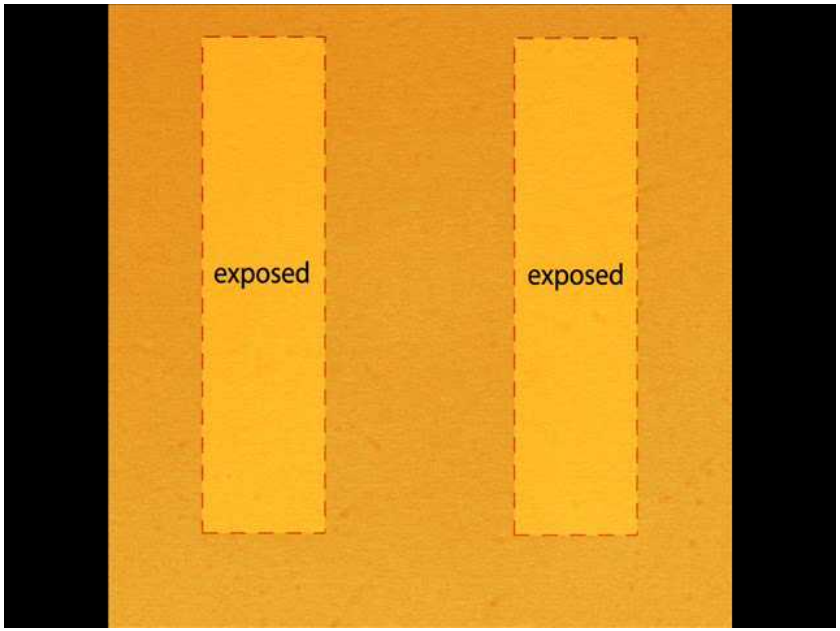

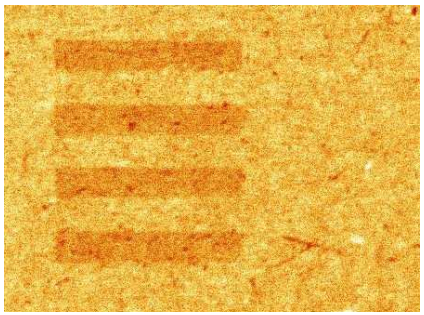

Flow Cell Adhesion

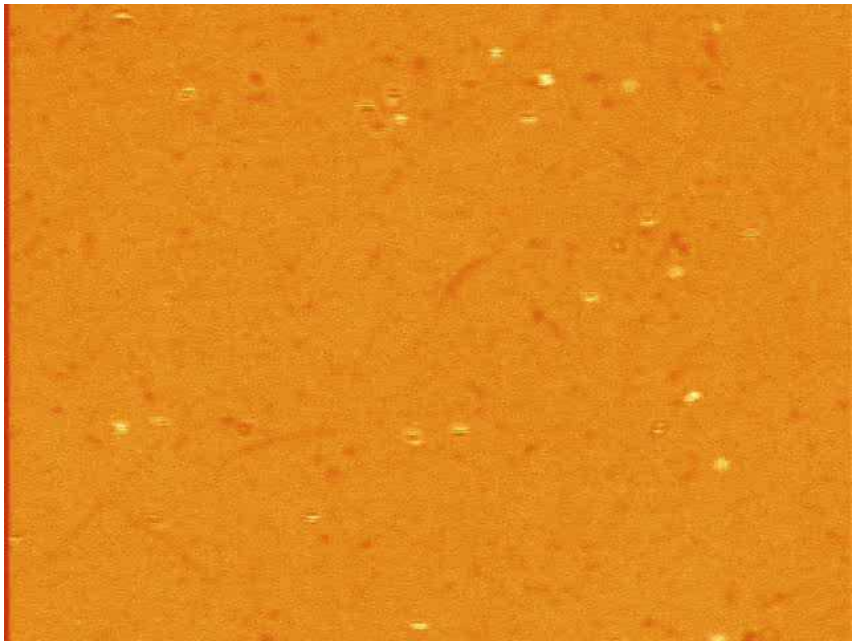

Conformation behavior under stimuli

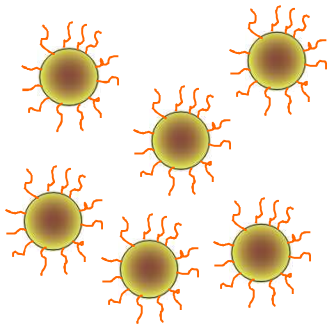

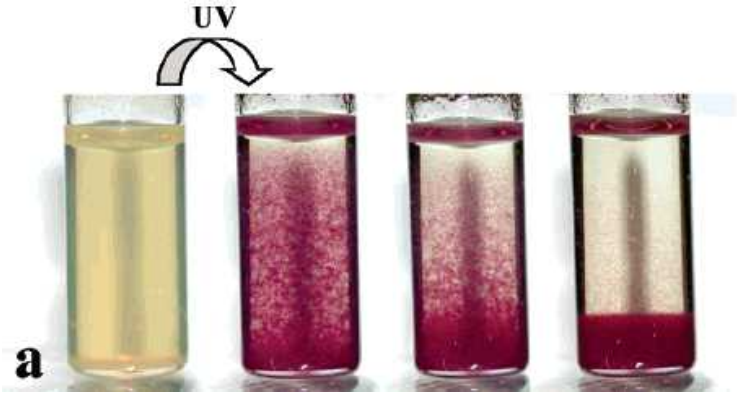

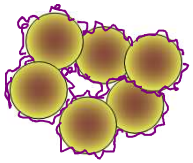

N. S. Bell, M. Piech, *Langmuir*, ***22*** *(2006)* 1420-1427

unexposed sediment

sterically stabilized colloidal glass

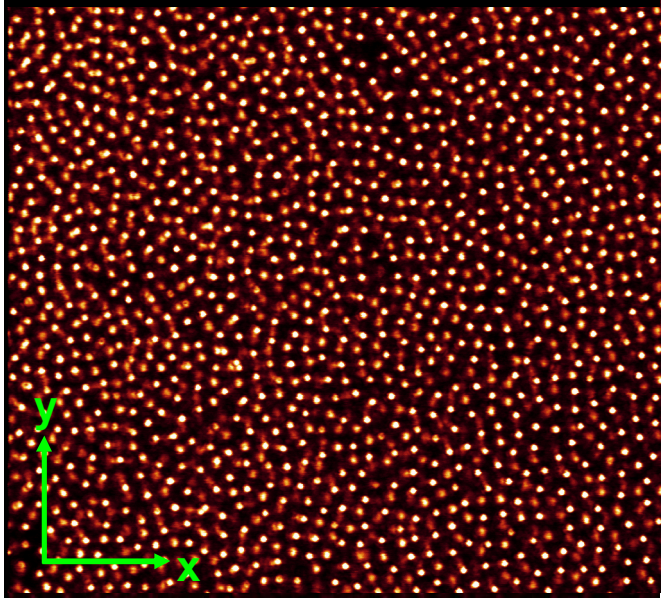

UV

Δ or Vis.

UV exposed sediment

colloidal gel

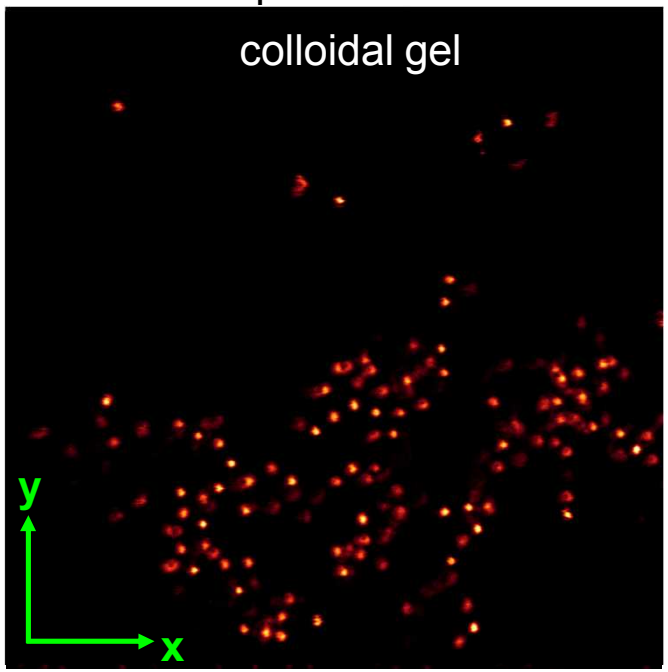

Photo-responsive Colloidal System

3D laser gel writing

Applications

- Trapped colloidal fluid
  - Study of confined colloidal fluids
  - Catalytic regeneration in microfluidic reactors
- Colloidal Ink based 3D photolithography
- Nanofiltration with dynamic remote control of pore size

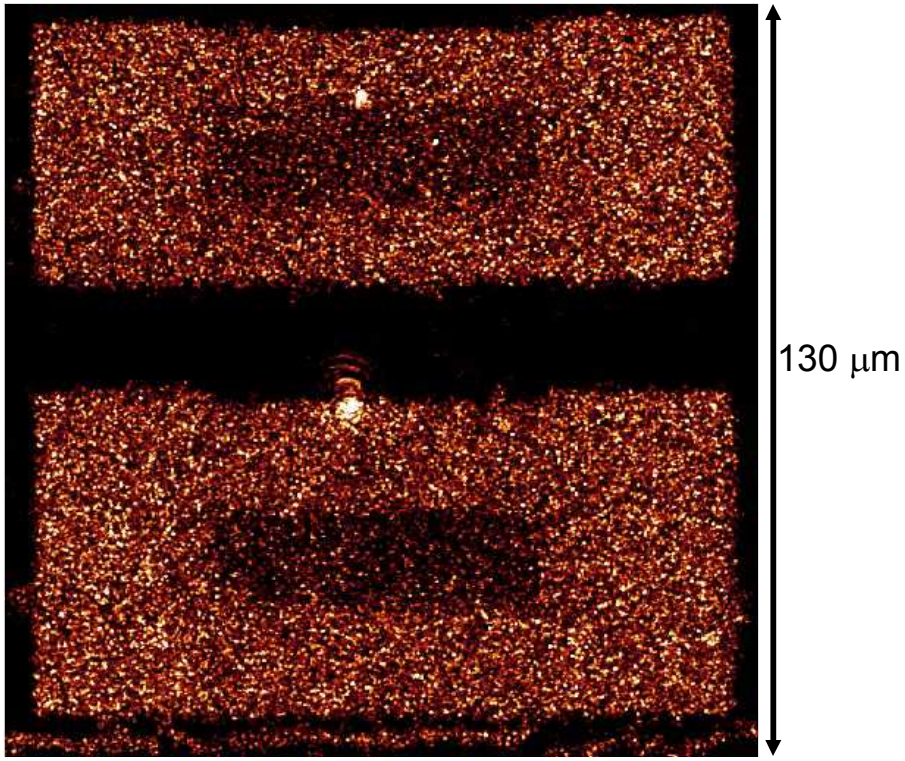

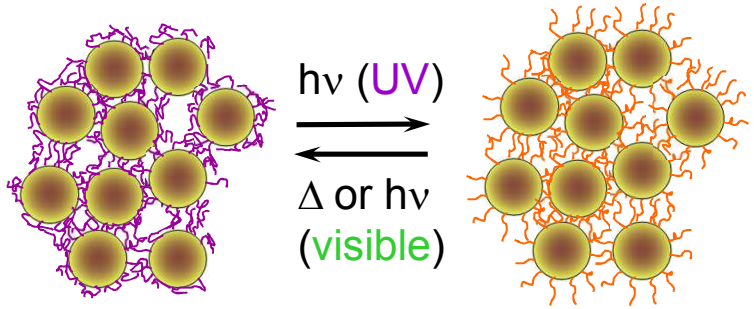

Reversible size selective photo-gating??

Multiple Epitaxial Growth of Complex ZnO Crystals

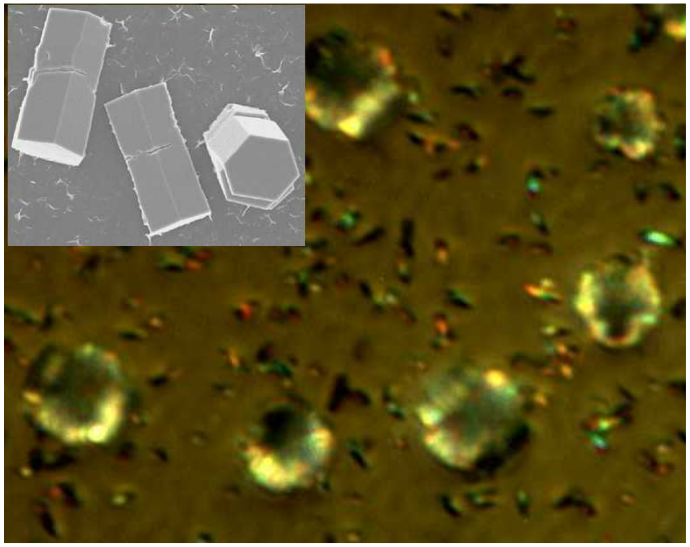

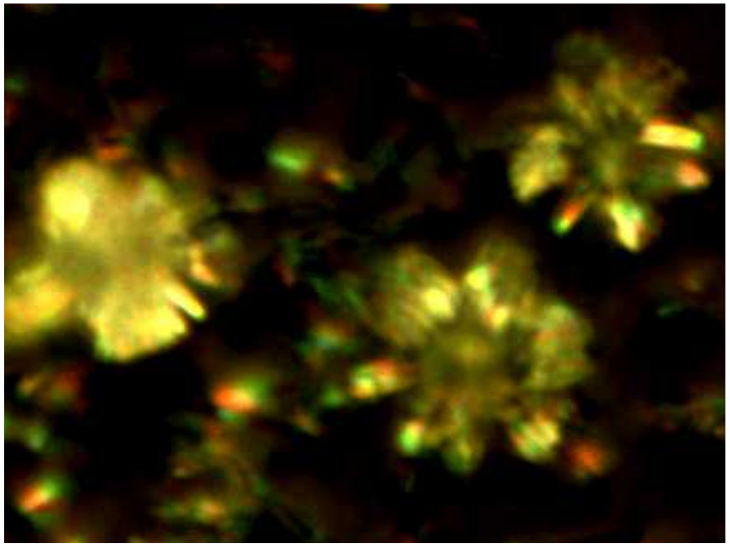

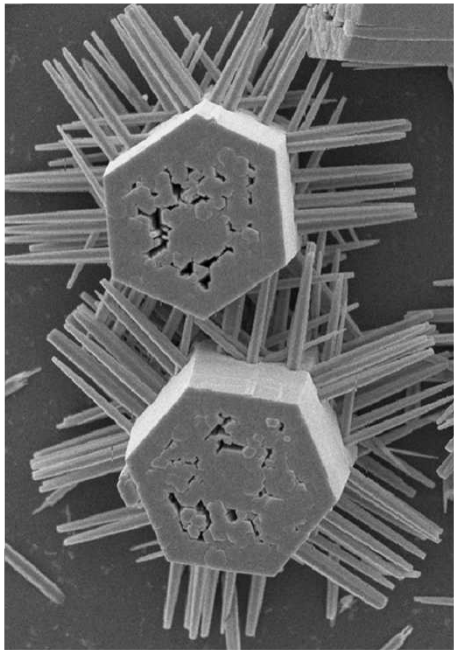

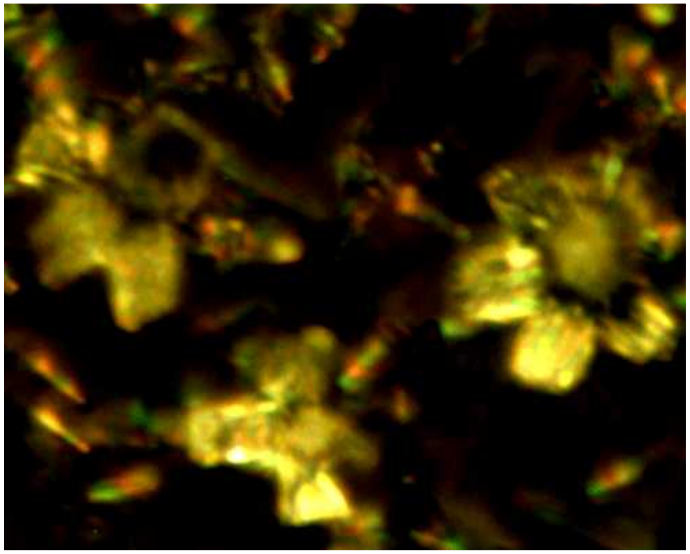

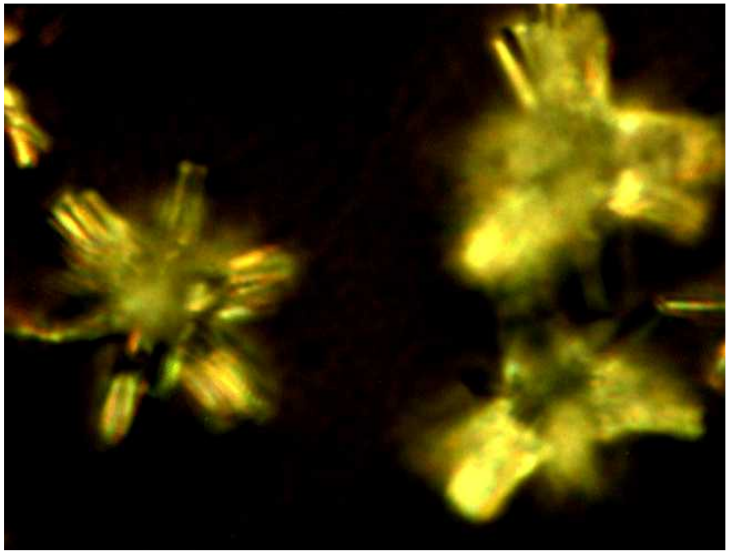

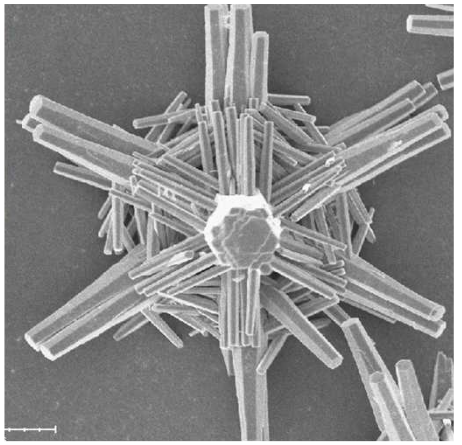

Colloidal Properties of Sol-gel derived ZnO Nanoparticles

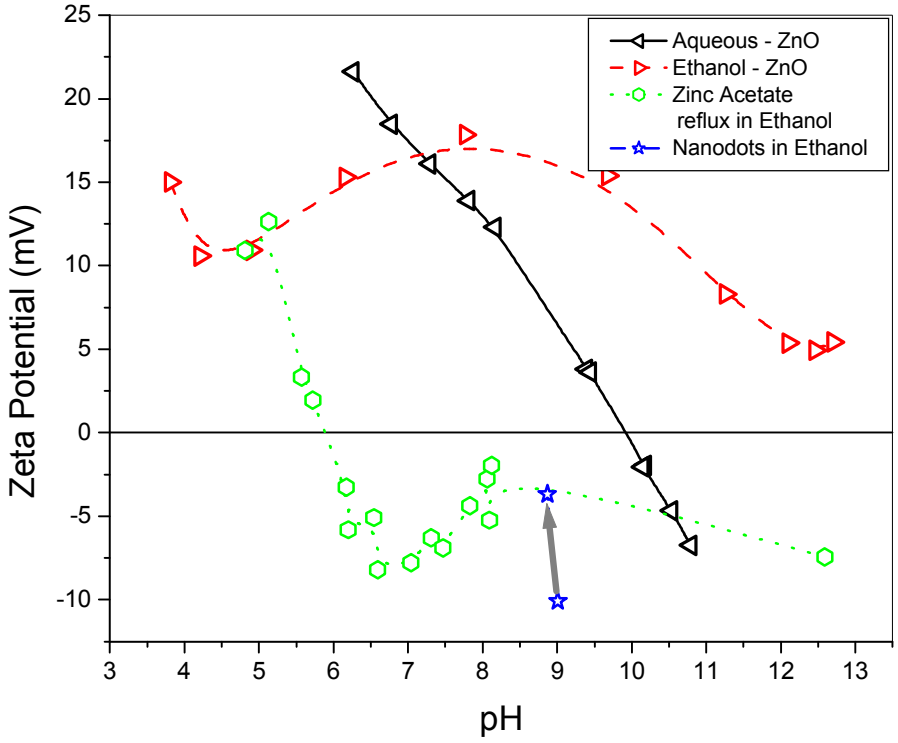

- There must be an aging reaction with the surface chemistry that lowers the surface charge, and affects colloidal stability.
- Particle size changes are not greatly affected.

Electrostatics is not strong enough to create a stable repulsion barrier to agglomeration.

zeta potential = -10 mV,
ethanol has a dielectric constant of 24.3

Acetate ions (CH_3COO^-) are too small to form a steric barrier. Dissociative adsorption favored on TiO_2 surfaces. The C-C bond adsorbs perpendicular to the surface, giving ~ 2.6 Å length.

Other potential stabilization mechanisms

Stern layer of TMA^+

negative charge of zeta potential will attract cation layer. Unknown repulsion strength

Hydrogen bonding with acetate-TMA+ ions

An extended $acetate^-$-TMA^+-Zn^{2+} "gel" layer may be stabilizing the ZnO core (i.e. silicic acid stabilization of SiO2)

Optical Characterization of ZnO Growth in 1,4 Butanediol

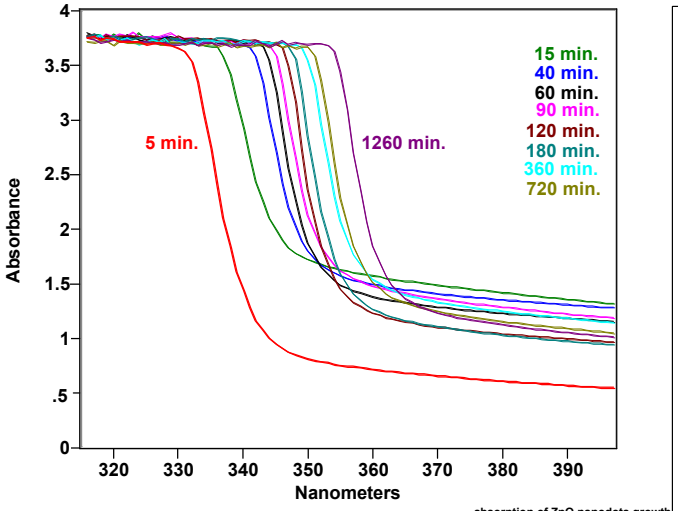

Figure 1. Absorbance of ZnO nanodots during growth at 30°C in butanediol

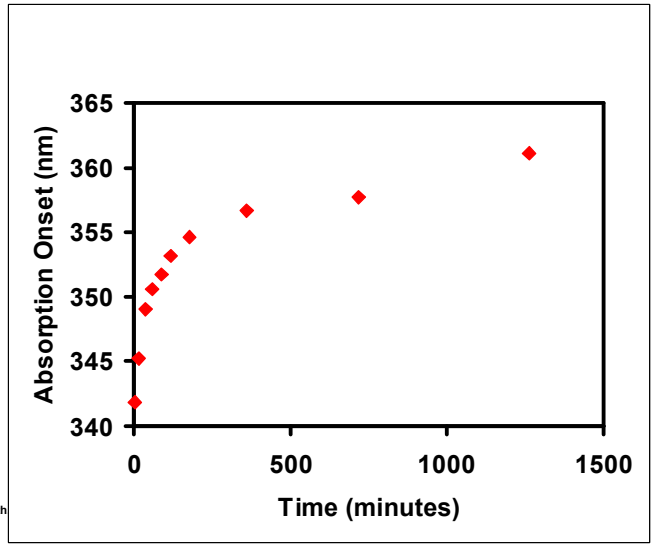

Figure 2. Absorption edge onset
of ZnO
ectra in

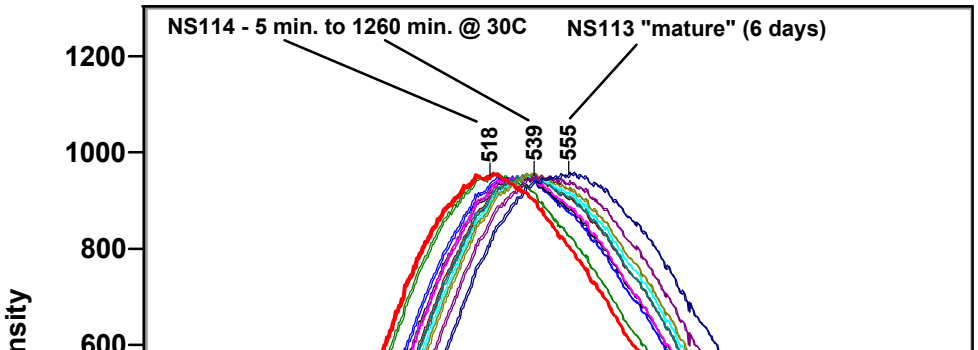

Figure 3. PL, obtained using 300 nm excitation, of ZnO nanodots during growth at 30°C. The intensities of the spectra have been normalized for ease of comparison.

Shape Evolution under Controlled Dissolution

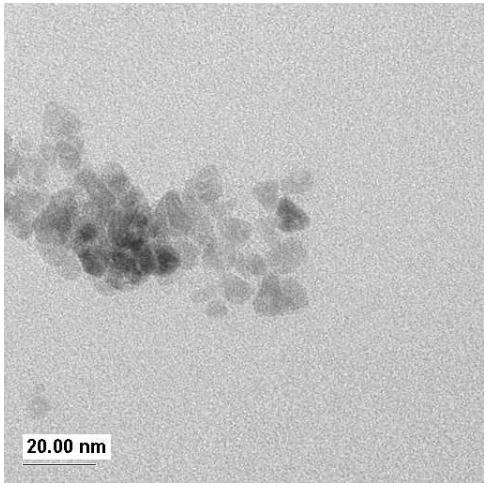

ZnO nanoparticles were formed in 1,4-butanediol solvent via the sol-gel process at room temperature.
The samples were diluted by a factor of 3, to promote the removal of the smallest particles via the solubility product equilization.
After 24 hours at 90 C, monodisperse septahedral particles are formed, which exhibit preferrential dimerization.

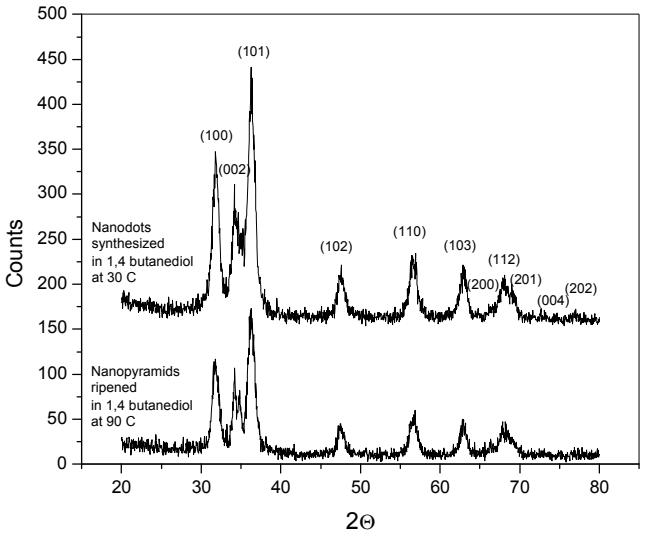

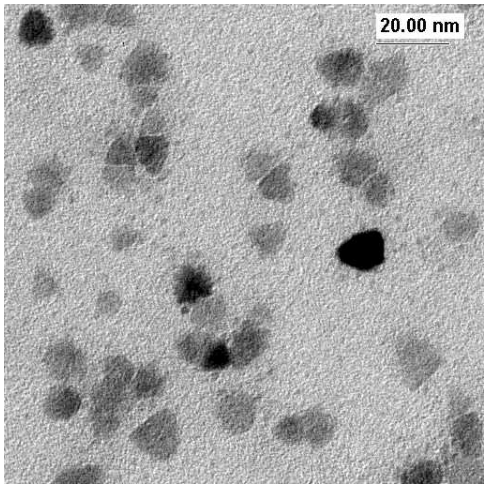

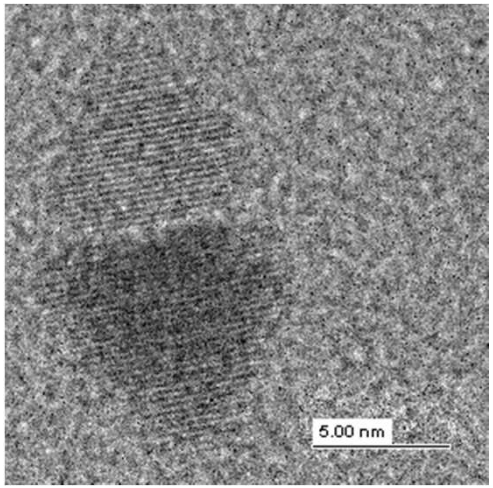

XRD Characterization of Crystal Size During Mg doping of ZnO

Estimates of crystal domain size were computed using the Scherrer Equation for line broadening

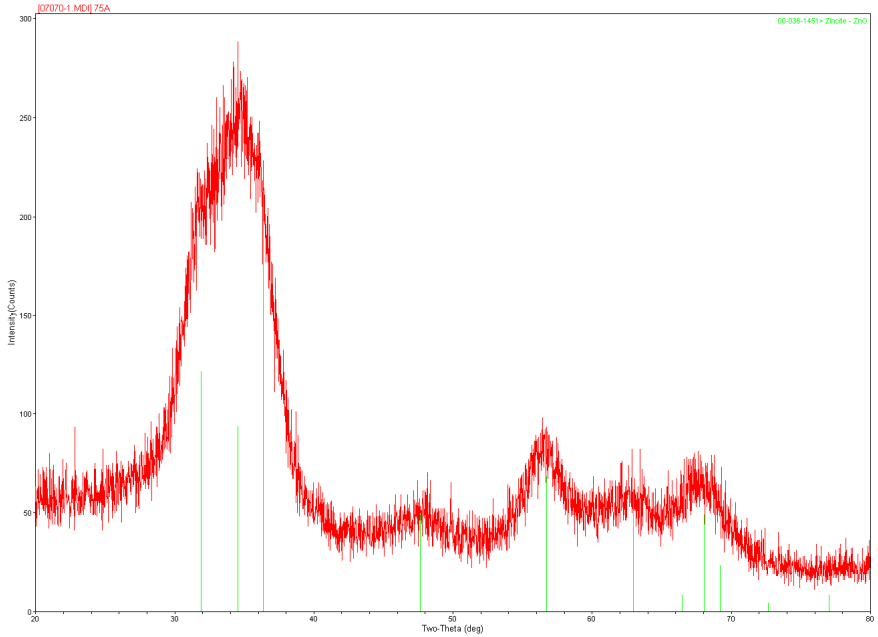

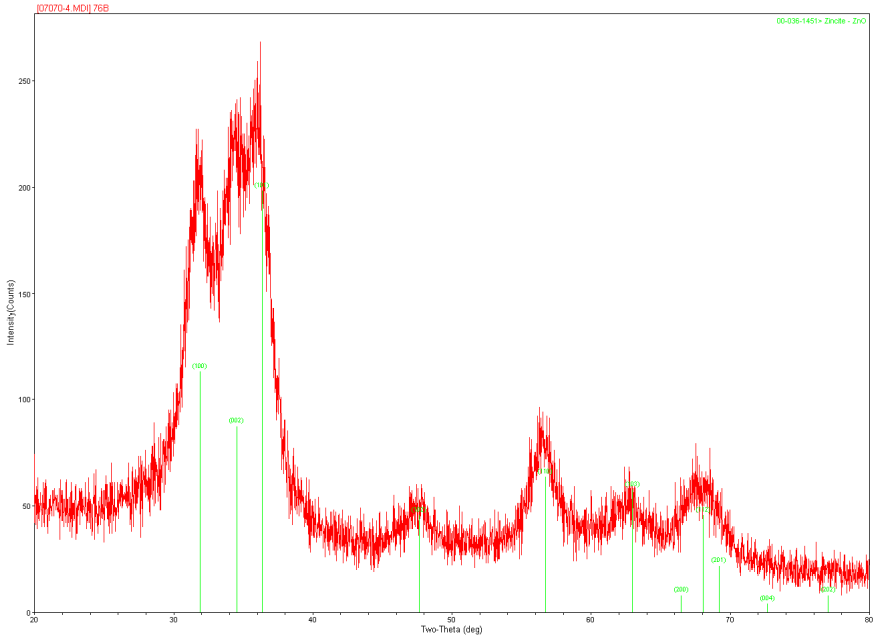

Plot data: 75A – 19 Angstroms
75B – 23 Angstroms
76A – 26 Angstroms
76B – 28 Angstroms

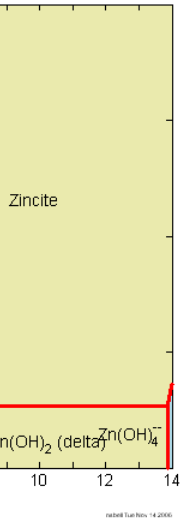

vs. T

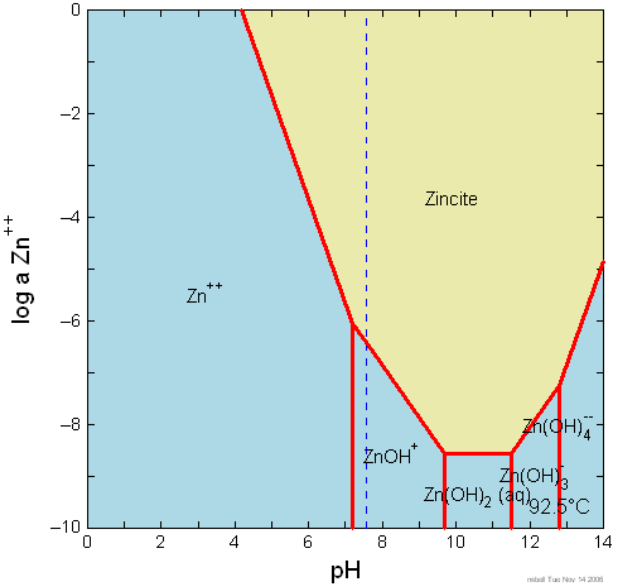

ammonia at 0.0001 M, T=92.5 C

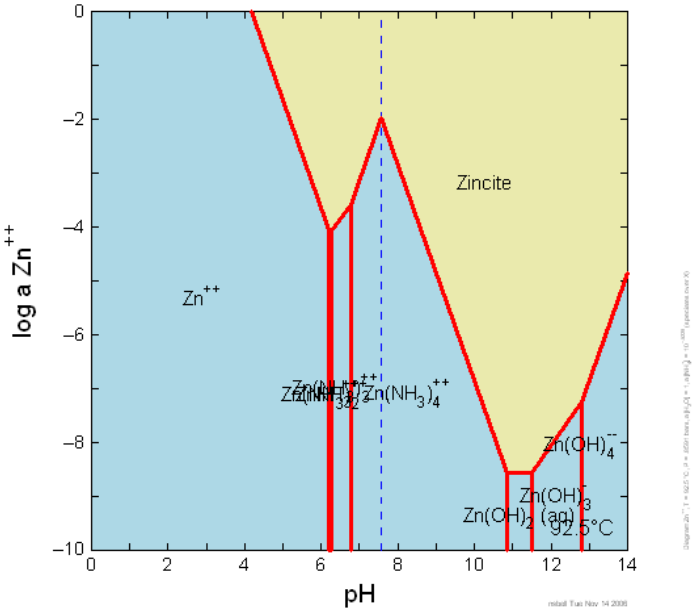

ammonia at 0.3 M, T=92.5 C

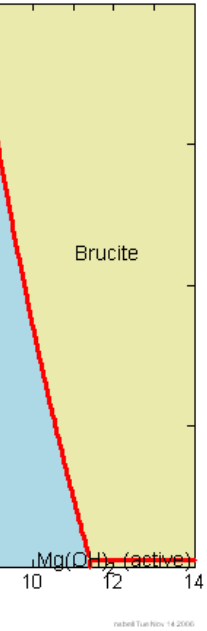

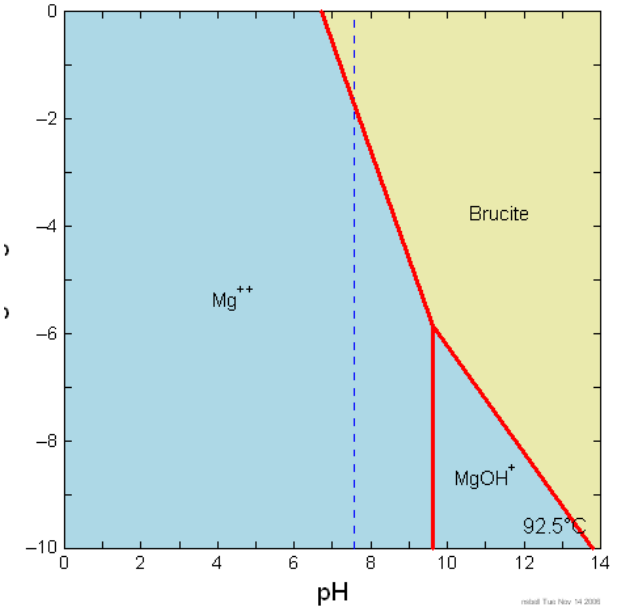

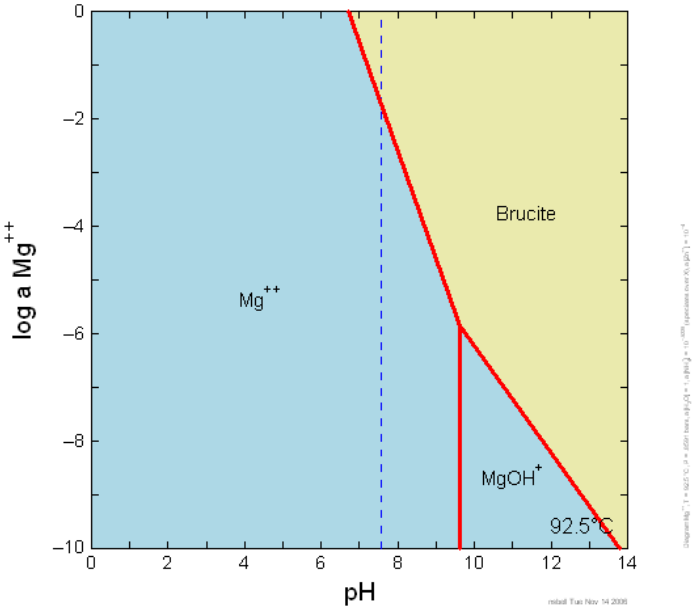

Kinetics of ZnO Nanoparticle Synthesis as affected by Mg Acetate

Microfluidic Synthesis Discovery Platform
CINT

Contributors

Nelson S. Bell, Tom Sounart,
James A. Voigt, Murat Okandan,
Ron Renzi, Bill Smith